Bending and Shear Behavior of Two-Layers Casting Reinforced Concrete Beams

A Thesis

Submitted to the Council of the Erbil Technical Engineering College at Erbil Polytechnic University in Partial Fulfillment of the Requirements for the Degree Master of Science in Civil Engineering

By

Halmat Burhan Najm

B.Sc. in Civil Engineering Techniques

Supervised by

Prof. Dr. Mereen Hassan Fahmi Rasheed

Erbil, Kurdistan

November-2022

بِسۡمِ ٱللَّهِ ٱلرَّحۡمَٰنِ ٱلرَّحِيمِ

﴿ قَالُوا سُبْحَانَكَ لَا عِلْمَ لَنَا إِلَّا مَا عَلَّمْتَنَا ۖ إِنَّكَ أَنتَ الْعَلِيمُ الْحَكِيمُ﴾

In the name of Allah, Most Gracious, Most Merciful

They said: "Glory to Thee, of knowledge we have none, save what Thou Hast taught us: In truth, it is Thou Who art perfect in Knowledge and wisdom."

Surat al-Baqarah, Ayat (32).

بەناوی خوای گەورە و میهرەبان

فریشتەکان وتیان: پاکو و بیگەردی و ستایش هەر شایستەی تۆیە خوای گەورە،ئێمە هیچ زانستێکمان نیە، تەنها ئەوە دەزانین کە تۆ فێرت کردووین، بەراستی تۆپەروەردگارێکی زاناو دانایت. (32)

سورەتی بەقەرە، ئایەتی (32)

DECLARATION

I declare that the Master Thesis entitled: Bending and Shear Behavior of Two-Layers Casting Reinforced Concrete Beams is my own original work, and hereby I certify that unless stated, all work contained within this thesis is my own independent research and has not been submitted for the award of any other degree at any institution, except where due acknowledgment is made in the text.

Signature:

Student Name: Halmat Burhan Najm

Date: / 22 / 12 / 2022

SUPERVISOR CERTIFICATE

This thesis has been written under my supervision and has been submitted for the award of the degree of Master of Science in Civil Engineering with my approval as supervisor.

Signature:

Name: Prof. Dr. Mereen Hassan Fahmi Rasheed

Date: 22 / 12 / 2022

I confirm that all requirements have been fulfilled.

Signature:

Name: Assist. Prof. Dr. Bahman Omar Taha

Head of the Department of Civil Engineering Techniques

Date: 22 / 12 / 2022

Signature:

Name: Assit. Lecture. Byad Abdulqader Ahmed

Postgraduate Office

Date: 22 / 12 / 2022

EXAMINING COMMITTEE CERTIFICATION

We certify that we have read this thesis: Bending and Shear Behavior of Two-Layers Casting Reinforced Concrete Beams and as an examining committee examined the student (Halmat Brhan Najm) in its content and what related to it. We approve that it meets the standards of a thesis in terms of scope and quality for the degree of master's in civil engineering.

Signature:

Name: Assist. Prof. Dr. Najmadeen M. Saeed

Member

Date: 22 / 12 / 2022

Signature:

Name: Assist Prof. Dr. Rahel Kh. Ibrahim

Member

Date: 22 / 12 / 2022

Signature:

Name: Prof. Dr. Mereen Hassan Fahmi Rasheed

Supervisor

Date: 22 / 12 / 2022

Signature:

Name: Prof. Dr. Ayad Zaki Saber

Chairman

Date: 22 / 12 / 2022

Signature:

Name: Prof. Dr. Ayad Zaki Saber

Dean of Erbil Technical Engineering College

Date: 22 / 12 / 2022

DEDICATION

To my beloved and first teachers, my parents, whose affection, love, encouragement faithful prayers, and teaching me to trust in ALLAH, and believe in hard work, make me able to get such successful work.

To my long-life companions, and my wife, whose support, understanding, and belief in me, make me proud of the work which I do in my life.

My friend who encourages and supports me,

For all the people in my life who touch my heart, I dedicate this research.

I am forever thankful

ACKNOWLEDGMENT

In the name of Allah, Most Merciful and Most Gracious

It is a genuine pleasure to express my deep sense of thanks and gratitude to my supervisor Prof. Dr. Mereen Hassan Fahmi Rasheed, for his esteemed suggestions, assessments, and guidance throughout all the stages of this research. His timely advice, meticulous scrutiny, scholarly advice, and scientific approach have helped me to a very great extent to accomplish this task.

In addition, special thanks are also directed to Dr. Bakhtyar Nassih, and Dr. Rafah Rasheed for their advice and useful notes throughout this study.

Furthermore, I abundantly thank Assist. Prof. Dr. Bahman Omar Taha head of the Civil Engineering Department for his continuous support and help from the beginning of the master's degree courses until the end of this thesis.

Special acknowledgment is presented to the Head of the Civil Engineering Department, Prof. Dr. Dana Khider Mawlood, and faculty members of the Civil Engineering Department- at Salaheddin University-Erbil.

I would like also to extend my thanks to the engineers' technical staff of the concrete laboratory, especially Mr. Muhammad Luqman, Mr. Hogr Himdad, Mr. Dana Iqbal, Mr. Lawan, and Mrs. Khanda, for their help. Finally,I would like to express my deepest thanks to my wife and all my friends, especially Eng.Saad Rasul for their help during this study.

ABSTRACT

Concrete it is very important in construction materials, for high rise building and bridge using high-strength concrete, to reduce the cost of high strength and the size of the beams can be used two-layer beams. This study investigates the bending and shear behavior of reinforced concrete beams consisting of two layers with different concrete strengths (grades), for beams with and without shear reinforcement (stirrups), considering the effect of layer compressive strength, the overlap casting time of the two layers, layer thickness, and the shear-span ratio. The experimental program consists of a total of nineteen reinforced concrete beams of dimension (125 mm x 250 mm) with a total length of 1200 mm, the beams are reinforced with longitudinal reinforcement (4Ø12mm) and using (Ø8mm) bar as transverse reinforcement (stirrups). The experimental results show that the crack pattern of the two-layer reinforced concrete is similar to the crack pattern of the control beam with one layer. Increasing the compressive strength of concrete of the top layer, the ultimate failure load increased by (8.35%, 15.6%, and 18.85%), with respect to the (control beam) with the full depth of normal concrete. By increasing the high-strength layer thickness, the value of cracking shear strength (Vc) and ultimate shear strength (Vu) increased linearly. The overlap casting time of up to (30min) can be used for casting two-layered reinforced concrete beams, which is recommended, beyond this time the cracking shear strength (Vc) and, ultimate shear strength (Vu) decrease. With increasing the shear span ratio (a/d) from (1 to 1.5 and 2) the ultimate load failure decreased by (33% and 50%). The shear strength capacity decreases with increasing stirrup spacing. Different equations are proposed to modify the ACI Code-2019 for two-layer beams to predict the shear strength of the beams in terms of the considered in this study. General equations are proposed using multi-linear analysis regression to predict cracking shear and flexural first cracking shear of two-layer beams in terms of the variables of this study.

LIST OF CONTENTS

Content **Page**

LIST OF TABLES

Table **Title** **Page**

LIST OF FIGURES

LIST OF MAIN NOTATIONS

Symbols	Meaning
a_v	Shear span (mm)
a/d	Shear span ratio
As	Area of reinforcement in tension zone (mm^2)
As'	Area of reinforcement in tension zone
bw	Width of the beam (mm)
C	Cement
CZ	Compression zone
COV	Coefficient of various
d	Effective depth of the beam (mm)
d'	Longitudinal compression steel cover
Ec	Elasticity modulus of concrete
Es	Young's modulus of steel reinforcement
fc'	Cylindrical compressive strength of concrete (MPa)
f_{cu}	Cube compressive strength of concrete (MPa)
f_{sp}	Splitting tensile strength (MPa)
f_r	Modulus of rupture of the concrete (MPa)
fy	Tensile yielding stress of steel reinforcement (MPa)
f_u	Ultimate Strength of steel (MPa)
FRLWC	Fiber-reinforced lightweight concrete
G	Aggregate
h	Height of the beam (mm)
HSC	High strength concrete
HPC	High-performance concrete
h_{HSC}	Depth of the layer (top layer) mm.
h_{NSC}	Depth of the layer (bottom layer) mm
ℓ	Effective length
Ig	Moment of inertia of the transformed section
L	Total length of the beam (mm)
LWAC	Lightweight aggregate concrete
LWC	Lightweight concrete
NSC	Normal strength concrete
Pu	Ultimate failure load (N)

P_{cr}	Cracking load (N)
R	The average ratio of (R) experimental shear force divided by theoretical shear force
R (max)	Maximum shear force ratio
R (min)	Minimum shear ratio
r	Coefficient of correlation
SP	Super plasticizer
SF	Silica Fume
s	Spacing of the stirrups (mm)
S	Sand
SHSC	Steel fiber high strength concrete
t	Time (min)
t_o	Initial setting time of cement (min)
TZ	Tension zone
Vc	Shear strength of the beam (kN)
Vc_1	Flexural first cracking shear (kN)
Vu	Ultimate shear strength (kN)
γ_c	Coefficient = 1.4
γ_m	Concrete partial factor of safety
y_t	Distance from the neutral axes to the tension face (mm)
σ	Standard deviation
ρ_l	Percentage of longitudinal reinforcement
ρ_t	Percentage of transverse reinforcement
ACI	American Concrete Institute
ASTM	American Society for Testing and Materials

CHAPTER ONE

INTRODUCTION

1.1 Background

Concrete is one of the most widely used construction materials in the world, it has many advantages such as cost-benefit, stable material supply, and a high level of durability (Choi et al., 2015). However, concrete also has a weak tensile strength, therefore cracking occurs quickly due to tensile stress and, it is strong in compression (Yang et al., 2018). Combination of concrete with steel reinforcement can become a highly durable material. Concrete is used in all kinds of structures to a large extend. Reinforced concrete structural components such as beams, columns, walls, slabs, etc. are designed to resist the external horizontal and vertical loads. Shear force and bending moments are developed in the beams shown in Fig. (1-1). Additionally, beams are characterized by cross-sectional shape, dimensions, and length of the beam, material used to make the beam, and support conditions. Beams made only from concrete cannot resist tension and it fails because of its brittle nature. The reinforcement is introduced into beams to carry the tension stresses and bending stress. While concrete would carry the compression stresses.

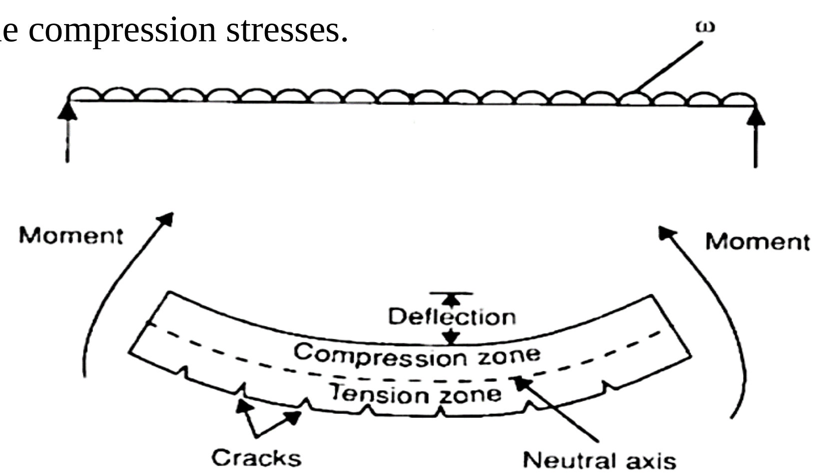

Fig.1-1 Bending of the beam (Adnan, 2018)

For the beam to be designed, flexural strength and shear strength need to be evaluated and then need to be checked for serviceability. The internal shear forces and bending moment forces carry major loads. The size of the concrete beam section and arrangement of the reinforcement is providing the required resistance for moments and shears developed in the element. High-strength concrete (HSC) provides a better solution for reducing the sizes and weights of the concrete structural element (Nilson, 1985, Swamy, 1985 , Wafa and Ashor, 1992).

1.2 High-strength concrete

In the construction of high-rise buildings and bridges, high-strength concrete has lots of advantages. In many areas in the world, concrete with the strength of 40 MPa and higher is produced commercially, in which normal coarse and fine aggregates are used along with the cement. Admixtures such as minerals and chemicals are used to have concrete with higher strength available.

The definition of high-strength concrete changes over time and place, based on building industry developments. (ACI Committee 363, 2005) high-strength concrete is defined as concrete with a specified compressive strength of 55 MPa (8000 psi) or higher.

High-strength concrete is more complicated to design than normal concrete, and it needs a careful mix of proportion, and high-quality materials, as well as a low water/cement ratio and high cement content. Of these, the use of a low w/c ratio (between 0.25 to 0.35) is essential, and this will invariably result in unworkable dry mixes unless admixtures are used. Chemical admixtures such as super-plasticizers, as well as mineral admixtures such as silica fume, slag, fly-ash and many more, different admixtures are added to help concrete to reach higher strengths.

1.3 Two-layer composite reinforced concrete beam consisting of NSC and HSC

The behavior of beams made of two layers of two different materials has been the subject of numerous investigations in recent years. Recently, researches was conducted on a continuous two-layer beam and a full-scale two-layer beam that used high strength concrete with steel fibre in the compression zone and normal strength concrete in the tensile zone (Iskhakov et al., 2014, Iskhakov et al., 2017). Other researchers have been focused on replacing the tension zone with Engineered Cementitious Composite (ECC) to improve the tensile strength of the concrete around the main steel reinforcement (Krishnaraja and Kandasamy, 2018, Ge et al., 2018). The essential objective of this study is to evaluate the strength and behavior of two-layer beams consisting of normal strength concrete in the tension zone and high-strength concrete in the compression zone shown in Fig. (1-2), the different variables have been chosen to study. The depth of each layer and compressive strength of normal and high-strength concrete were variables of this study.

1.4 Problem Statement

High-strength concrete is used to reduce the size of the beams in addition to enhancing the strength, this leads to overestimated cost in comparison with normal strength concrete while using normal strength concrete leads to the overestimated amount of concrete (layer size) of the beam section. For balancing the condition between the cost and size of beams, the benefit of both materials is used, by using beams in two layers, high-strength concrete in the compression zone (top layer), which is more beneficial for beam strength, and normal strength concrete in tension zone (bottom layer), which is no need to use high strength concrete in the tension zone.

1.5 The benefits of Two-layers Reinforced Concrete Beams

1. To provide an economic from of a reinforced concrete beam by replacing normal strength concrete instead high strength concrete in tension zone
2. To enhance the strength in compression zone

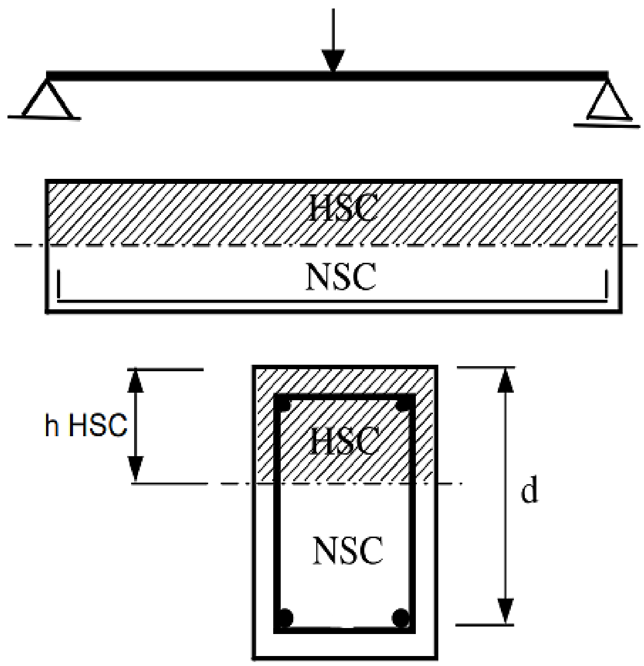

Fig.1-2 Two-layer composite beams

1.6 The Aim of the study

The main aim of the thesis is: -

1. Study the flexural and shear behavior of reinforced concrete beams consisting of two layers with different concrete strength (grades), for beams with and without shear reinforced (stirrups), considering the effect of shear-span ratio, layer thickness, layer compressive strength, and the overlap casting time of the two layers.

2. Propose empirical equations to predict the shear capacity and flexural of the concrete beams including the effect of the study variables and comparing the theoretical results with the data obtained in the lab by experimental.

1.7 The objectives of the study

Study of flexural and shear behavior of two-layer reinforced concrete beams, considering the following variables for beams with and without stirrups, using normal strength in the location that is subjected to tension and, in the location of compression that has a high strength, the following objective were focused on

1. To study effect of concrete compressive strength ratio of the two layers $\frac{fc'HSC}{fc'NSC}$
2. To evaluate effect of overlap casting time of the two layers.
3. To Calculate effect of layer thickness normal and high strength concrete.
4. To investigate effect of shear span ratio $\frac{a}{d}$.
5. Effect of spacings stirrups.

1.8 The structure of the thesis

This thesis is consisting of six chapters:

Chapter One gives a brief introduction to the topics. While Chapter Two is an extensive review of the literature on the behavior of flexural bending and shear of two-layer reinforced concrete beams. In addition, Chapter Three gives detailed information on the materials, testing instrument, testing procedures, and experimental program. Later, in Chapter Four, the experimental work results are discussed, and the experimental results are compared with the theoretical results obtained from the different available equations from literature and codes. Then

Chapter Five presents a theoretical study to predict the bending moment and shear capacity of the beams and purpose an empirical equation and compares the results with the experimental data. Finally, the conclusions of the research are presented in Chapter Six precisely, the chapter also suggests recommendations for the fellow researchers in the future.

CHAPTER TWO

LITERATURE REVIEW

2.1 Introduction

In this chapter a review of the previous theoretical and experimental works has been conducted. Several recent studies focused on the flexural behavior of two-layer reinforced concrete consisting of normal strength NSC in tension zone and steel fiber high strength in locations that are subjected to compression SHSC or NSC with steel fiber lightweight concrete. While this current investigation concentrated on the flexural behavior of two-layer reinforced concrete consisting of normal strength concrete NSC in the tension zone and high strength concrete HSC in the compression zone. The flexural behavior of the reinforced concrete beam is affected by several factors, including the concrete compressive strength, the amount of rebar, layer thickness, shear span ratio, and the cross-section area of the member.

2.2 Two-layer RC beams made of NSC and lightweight concrete

Adnan et al. (2021) were tested twelve concrete beams with two different concrete layers were tested as simply supported beams under four-point loads. The beams were made using two different types of concrete layers: normal-weight concrete (NWC) and lightweight aggregate concrete (LWAC). The thickness of lightweight concrete to a total depth of beams ($\frac{h_{LW}}{h}$), was examined. All the beams have a 140 x 200 mm cross-section and a total length of 1700 mm in four different sets. The first set was categorized according to the thickness of the LWAC layer about the overall depth of the beam ($\frac{h_{LW}}{h}$): 0, 25, 50, 75, and 100 percent, with the LWAC in the tension zone (TZ). The second and third groups investigate the effect of NWC and LWAC on compressive strength in the compression zone (CZ), while the fourth group investigates the compressive strength of LWAC in the tension zone (TZ). The specifications of tested beams are summarized in Fig. (2-1) and Table (2-1).

Table 2-1 Specification of beams (Adnan et al. 2021)

Beam	Layer thickness of		h_{LW}/h	Type of concrete	
	NWC (mm)	LWAC (mm)		Top layer	Bottom layer
B1N	-	-	0%	NWC	-
B1N-1L25	150	50	25%	NWC	LWAC
B1N-1L50	100	100	50%	NWC	LWAC
B1N-1L75	50	150	75%	NWC	LWAC
B1L	-	-	100%	-	LWAC
B1L-1N50	100	100	50%	LWAC	NWAC
B2L-1N50	100	100	50%	LWAC	NWAC
B3L-1N50	100	100	50%	LWAC	NWAC
B1N-2L50	100	100	50%	NWC	LWAC
B1N-3L50	100	100	50%	NWC	LWAC
B2N-1L50	100	100	50%	NWC	LWAC

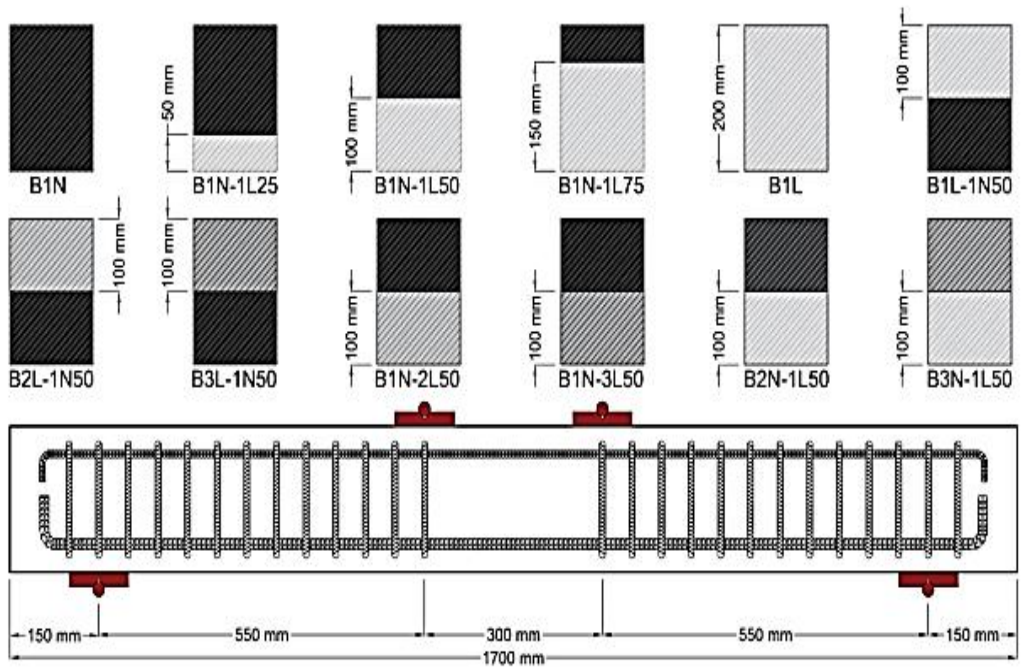

Fig. 2-1 layout of beam and distribution of reinforcement (Adnan et al. 2021)

Based on this study results the following conclusions were obtained:

• Except for crack spacing, the behavior of both control and two-layer beams was the same. The cracks of two-layer beams were closer to each other than the cracks of control beams, and all the beams failed in flexure.

• Flexural strength: increasing the lightweight aggregate layer thickness in the tension zone from 0% to 25%, 50%, 75%, and 100% reduces the ultimate load capacity of beams by 0.13 %, 0.44 %, 3.4 %, and 8.65 %, respectively.

Jamal et al. (2019) the research by Jamal et al. presents an experimental investigation of the layered beam to study the possibility of using the weak effect of concrete at the tension zone of a simply supported concrete beam that places at this zone practically by using lightweight concrete as a part of this region to produce a beam that is lighter than a homogeneous RC beam. Eight beams' specimens with dimensions of (150 * 200 * 1000) mm was cast, with longitudinal reinforcement of 3 Φ10 mm at tension zone and 2 Φ6 mm at compression zone and shear reinforcement stirrups of Φ6mm @50mm. Table (2-2) and Fig. (2-2) illustrate the specifications of each beam specimen. Where the section of rectangular beams (150*200*1000) mm is cast with Light-weight concrete (LWC) (produced by replacing the coarse aggregate of the main normal concrete mix with a crash limestone once and another time by replacing half of the normal coarse aggregate with chopped rubber tire) in the tension zone and normal strength concrete in the rest of the section and compared to control beams. Three different levels of lightweight layers (1/3,1/2, and 2/3 of beam thickness) were investigated, and all beams were tested under a two-point load until it breaks.

Table 2-1 Beams details (Jamal et al. 2019)

Beam type	The thickness of LWC mix mm	The thickness of NSC mix mm	No. of specimen
HRC	-	200	2
LRC1	67.7	133.3	2
LRC2	100	100	2
LRC3	133.3	67.7	2

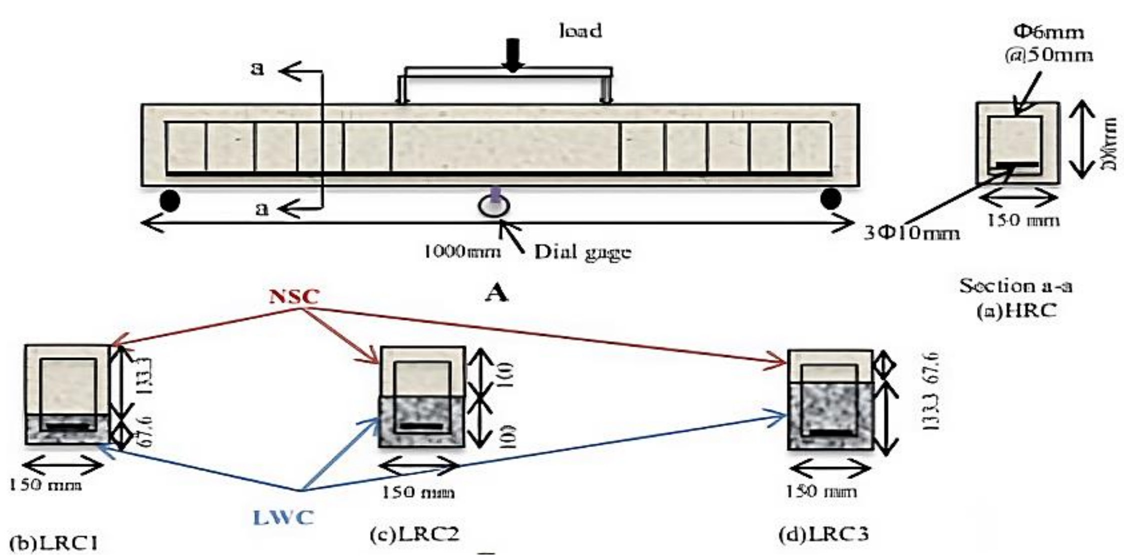

Fig. 2-2 Loaded simply supported beam (Jamal et al. 2019)

The results of this investigation (for all different thickness that are replaced) showed that the load-deflection curve of the layered beams (LWC) and (HRC) beam are similar, the slope of the curve of the (LWC) beams is stepper than the (HRC), this means that (LWC) beams, with limestone crushed aggregate has a higher stiffness than the (HRC) beam with normal concrete as shown in Fig. (2-3).

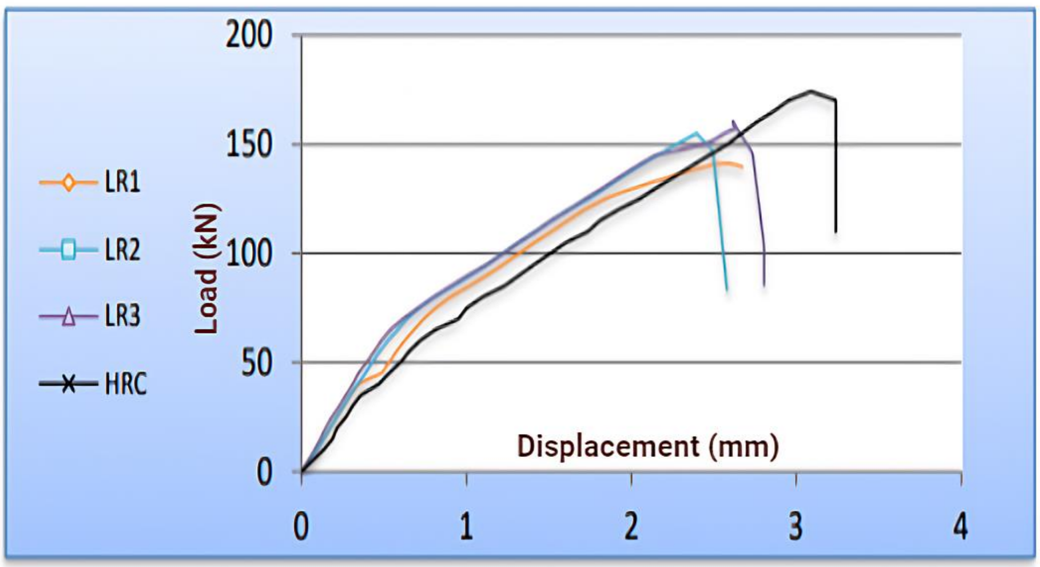

Fig. 2-3 Load-displacement relation for HRC beam and layered beams of LWC with limestone (Jamal et al. 2019)

Fig. (2-4) shows the cracking and failure load of the tested beam, the crack load of the LR1, LR2, and LR3 beams is smaller than that of the HRC beams by 18.03 %, 11.50 %, and 3.13 %, respectively. Furthermore, the breaking was 18.96%, 8.39%, and 7.70% less than HRC beams, respectively.

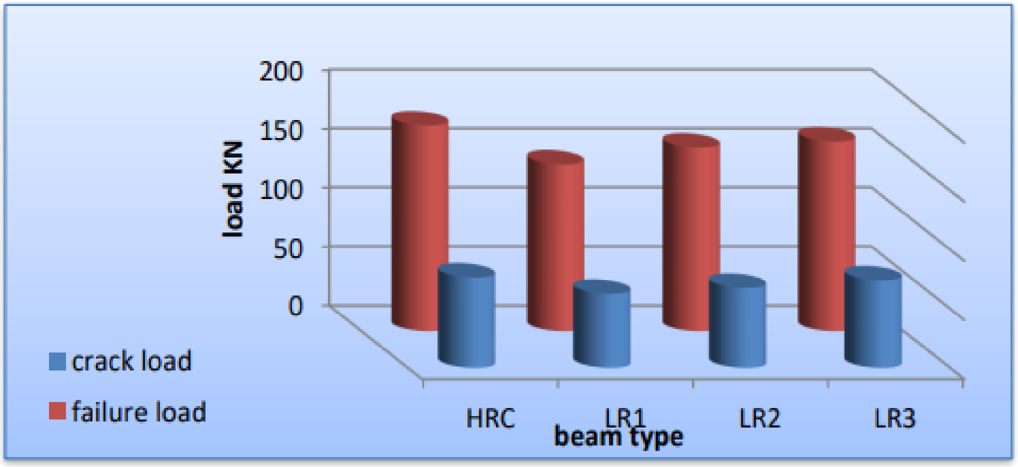

Fig. 2-4 Failure load and crack result of the beams (Jamal et al. 2019)

Nes and Overli, (2015) the research by Nes and Overli. made of two layers of various types of concrete beams. In the top layer, normal density concrete (NC) was mixed with a layer of fiber-reinforced lightweight concrete (FRLWC). The experimental program included 16 simply supported concrete beams with similar cross-sections. Eight beams were developed for shear failure, and eight beams were developed for bending failure. The beams were made up of a 50 mm top layer of NC and a 200 mm bottom layer of fiber-reinforced lightweight concrete (FRLWC), as illustrated in Fig. (2-5). A four-point loading system was used to test the beams in flexure.

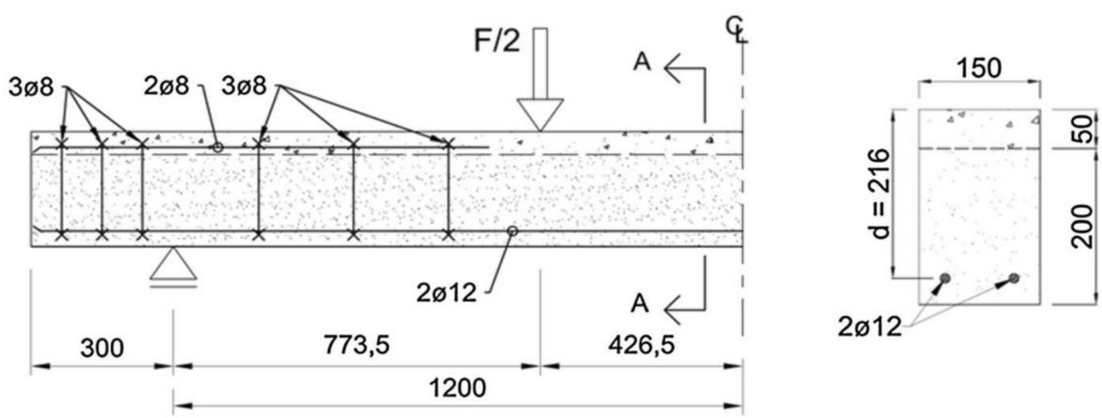

Fig. 2-5 The concept of design for hybrid concrete and cross-section (Nes and Overli, 2015)

This study found that steel fiber reinforcing of lightweight concrete increased the ductility in tension and decreased the amount of normal shear reinforcement. Additionally, compared to a normal reinforced concrete beam, these composite beams' bending failure is less ductile. The shear capacity increased with the amount of fiber, though the distribution and orientation of the fibers greatly influence the results. Fig. (2-6) illustrates the crack patterns for beams that failed in bending with 0.5% and 1.0% fiber reinforcement. The number of cracks in 0.5 % fiber beams was significantly higher than in 1 % fiber beams.

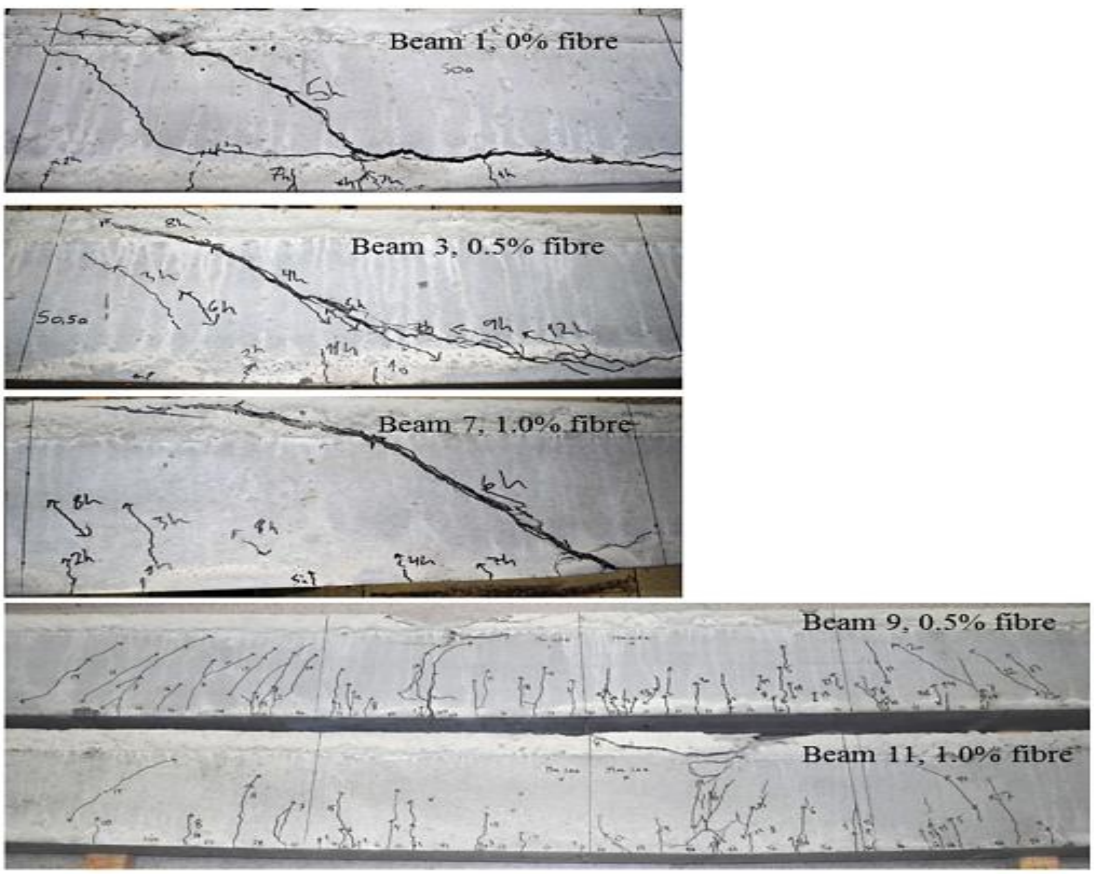

Fig. 2-6 Crack pattern and failure mode for beams 1, 3, and 7 failing in shear, and beams 9 and 11 failing in bending (Nes and Overli, 2015)

2.3 Two-layer RC beams made of NSC and steel fiber RC beam

Iskhakov et al. (2014) the experimental study of two-layer beams (TLB) using steel fibered high strength concrete (SFHSC) in the compression zone and normal strength concrete (NSC) in the tensile zone. The dimensions of the TLB tested in this study were 15 × 30 × 300 cm. Fig. (2-7) shows a beam construction technique. The NSC layer was 21 cm deep, while the SFHSC layer was 9 cm deep. Fig. (2-8) shows a general overview of the TLB that was tested.

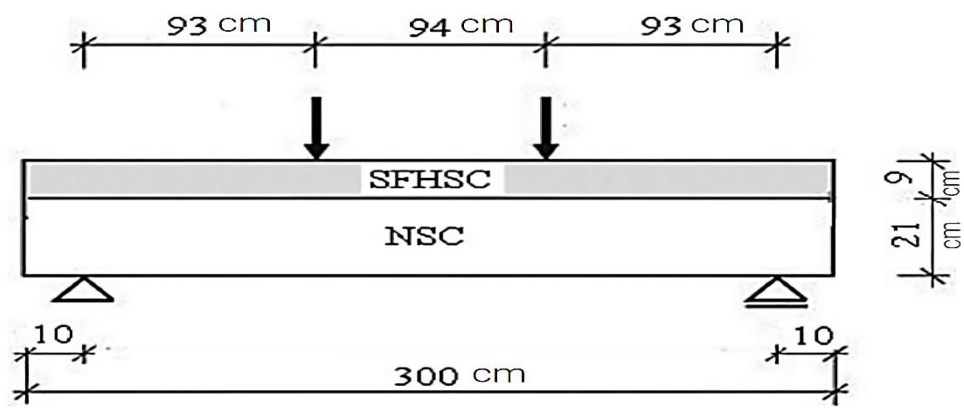

Fig. 2-7 A four-point loading test setup: NSC and SFHSC (Iskhakov et al. 2014)

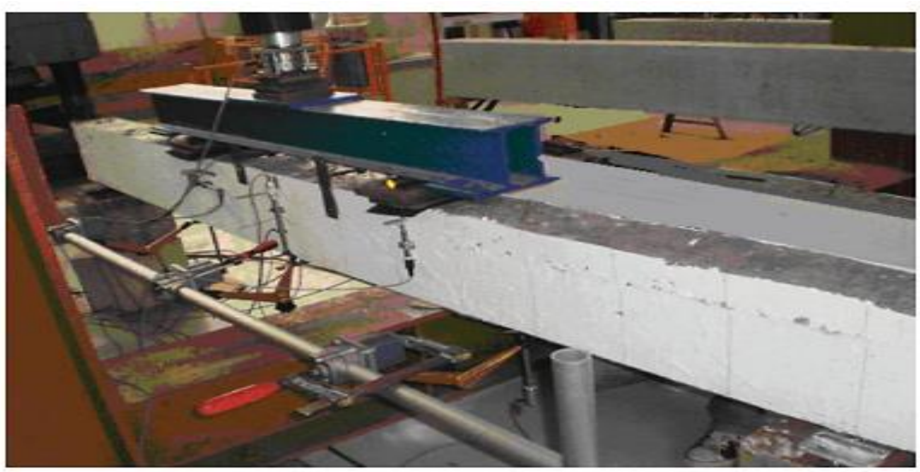

Fig. 2-8 A general view of the tested two-layer beam (Iskhakov et al. 2014)

For the concrete that has normal strength class C25/30 of concrete was chosen and, the C70/85 concrete class was selected for SFHSC. After the NSC hardening, the SFHSC layer was cast. The force-deflection curves obtained experimentally were smooth until failure. A horizontal crack occurred at the failure stage due to de-bonding between the SFHSC and NSC layers. TLB has been improved to be more effective, and it has been shown that using the optimum steel fiber weight ratio in HSC allows for high-performance bending elements with similar elastic-plastic behavior to regular NSC bending elements. Two-layer beams have the same bearing capacity as HSC-only beams and are less expensive because high-strength concrete and steel fibers are only used in the compression zone of the concrete.

Martínez-Pérez et al. (2017) studied the flexural behavior of layered beams with steel fiber reinforced concrete (SFRC) external layers and RC internal layers. The behavior of these beams is compared to SFRC and normal RC beams. The testing program consisted of eight beams with the dimensions of 300 cm, 150 cm, and 30cm of length, width, and height respectively. Two reinforced concrete beams, beams 1 and 2 are identified as RC, and two kinds of beams with different layer heights - beams has 5 cm and 10 cm of external steel fiber reinforced concrete layers were created, beams 3 and beams 4, identified as MC1. For beams 5 and 6, they are identified as MC2. The final group is made of monolithic beams that is concrete and has reinforcement in then with steel fiber, locations 7 and locations 8 are identified as SFRC. This is illustrated in Fig. (2-9).

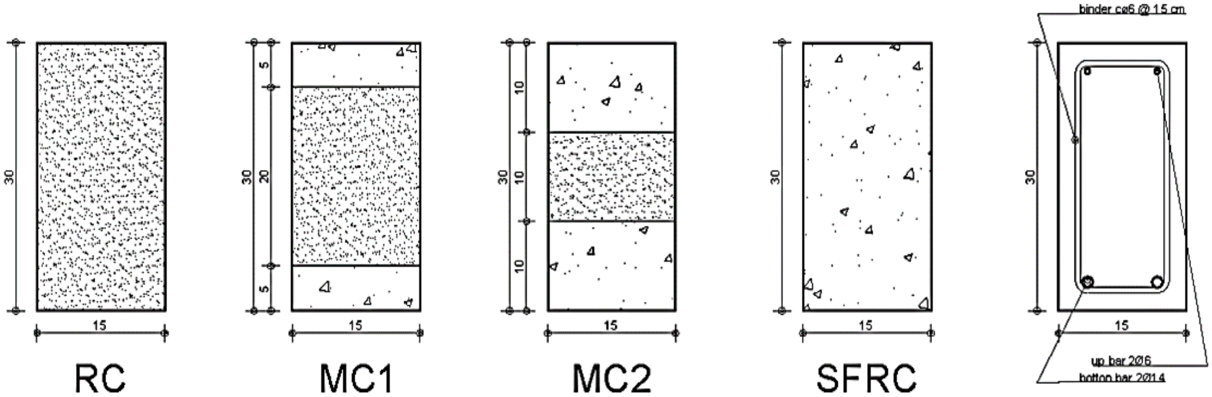

Fig. 2-9 Cross-section and reinforced of the tested beams (Martínez-Pérez et al. 2017)

The study showed that there is a significant difference in deflection between the control beam and the layered beam, the deflection layered beam was (42%) higher than the control beam, control beam showed less cracking than the layered beam. The deflection monolithic reinforced concrete beam was (0.7%) larger than the monolithic SFRC beam. The comparison of the moment and deflection of all beams are shown in Fig. (2-10).

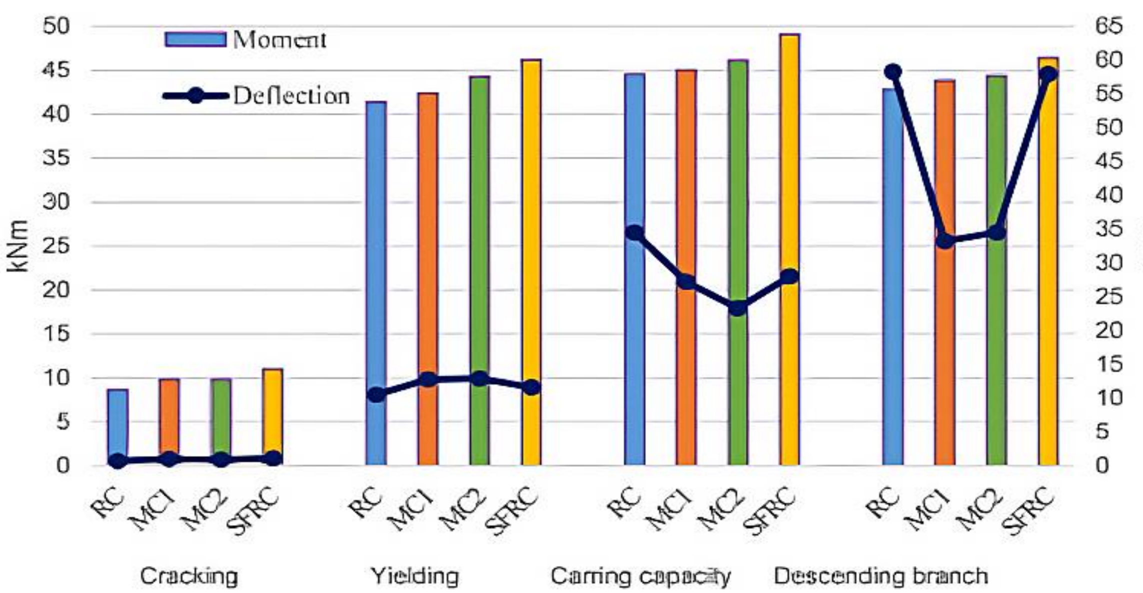

Fig. 2-10 Comparison of moments and deflections of all beam types tested (Martínez-Pérez et al. 2017)

Li et al. (2022) have investigated the flexural behavior of concrete beams hybrid reinforced by continuous basalt fiber reinforced polymer (BFRP) bars and discrete steel fibers. Eleven beams were prepared and tested using four-point bending. With a clear span of 1800 mm and a shear span of 600 mm, all beams had the same size of 150 × 300 × 2100 mm. The concrete cover was 15 mm thick. The beams were also reinforced with longitudinal bars with a diameter of 2 Ø 14 mm and transverse bars with a diameter of Ø10 mm. Fig. (2-11) is showing the cross-section details of the beam series with different SFRC layer thicknesses.

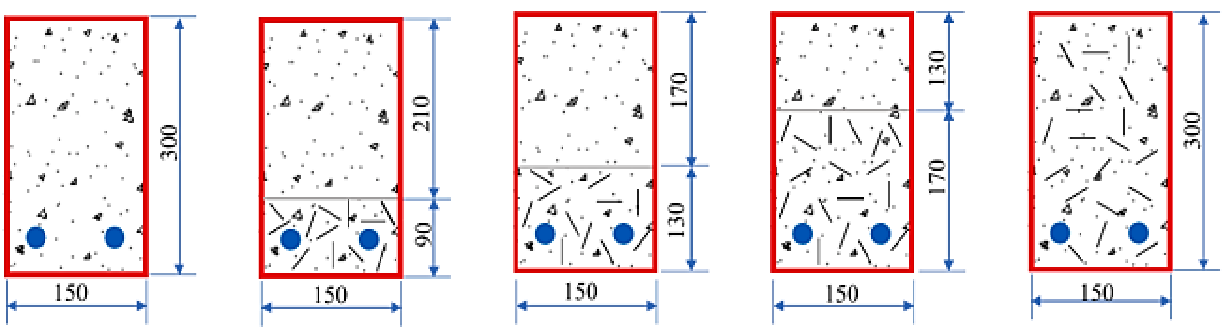

Fig. 2-11 Cross-section details of steel bar distribution (Li et al. 2022)

According to this study, an increased amount of steel fiber reduced deflection and crack width. At the service stage, increasing the steel fiber volume ratio had a larger effect than at the final stage. The displacement and cracking response of the beam with a 2.0 % steel fiber volume ratio were like those of the beam with a 1.5 % steel fiber volume ratio. The maximum steel fiber volume ratio for SFRC in FRP bar reinforced concrete is suggested to be 1.5 %. As shown in Fig. (2-12), the deflections and cracking widths of the BFRP were significantly reduced when the BFRP reinforcement ratio was increased. The flexural strength increased by 6% using the larger amount of reinforcement of BFRP by 63%.

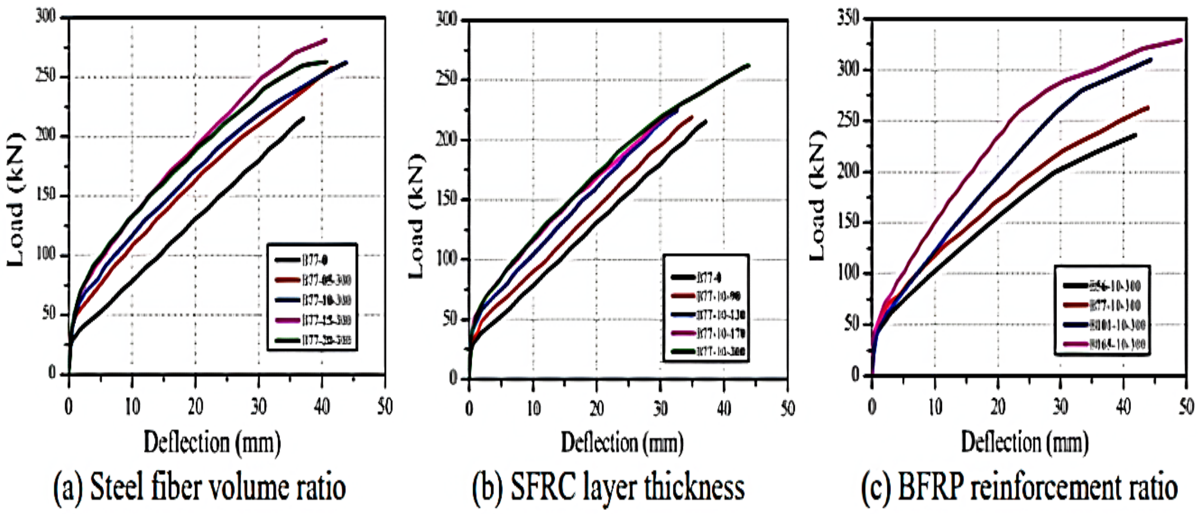

Fig. 2-12 Mid-span load-deflection curves of tested beams (Li et al. 2022)

2.4 Bond strength and cold joint of two-layers reinforced concrete beam

Dybeł and Wałach. (2017) investigated the development of bond strength in concrete-to-concrete composite elements. The work was done to note the bond improvement when having two layers of concrete. For this purpose, two kinds of concrete used. The first type was the concrete of normal strength, and the other type was the concrete of high strength performance. NC-HPC and HPC-HPC substrate and overlay composite specimens, as well as reference NC-NC specimens, were produced. The bond strength was evaluated using 150x150x150 mm composite cubes that were submitted to splitting tension tests after 3, 7, 14, and 28 days of concrete overlay curing. As shown in Fig. (2.13).

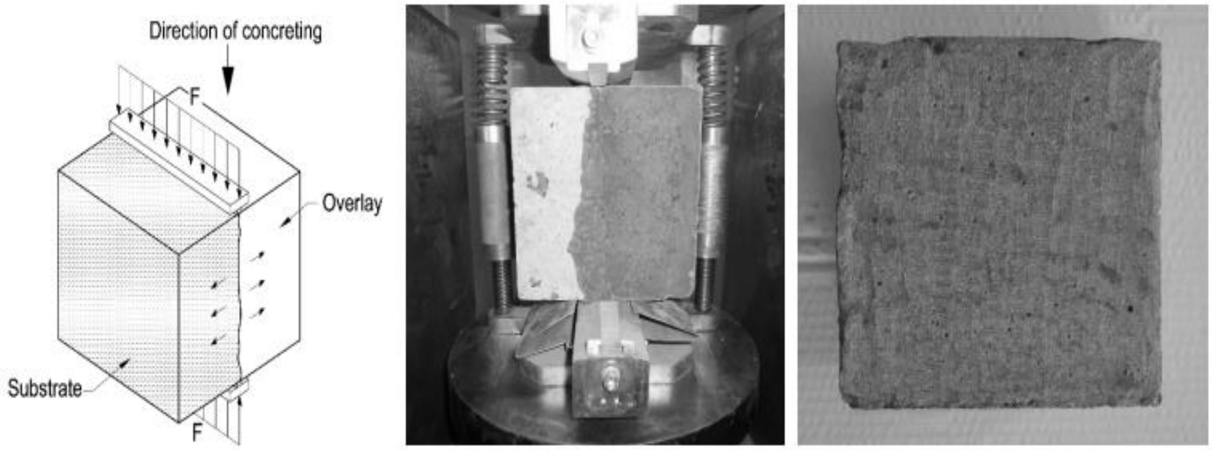

Fig. 2-13 Model of specimen used in tests of tensile bond strength and substrate surface prepared with (Dybeł and Wałach. 2017)

the study's results demonstrated that adhesion between concrete layers, which develops with the curing of the concrete overlay, is the fundamental phenomenon that affects bond strength. The composite specimens showed the highest increase in tensile bond strength during the first three days of curing. During this time, the NC-NC composite reaches 53% of its 28-day tensile bond strength, the NC-HPC specimen 67 %, and the HPC-HPC 74 %. The lab work showed that the failure in the interface had different patterns and that is affected by class of the concrete in the specimens that are composite. In the case of composite specimens NC-NC and HPC-HPC the observed dominant interface failure mode occurred within the overlay transition zone. For the NC-HPC specimens, the interface failure mode was observed both in the overlay transition zone and in the substrate made of NC.

Korol and Vu. (2020) developed shear bond strength between two concrete layers in a three-layer sandwich concrete developed. Two types of concrete were employed in this research: normal concrete (NC) and lightweight concrete (LWC) - polystyrene concrete. The test was carried out using 200x200x200 mm composite cubic specimens. Normal concrete with a thickness of 40mm was first placed, after that lightweight concrete with a Thickness of 120mm was placed. Finally, construct the external layer of normal concrete with a Thickness of 40mm shown in Fig. (2-14). with varying time intervals between laying layers of concrete of different densities from 30 minutes to 4 hours in steps of 30 minutes, this method was taken to create an inventory of samples. A total of 27 samples were examined over 28 days to determine the shear bond strength. All tests can be classified into 9 groups based on the time spent between concreting two adjacent layers, ranging from 0 to 4 hours. Fig. (2-15) shows the results of the experiments.

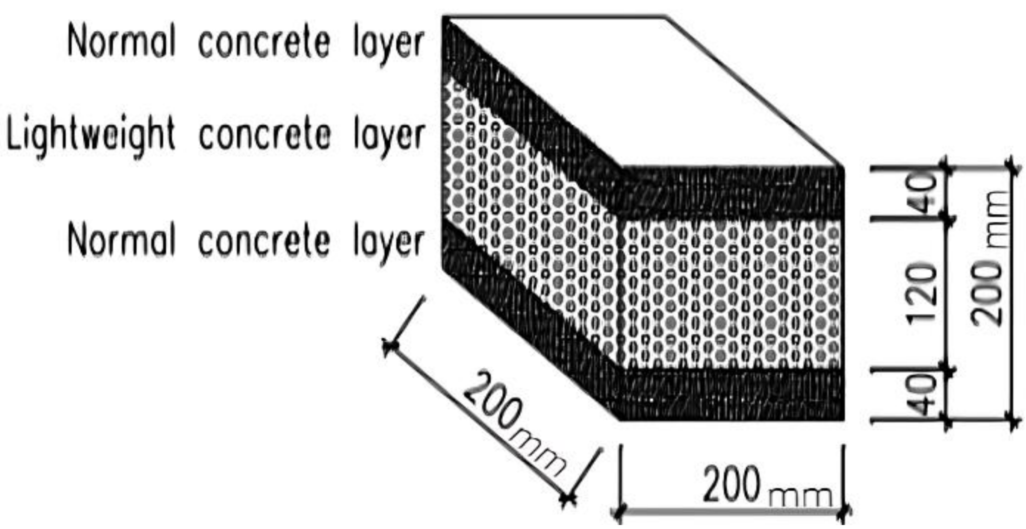

Fig. 2-14 Sample three-layer concrete for shear test (Korol and Vu. 2020)

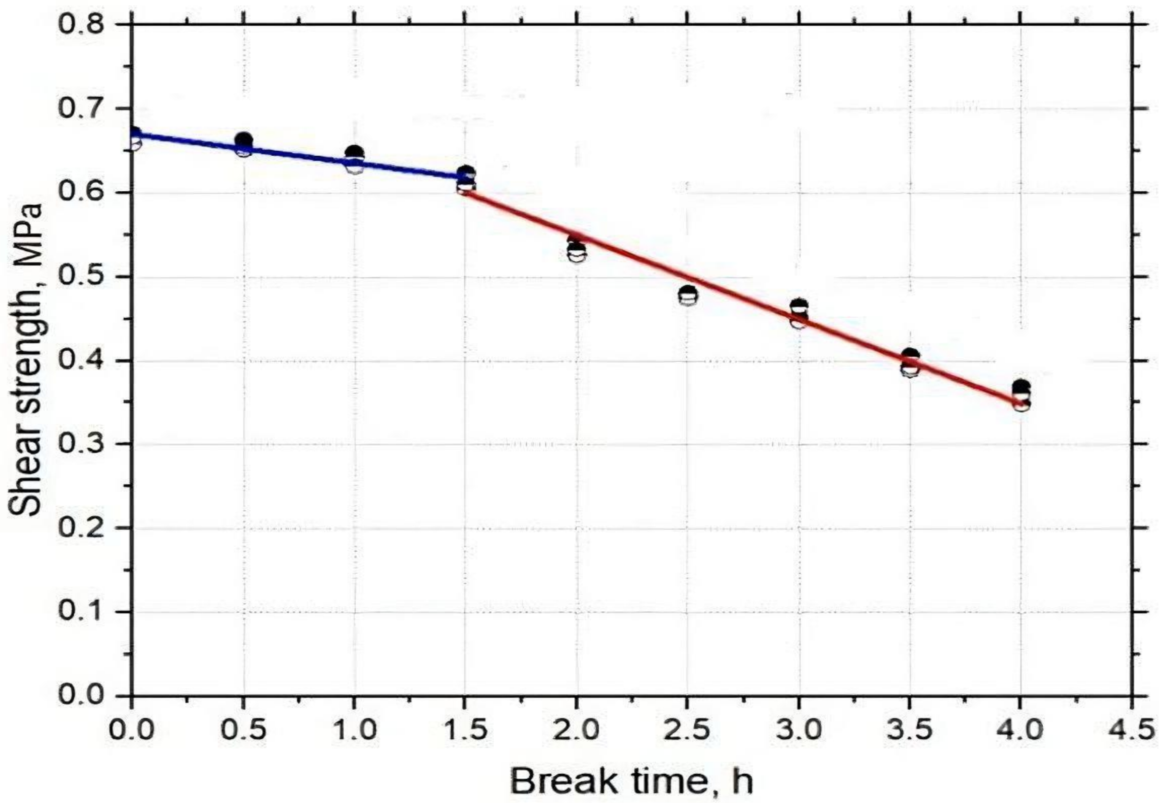

Fig. 2-15 Shear strength - breaking time for samples with three layers obtained from tests (Korol and Vu. 2020)

Bekem Kara, (2021) searched the cold joint's effects on the properties of concrete in terms of durability and strength. The horizontal cold joint was made by casting concrete to mid-height of the mold, and then additional concrete was poured on top of the molds after 0, 60, 120, and 180 minutes. Compressive, flexural, splitting tensile, and concrete–steel rebar pullout tests were performed on the specimens. Two types of concrete were created in the second part of the investigation to conduct durability tests. 15 x 15 x 15 cm cubic, 10 x 10 x 40 cm prisms, and cylinders with 15 cm of diameter and 30 cm of height were preferred for the strength tests. The specimen dimensions, cold joint formation periods, and loading circumstances are shown in Fig. (2-16) and Table (2-3).

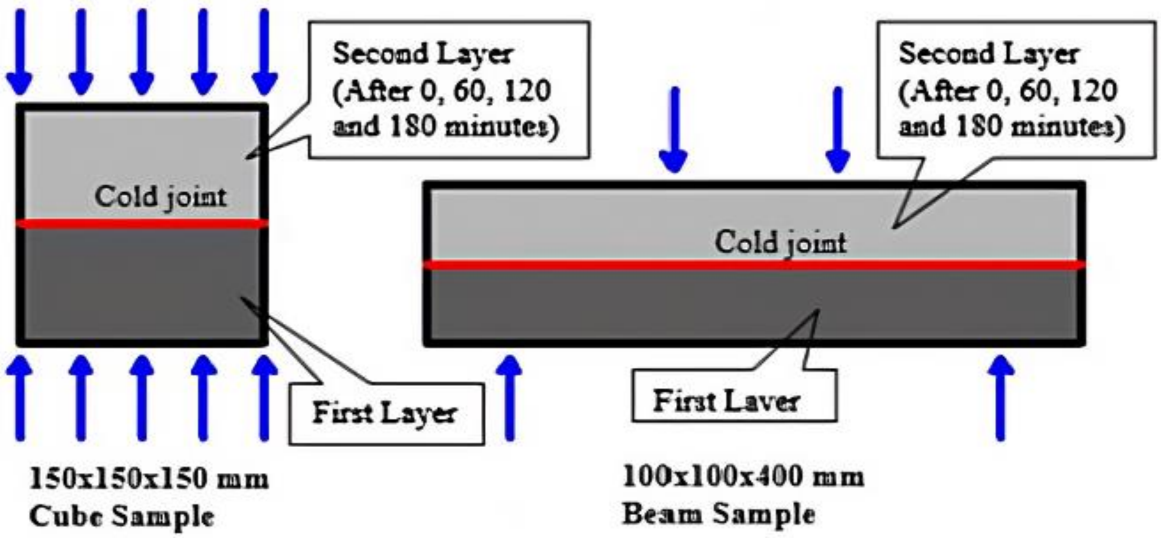

Fig. 2-16 Cold joint formation line in the concrete specimens and loading situations (Bekem Kara. 2021)

Table 2-2 Concrete types and codes for the strength experiments (Bekem Kara. 2021)

Concrete pouring details	Code
First layer after 0 min, followed by second layer (concrete without cold joint)	CJ0
First layer after 60 min, followed by second layer (concrete has a cold joint)	CJ1
First layer after 120 min, followed by second layer (concrete has a cold joint)	CJ2
First layer after 180 min, followed by second layer (concrete has a cold joint)	CJ3

The compressive, splitting, tensile, and flexural strengths of concrete decreased as the time between casting two layers of concrete increased, as shown in Fig. (2-17). While the concrete without cold joints had a compressive strength of 30.28 MPa, the concrete with cold joint pouring delays of 60, 120, and 180 had compressive strengths of 29.96, 29.65, and 29.60 MPa, respectively.

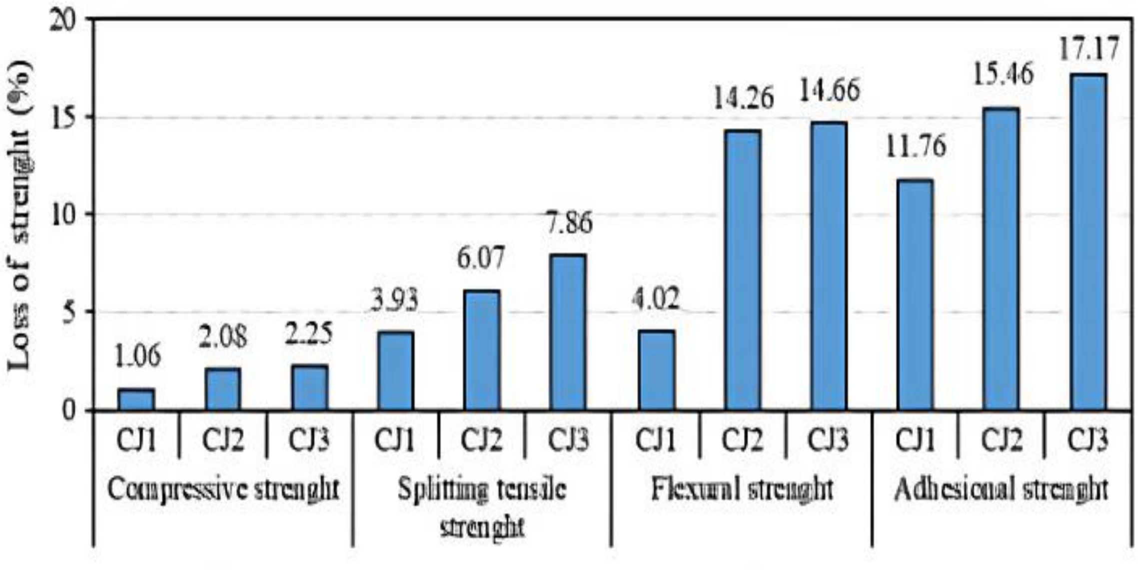

Fig.2- 17 Strength losses of CJ1, CJ2, and CJ3 compared to CJ0 (Bekem Kara. 2021)

Yehia, (2020) investigated the flexural behavior of slab consisting of two-layers reinforced concrete that is high in strength in the locations of compression and concrete that is normal in strength in the locations of tension by effecting delay overlap time between two-layer concrete (15 minutes and 60 minutes). Two slab specimens with dimensions (500 * 150 * 3200) mm were cast shown in Fig. (2-18) after 15 minutes second layer of HSC was placed over the first layer of NSC for the first slab (S1), and for the second slab (S2) after 60 minutes second layer HSC was placed over first layer NSC. With increasing overlap time from 15 minutes for S1 to 60 minutes for S2 the ultimate load increased by 53.3%. Also, the yielding load increased by 36.6% for S2 than S1. Before slab S2 reached the yielding load, slab S1 reached the maximum load (70.15 kN) (78.66 kN). Therefore, using the HSC at the compression zone with a 60-minute time overlap between casting the two layers indicates a significant improvement.

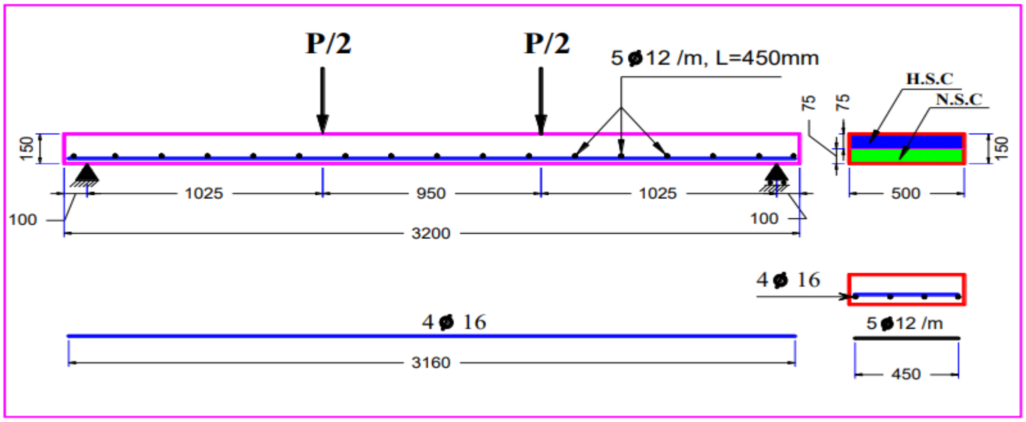

Fig. 2-18 Details of specimens (Yehia, 2020)

Zega et al. (2021) studied the compressive and flexural strength of the cold joint in concrete. The waiting time between first concrete and the second concrete (cold joints) was two hours to four hours, respectively. Cold joints were tested for the strength in compression and flexural strength in both the vertical and horizontal directions shown in Fig. (2-19). the dimension of the cube specimens was $100 \times 100 \times 100$ mm and used for strength in compression testing was performed. Normal concrete with a compressive strength of 35 MPa, concrete with a strength that is high in compression using the superplasticizer, and concrete containing polypropylene fiber as an additional material also were used in this investigation. At 3, 7, 14, and 28 days, compressive and flexural strength testing was conducted.

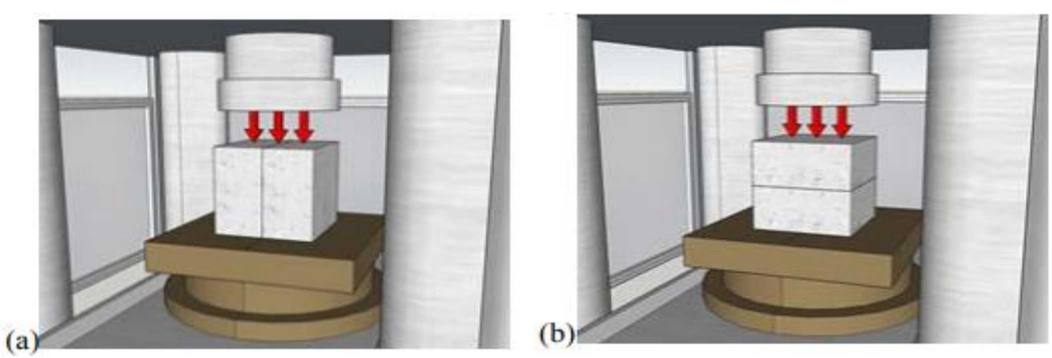

Fig. 2-19 Compressive strength test (a) Vertical direction (b) horizontal direction (Yehia, 2020)

The results from the lab work indicated that specimens with a cold joint connection in normal concrete, as well as concrete with a superplasticizer (high early compressive strength), have lower quality (flexural and compressive), although concrete with fiber has a higher strength than concrete that is normal and has no joints (cold joint connection), shown in Fig. (2-20).

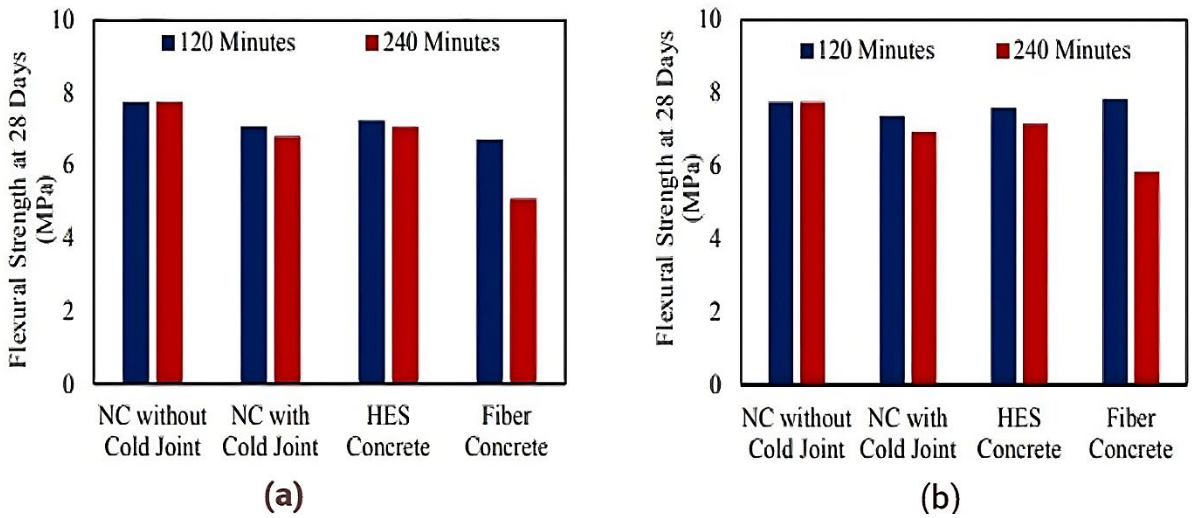

Fig. 2-20 Flexural strength at 28 days (a) Vertical direction (b) Horizontal direction (Yehia, 2020)

2.5 Bending and shear behavior of two-layer different types of concrete

The research by Ataria and Wand (2019) shows the results from a lab work, investigates the behavior of a reinforced concrete beam that has a simple support in shear and bending moment, which made with two layers of concrete, each concrete has different concretes in strength. The top (1/3) of total section depth layer of concrete is of higher grade, and the bottom (2/3) layer of rubber recycled aggregate concrete is of low grade, in tension. A total of eight simply supported reinforced concrete beams were examined, with six bending resistance (bending tests) and two of them for shear resistance (shear test). The beam has dimensions of 150 mm × 150 mm × 1500 mm. The results show that the two-layer beam has the same bending resistance the control reinforced concrete beam made entirely of higher-grade concrete compared with two-layer beam has lower shear resistance than the control beam in beams without shear reinforcement, Figs. (2-21) and (2-22) showed the failure mode of the bending and shear respectively. Fig. (2-23) shows the load-deflection curves of bending test beams.

Fig. 2-21 The failure patterns in bending of the beams (Ataria and Wang, 2019)

Fig. 2-22 The failure patterns in shear of the investigated beams (Ataria and Wang, 2019)

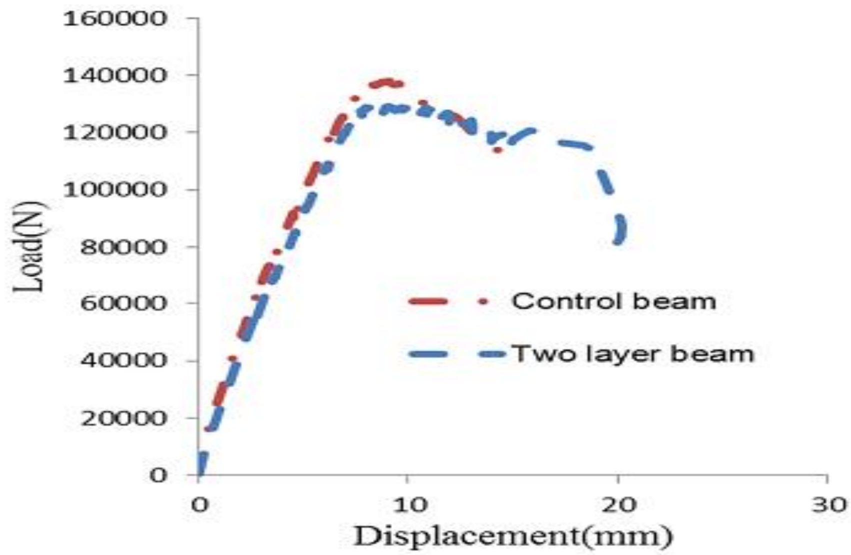

Fig. 2-23 Curves of load verses displacements for the tested beam in bending (Ataria and Wang, 2019)

Butean and Heghes, (2020) compared the flexural behavior of a two-layer high-strength reinforced concrete beam with a single-layer high-strength reinforced concrete beam. The experimental program consisted of a reinforced concrete beam with two different concrete grades, as well as constructing a reinforced concrete beam of the high concrete grade to compare the flexural of the two-layer beam with the single-layer beam. The single-layer beam (CB 1-1) had a mean compressive strength of approximately 110 MPa, whereas the two-layer beam (CB 1-2) had a mean compressive strength of 80 MPa for the tension zone and 110 MPa for the compression zone. Both beams have a section of 120x240mm and a constant length of L=2000mm. The transversal reinforcement was the same for both beams, with stirrups Φ6mm @100mm at the ends and Φ6mm@150mm at the middle. The behavior was similar for both beams as a braking force: 137 kN for beam CB 1-1 and 139 kN for beam CB 1-2, as well as the deflections. Working beam stages were similar, the first visible crack appeared on the same loading (25 kN), and the recommended deflection limit l/250 appeared between 100-110 kN load, representing approximately 75% of the maximum load. As shown in Fig. (2-24).

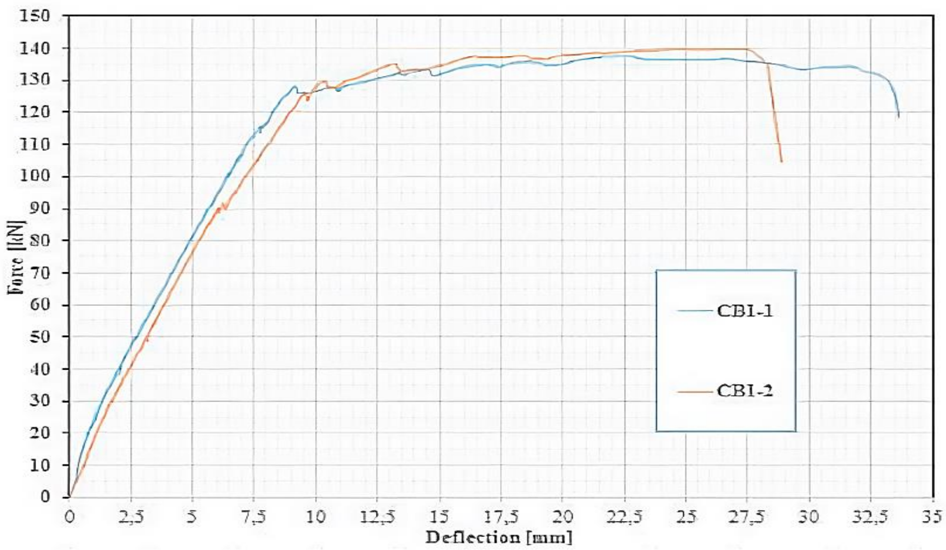

Fig. 2-24 Load deflection curve of CB1-1 and CB1-2 (Butean and Heghes, 2020)

Pratama et al. (2019) study the behavior of the functionally graded (FGC). Four beams with 120 x 240 x 2200 mm were produced with concrete strengths of 25 MPa one layer configuration (NA), 30 MPa (NB), 30-20 MPa two-layer configuration (GBA), and 30-20-30 MPa three-layer configuration (GBAB). A four-point bending method was used in the lab to evaluate the specimens. The illustration of the concrete casting configuration for GBA and GBAB is displayed in Figure (2.25). The results show that the GBAB had 0.83 % higher maximum loads than the GBA; the GBAB deflected 29.52 % less than the GBA; the GBAB had stiffness 12.03 % higher than the GBA; the GBAB had higher resulting yield points and ultimate state than the GBA at the moment-curvature relationship; and the GBAB was 20.06 % less ductile than the GBA.

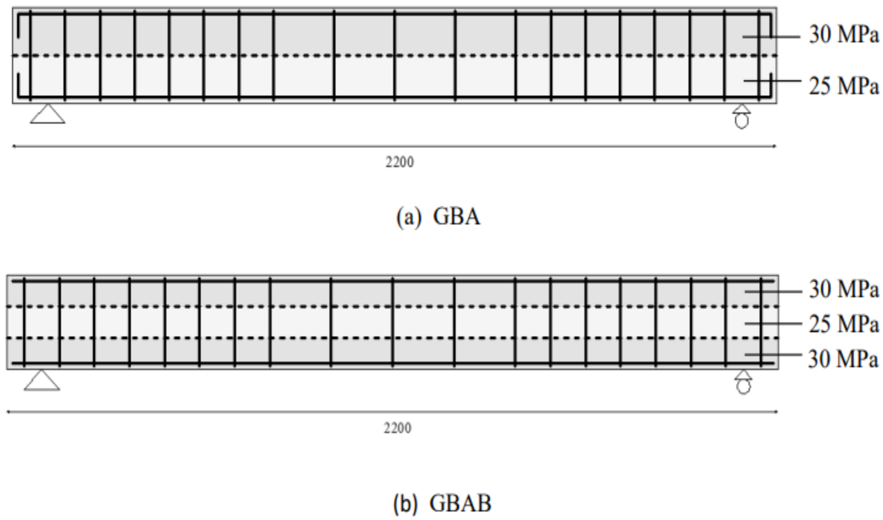

Fig. 2-25 Casting configuration of (a) GBA and (b) GBAB (Pratama et al. 2019)

2.6 Summary

Based on the previous literature review, the following points can be made:

1. Previous studies focused on the behavior of crack pattern and deflection of two-layer beams consisting of two-layer reinforced concrete beams made of normal strength concrete and lightweight concrete, or two-layer reinforced concrete beams using steel fiber high strength concrete in compression zone and normal concrete in tension zone without analysis or improved new equations of bending moment and shear strength and some study investigate the bond strength and cold joint of tow-layers reinforced concrete beams.
2. There is not cover properly of literature on the flexural of beams made of two layers of concrete, one of the layers is using normal strength concrete in tension zone and using high strength concrete in compression zone.

CHAPTER THREE

EXPERIMENTAL WORK

3.1 Introduction

The main purpose of this chapter is to present a comprehensive description of the experimental program carried out in the present thesis. This chapter describes the dimensions and reinforcement details of all groups of the test specimens. The proportions of mix design of concrete which were used herein have been conducted. In addition, the characteristics of the materials such as cement, mixing water, coarse and fine aggregates, silica fume, Superplasticizer, and reinforcement are evaluated. Moreover, the loading setup, the measuring apparatus, and the testing procedures are also described in this chapter.

3.2 Description of the test specimens

The experimental work is planned and carried out to achieve the study objectives. The focus of the experiments was the bending and shear behavior of two layers of reinforced concrete beams. The experimental program consists of nineteen beams in total, the beams are rectangular in shape with the cross-section dimensions of (125 x 250) mm and the length of the beam is 1200 mm, all prepared for this work, which was sorted into six groups, the beams are reinforced with (4Ø12mm) longitudinal reinforcement, and (Ø8mm) bar used for transverse reinforcement (stirrups).

3.3 Material Properties

3.3.1 Cement

Mass's Ordinary Portland Cement is used to design mixes of concrete for both concretes, first is normal strength and the second is high strength. The properties of cement were tested physically and chemically and verified according to the specifications of (ASTM - C150). As shown in Table (3-1 and 3-2).

3.3.2 Fine Aggregate (Sand)

Locally available sand from Aski-Kalak source was used. The sand is cleaned, and the nominal particle size was (4.75 mm), specific gravity of fine aggregate was (2.55), and the grading curve of the fine aggregate is shown in Fig. (3-1). Also tested within the upper and lower limits of the (ASTM - C33) specification. Which are displayed in Table (3-3).

3.3.3 Coarse Aggregate

The coarse aggregate used in the present experimental program was rounded river coarse aggregate, the locally available gravel was utilized, the specific gravity of coarse aggregate was (2.69), and the bulk density of coarse aggregate was (1695 kg/m^3), the sieve analysis of the aggregate of maximum nominal size (12.5 mm) is shown in Fig. (3-2), and the test result within the allowable limits of the specification of (ASTM-C33). As shown in Tables (3-4).

3.3.4 Water

The water used during the experimental program in producing concrete and in curing all beams specimens, was tap clean drinking fresh water free from impurities.

Table 3-1 Physical properties of the cement

Physical Tests	Results	ASTM C150-10
Initial setting time	120 min.	At least to be 45min.
Final setting time	305 min.	Not more than 600min.
Compressive strength 3 days age	22.68	14.7 MPa, a lower limit
Compressive strength 28 days age	32.25	22.5 MPa, a lower limit
Specific gravity	3.15	
Density	1400 kg/m^3	

Table 3-2 Chemical tests for cement investigated by Directorate of Erbil Construction Laboratory

Chemical tests	Results	Specification
Lost in ignition	2.22%	4% Max.
Insoluble material	0.5%	1.5 Max.
SiO2	20%	
Cao	63.5%	
$AL2O3$	4%	
$Fe2O2$	4.5%	
MgO	2.15%	5% Max.
SO3	2.1%	28% Max.
C3A	3%	
L.S.F	0.97%	(0.66 – 1.02)
C3S	67.2%	
C2S	6.9%	
C4AF	13.7%	

Table 3-3 Grading of the Fine Aggregates (sand)

Sieve size (mm)	Passing %	ASTM Limits	
		Lower	Upper
9.5	100	100	100
4.75	95.334	95	100
2.36	82.334	80	100
1.18	68.987	50	85
0.6	50.536	25	60
0.3	19.207	5	30
0.15	3.343	0	10

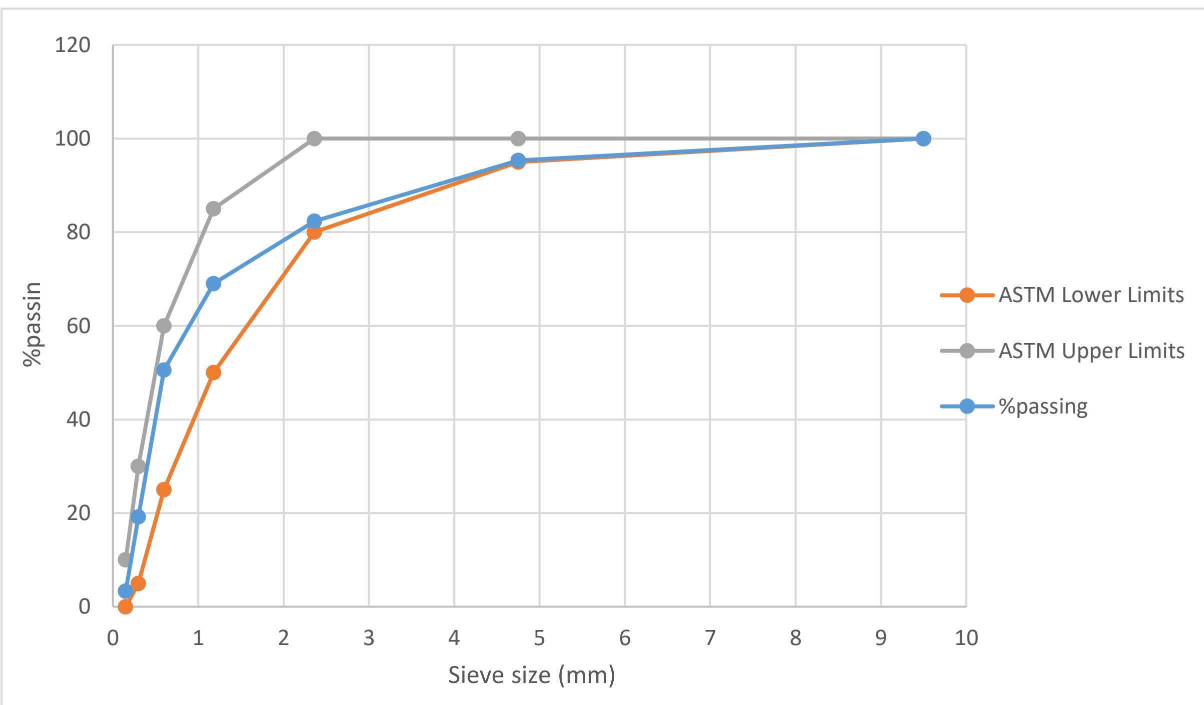

Fig.3-1 The fine aggregate curve of grading is falling with in ASTM limits

Table 3-4 Grading of the Coarse Aggregates

Sieve size (mm)	Passing %	ASTM Limits	
		Lower	Upper
19	100	100	100
12.5	91.64	90	100
9.5	52.37	40	70
4.75	3.02	0	15
2.36	0.18	0	5

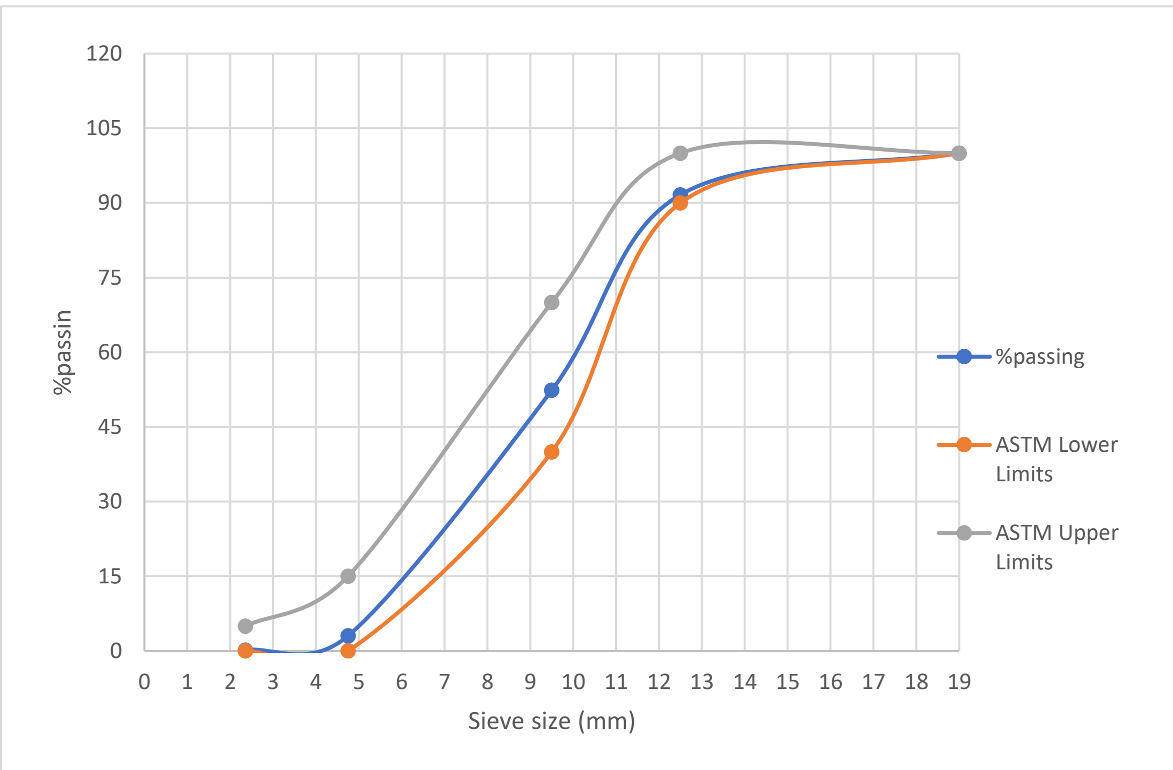

Fig. 3-2 Grading curve for coarse aggregate with ASTM limits

3.3.5 Silica Fume

Silica Fume is a binder material that can be added directly to concrete or combined with cement. It is used to enhance concrete properties. The silica fume used in the present study is in the production of ECA MICRO SILICA-D which has the properties of increasing compressive and flexural strength, reducing permeability, and increasing durability. The physical and chemical properties of the silica fume are tested and checked according to the specification of (ASTM-C1240). The physical and chemical properties are shown in Tables (3-5) and (3.6).

Table 3-5 Silica fume physical properties

Physical properties	Results	ASTM C1240 (2017)
Appearance	Ultra-fine amorphous light to dark grey, colored powder	Light to dark gray
Specific Gravity	2.25±15 % at 20°C	Approximately 2.2
Bulk Density	≥650 kg/m3	(130-430) kg/m^3
Freezing Point	N.A	
Air Entrainment	Nil.	

Table 3-6 Chemical Analysis of Silica fume

Cement contents %	Results	ASTM C1240 (2017)
SiO_2	90 % min	85 min.
Sulphate Content	<1.0% as S03	

3.3.6 Superplasticizer

Superplasticizer is the most popular admixture to the concrete mix. It is available generally in a liquid. The superplasticizer used in the present study is in the production of Sika ® ViscoCrete ® -1316 Hi-Tech meets the requirements of (ASTM C-494). It is a high-range water-reducing, retarding, and slump retaining admixture. It is added to the mix with a ratio of about (0.1% to 2%) of cement weight. Superplasticizer was added to the mix on-site to bring the workability to the desired level, increase the liquidity of the mix while no change in (W/C) ratio, highly improve the strength of the fresh concrete, and enhance the properties of hardened concrete to have the required High Strength Concrete (HSC). The main role of a Superplasticizer in the concrete mix is to separate any accumulative cement particles from each other and so make a homogenous distribution of water in the mix and make good contact between the water and the cement particles to increase the workability of the concrete mix.

3.3.7 Reinforcing Steel

Deformed steel bars of 12mm and 8mm diameter were used. 12 mm diameter bars are used for the main reinforcement, and 8 mm bars are used for stirrups. The strength properties of the steel bars have been determined boom testing three samples of each type by hydraulic machine to test tensile (600 kN), as shown in Fig. (3-3). The testing results are shown in Table (3-7)

Fig. 3-3 Tensile testing machine for steel bar

Table 3-7 Properties of reinforcing steel for the experiment

No.	Diameter (mm)	Lo (mm)	L_1 (mm)	fy (yield) (MPa)	Avg. (fy) MPa	Fu (ult) (MPa)	Avg. (Fu) (MPa)	Elongation %
1	8	202	224	445.9	443.87	640.92	637.47	22
	8	202	226	441.9		634.95		24
	8	202	225	443.8		636.56		23
2	12	202	222	555.6	568.27	703.29	736.02	20
	12	202	225	548.5		714.79		23
	12	202	221	600.7		789.99		19

3.4 Mixing and Mix Proportions

According to the American Concrete Institute Code (ACI) 318M-19, several mixes were tried to design the concrete with the nominal size of coarse aggregate (12.5mm) to obtain the concrete compressive strength, thirteen trial mixes were done to get different classes of strengths, for each concrete mix, six 150 mm^3 cubes were cast three of them were tested at age of 7 and 28 days. The cubes were subjected to a standard curing regime at 20° C, and then normally cured in the laboratory temperature and humidity until 28 days. The marked mix proportions from Table (3-8) and were selected to obtain the required different concrete compressive strength and compositions for a series of remaining tests in the planned schedule; the amounts of materials required for (1 m^3) of concrete in each mix, are listed in Table (3-9). For determining the HSC compressive strength 150 mm^3 cubes were used according to BS 1881 part 116.

Table 3-8 Trial Mixes (by Weight)

Trail No.	fc' (MPa)	Binders		Aggregate		% SP	Water	
		C	SF	S	G		w/c	w/b
1	30	1	-	1.65	2	-	0.45	
2		1	-	1.8	2.2	-	0.48	
3		1	-	2.35	2.75	-	0.51	
4*		1	-	2.5	3	-	0.53	
5	45	1	-	1.25	1.75	-	0.4	
6		1	-	1.22	1.58	-	0.38	
7*		1	-	1.2	1.7	-	0.36	

8		0.90	0.1	1.35	2	0.4		0.34
9	60	1	-	1	1.6	0.6	0.3	
10*		1	-	1	1.65	0.42	0.32	
11		0.89	0.11	1.18	1.78	0.7		0.27
12	75	0.88	0.12	0.75	1.34	0.9		0.24
13*		0.9	0.1	0.8	1.5	0.62		0.25

* Mix proportions selected for a series of planned tests.

C: Cement, SF: Silica Fume, G: Gravel, S: Sand, SP: Super-Plasticizer, W: Water, b: Binders (cementations materials).

Table 3-9 Selected concrete mixes per one meter cube of concrete

Trail No.	fc' (MPa)	C	SF	S	G	SP	Water
		Kg				Liter/m^3	
4	30	325	-	812	975	-	172
7	45	550	-	655	940	-	198
10	60	600	-	600	990	2.52	192
13	75	650	65	572	1072	4.03	178

3.5 Beam Formworks

The formwork was made of plywood block sheets of dimensions (1220×440×18) mm. Later, molds were created from these plywood block sheets, and the size of the beam formworks are (125 × 250 ×1200mm). Before putting the reinforcement cage and casting, the mold was cleaned and oiled. Fig. (3-4) depicts the formwork for beam specimens.

Fig. 3-4 Molds of the tested specimens

3.6 Cages and Reinforced Placement

All specimens are provided with steel reinforcement with different diameters and types. High tensile steel bars with 4Φ12 mm diameter was used for the longitudinal top and bottom bars, respectively, two at the bottom and two at the top. Steel bars of 8 mm diameter were used for stirrups. Thirteen beams with stirrup spacing of 150 mm were designed, one beam with stirrup spacings of 100 mm was designed, and one beam had 200 mm stirrup spacings. This is in addition to another four of the beams that had no stirrups. Stirrups are shown in Fig (3-5). The properties of reinforcing steel bars obtained from results of tension tests carried out for three samples of bars for each diameter are shown in Table (3-7). Bottom longitudinal steel reinforcement consisted of straight bars with a 90- degree hook to provide adequate anchorage.

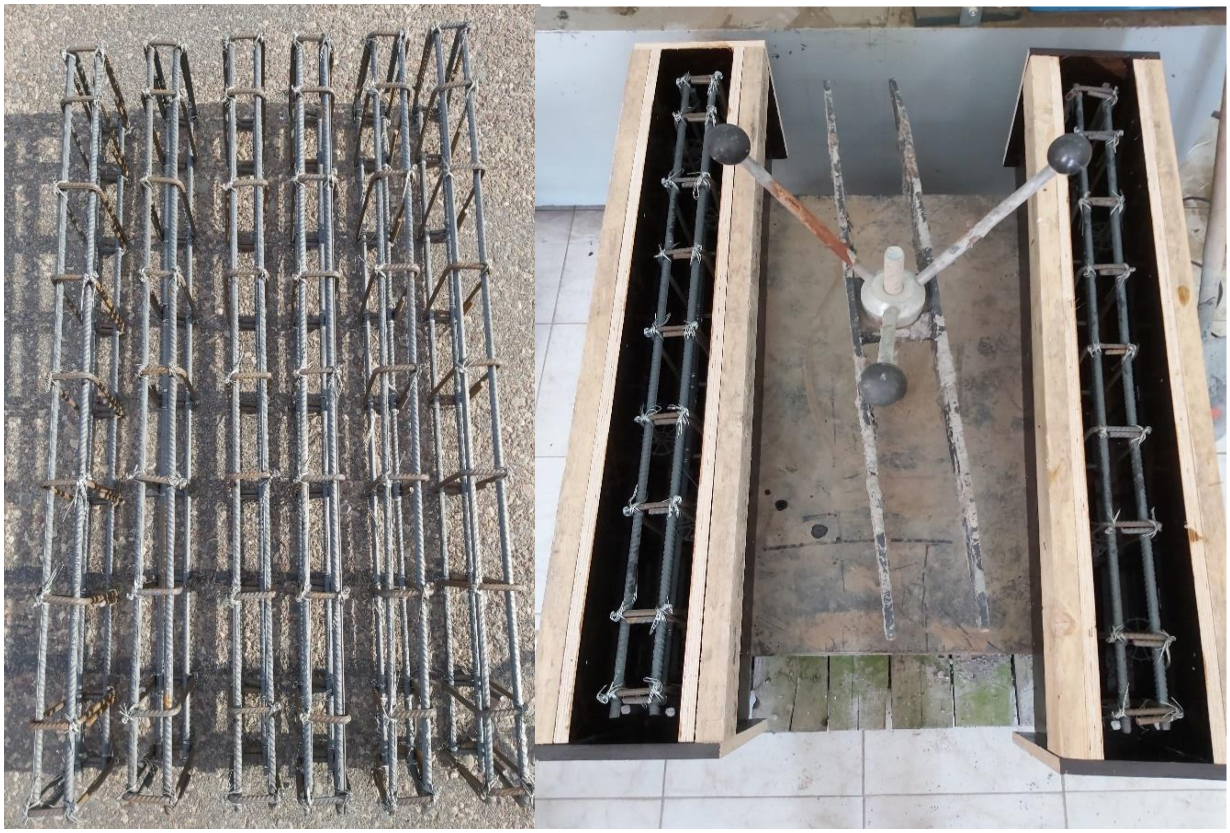

Fig. 3-5 Reinforcement cages and molds

3.7 Casting of Concrete

All beams were mixed by Mechanical Rotary Drum Mixer. The molds were cleaned and then brush oiled to avoid sticking concrete to the inside face of the mold. The steel cage was set carefully inside the mold, and the dimensions of the two-layer beams were 125 × 150 × 1200 mm shown in Fig (3-6). The beams' production included two stages. In the first stage, normal strength concrete (NSC) was made and the lower layer (tensile zone) of the beams was cast. After casting, the first layer of the beams was vibrated for 15 sec on a vibrating table. The second stage included making high-strength concrete (HSC) and casting the upper layer of the beams (compressed zone) and the overlap time arrange between 15 minutes till 100 minutes. After casting the second layer the beams were again vibrated for 10 sec. Three cubes of (150 × 150 × 150) mm, were cast to determine compressive strength at the age 28 days was determined.

Fig. 3-6 Casting of specimens and Mechanical Rotary Drum Mixer

3.8 Vibrating Table

Concrete Vibrating Table is used for consolidating fresh concrete when forming a cylinder, cube, and beam molds, according to the ASTM C192/C192M. Using the electrical vibrator, shown in Fig (3-7), the first layer and second layers of fresh concrete were subjected to 15 seconds and 10 seconds of vibration, respectively.

Fig. 3-7 Electrical vibration of specimens

3.9 Curing

After casting, the samples were kept in the molds for 24 hours before removing the molds and keeping the samples for curing. ASTM-C31(2007) instructions applied for curing by covering the samples and specimens with moist burlap. This is shown in Fig (3-8).

Fig. 3-8 Curing of specimens

3.10 Concrete Mechanical Properties

3.10.1 Compressive Strength

Compressive strength is the capacity of a material or structure to resist or withstand compression. The compressive strength of concrete is given in terms of the characteristic compressive strength of 150 mm size cubes tested at 28 days (f_{ck})- as per British Standards, (ACI standards use a cylinder of a diameter of 150 mm and height of 300 mm). Three cubes with dimensions of (150 X 150 X 150) mm casted with concrete. These cubes were tested at 28 days. This process included the beams. Shown in Fig. (3-9). The results of trial mixes of compressive strength for normal and high strength concrete are shown in Table (3-10).

Table 3-10 Compressive Strength of Control Mixes (MPa)

Trial No.	f_{cu} (MPa)	Slump (mm)	f_{cu} (MPa)		fc' (MPa)	
			7 days	28 days	7 days	28 days
1	C 30		44.14	53.62	35.312	42.9
2			40.76	48.73	32.61	39
3			36.41	44.29	29.128	35.432
4*		110	33.52	40.95	26.816	32.76
5	C 45		37.2	49.73	31.62	42.27
6			43.03	53.16	36.575	45.186
7*		95	46.74	57.53	39.729	48.9
8	C 60		53.34	62.73	45.339	53.320
9			65.9	73.64	56.015	62.59
10*		240	60.68	68.56	51.578	58.276
11	C 75		68.32	77.95	58.072	66.257
12			82.64	91.57	70.244	77.834
13*		250	74.38	83.97	63.223	71.374

fc' = compressive strength of cylinder specimen

f_{cu} = compressive strength of cubes specimen

fc' = $f_{cu} \times 0.80$ for normal strength concrete (Elwell and Fu, 1995)

fc' = $f_{cu} \times 0.85$ for high strength concrete (Elwell and Fu, 1995)

Fig. 3-9 Compressive strength of specimens

3.10.2 Splitting Tensile Strength

For each sample beam, three cylinders casted for testing tensile strength. These cylinders were Φ10 mm diameter and 200 mm height. The tests were performed according to ASTM (ASTM-C469). Moreover, the YKSEL material testing equipment with the capacity of 2000 kN was used for the performance of the splitting tensile test, as shown in Fig (3-10).

Fig. 3-10 Splitting test of specimens

3.10.3 Slump Test

Generally, the concrete slump value is used to determine workability, which reflects the water-cement ratio. However, the concrete slump value is affected by a variety of elements such as material qualities, mixing methods, dosage, and admixtures, among others. According to ASTM C 143 (2007), the purpose of a concrete slump test, also known as a slump cone test, is to measure the workability or consistency of a concrete mix made in the laboratory is presented in Table (3-10). Fig (3-11) shows the experimental slump.

Fig. 3-11 Slump of concrete

3.11 Experimental Program

The experimental program consists of nineteen beams that are rectangular in the cross-section, beams are supported simply and tested under a four-point loads. The beams are divided into groups, some groups have transverse reinforcement (stirrups), and some beams are with no transverse reinforcement. The beams are made of concrete with different compressive strengths. All the beams are made with same dimensions of (125*250*1200) mm shown in Fig (3-12), with maximum nominal aggregate sizes of (12.5) used in the concrete mixes. The specimen beams were divided into six groups shown in Table (3-11), the beams are reinforced with longitudinal reinforcement (4Ø12mm), and the reinforcement used for stirrups was (Ø8mm). In beams B1 to B3, the beams were subjected to the effect of the ratio of compressive strength of high strength to normal strength with stirrups, group (A) as shown in Fig. (3-13). Beams B4 to B7 are subjected to the effect of overlap time, group (B) as shown in Fig (3-13). Beams B8 to B11 are subjected to the effect of layer thickness group (C) shown in Fig (3-14). Group (D) consist of beams (B12, B13, and B2) to study the effect of shear span ratio (a/d), shown in Fig. (3-15). Beams B15 to B 17 are subjected to the effect of the concrete compressive strength ratio without stirrups group (E). The last beams, B18 and B19 are subjected to the effect of stirrups space group (F) shown in Fig. (3-16). The loading process for all the beams was videoed for recording the crack behavior of the beams.

Table 3-11 Experimental program of beam specimens

Groups	Beam No	$fc`_{NSC}$ (MPa)	$fc`_{HSC}$ (MPa)	$\frac{fc`HSC}{fc`NSC}$	h_{HSc} (mm)	h_{NSc} (mm)	$\frac{h_{HSc}}{h_{total}}$	Overlap time (min)	$\frac{a}{d}$	Note
A	1	30	45	1.5	125	125	0.5	30	2	Effect of $\frac{f\bar{c}_{HSc}}{f\bar{c}_{NSc}}$
	2	30	60	2	125	125	0.5	30	2	
	3	30	75	2.5	125	125	0.5	30	2	
B	4	30	60	2	125	125	0.5	15	2	Effect of overlap time
	2	30	60	2	125	125	0.5	30	2	
	5	30	60	2	125	125	0.5	60	2	
	6	30	60	2	125	125	0.5	80	2	
	7	30	60	2	125	125	0.5	100	2	

C	8	30	-	-	-	250	-		2	Full NSC
	9	30	60	2	62.5	187.5	0.25	30	2	Effect of layer thickness
	2	30	60	2	125	125	0.5	30	2	
	10	30	60	2	187.5	62.5	0.75	30	2	
	11	30	60	2	250	-	1	-	2	Full HSc
D	12	30	60	2	125	125	0.5	30	1	Effect of ratio $\frac{a}{d}$
	13	30	60	2	125	125	0.5	30	1.5	
	2	30	60	2	125	125	0.5	30	2	
E	14	30	-	-	-	250	-	-	2	Control beam
	15	30	45	1.5	125	125	0.5	30	2	Effect of $\frac{f\bar{c}_{HSc}}{f\bar{c}_{NSc}}$
	16	30	60	2	125	125	0.5	30	2	
	17	30	75	2.5	125	125	0.5	30	2	
										Ø8 mm stirrups spacing
F	16	30	60	2	125	125	0.5	30	2	0
	18	30	60	2	125	125	0.5	30	2	100
	2	30	60	2	125	125	0.5	30	2	150
	19	30	60	2	125	125	0.5	30	2	200

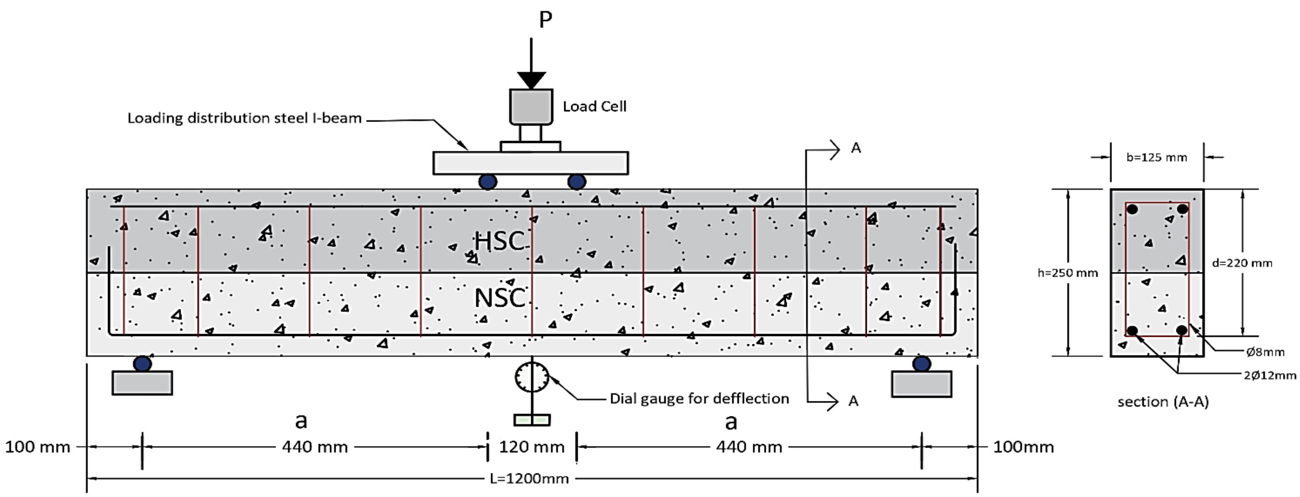

Fig. 3-12 Longitudinal and transverse cross section view

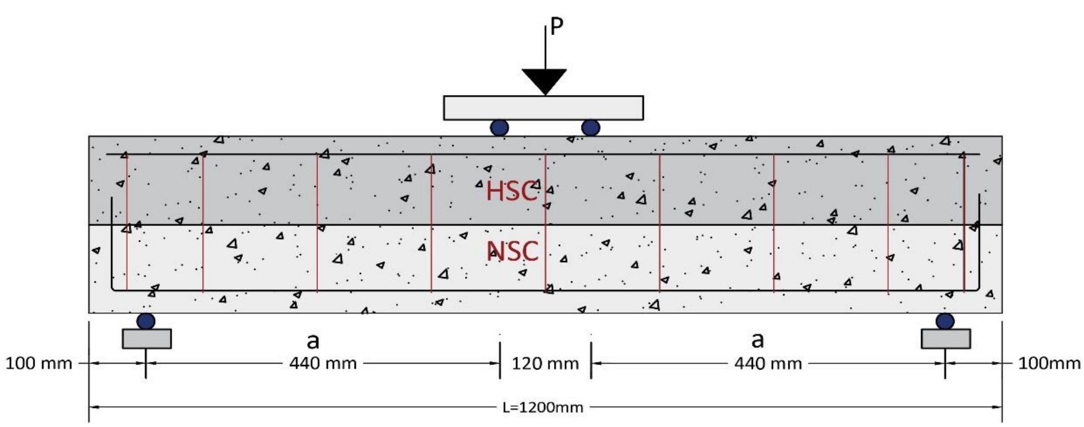

Fig. 3-13 Details of beams for groups (A, B)

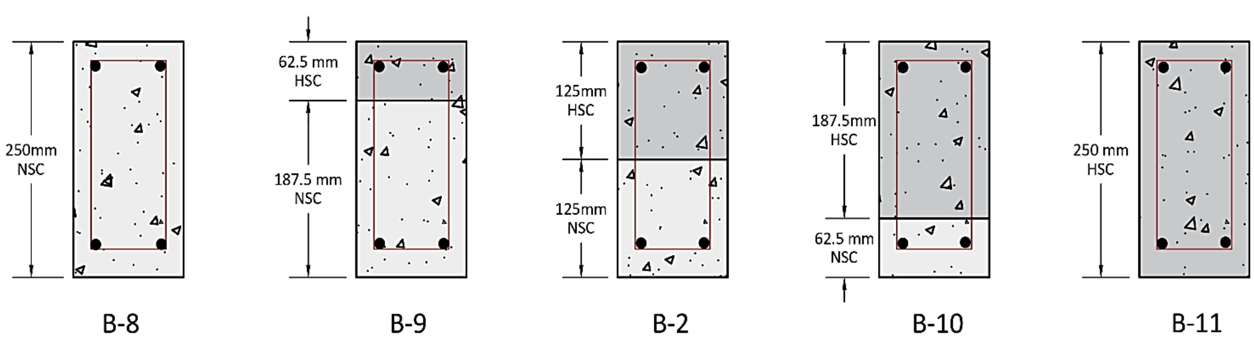

Fig. 3-14 Cross-section details of distribution concrete layers group (C)

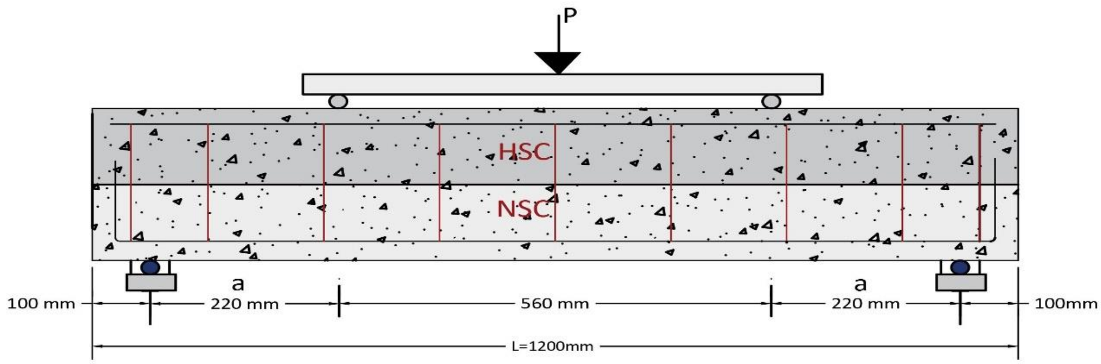

longitudinal section B-12

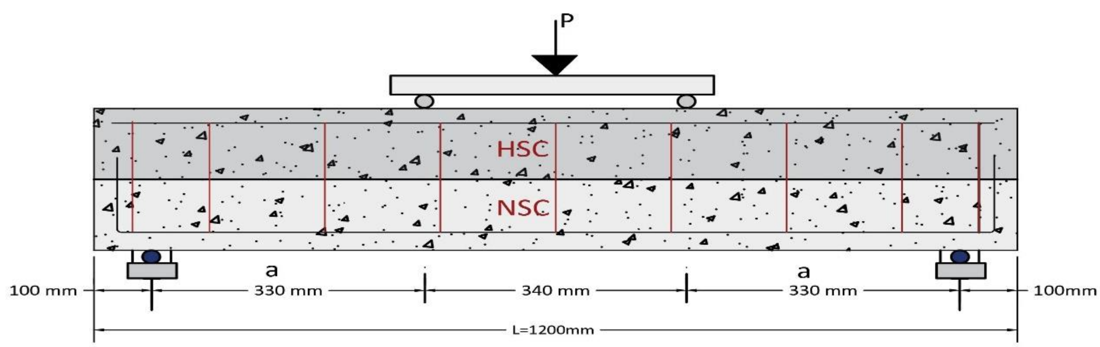

longitudinal section B-13

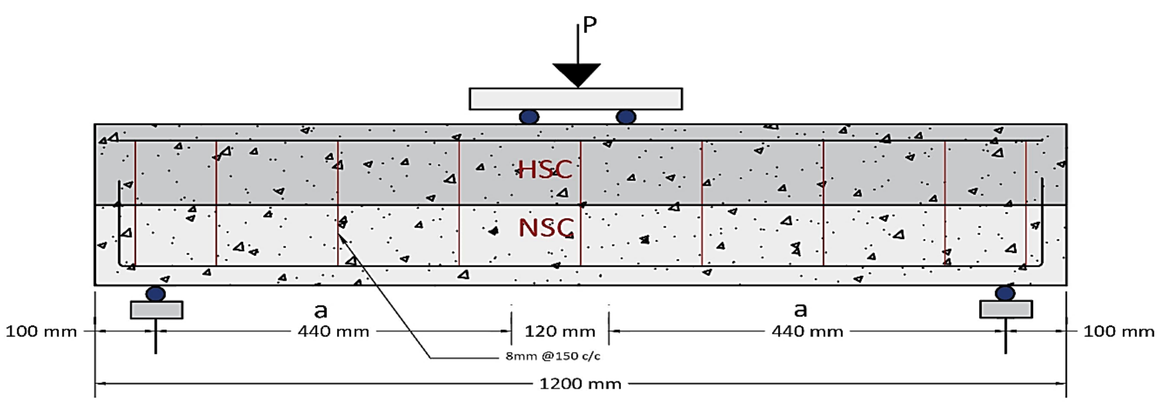

longitudinal section B-2

Fig. 3-15 Details of beams for group (D)

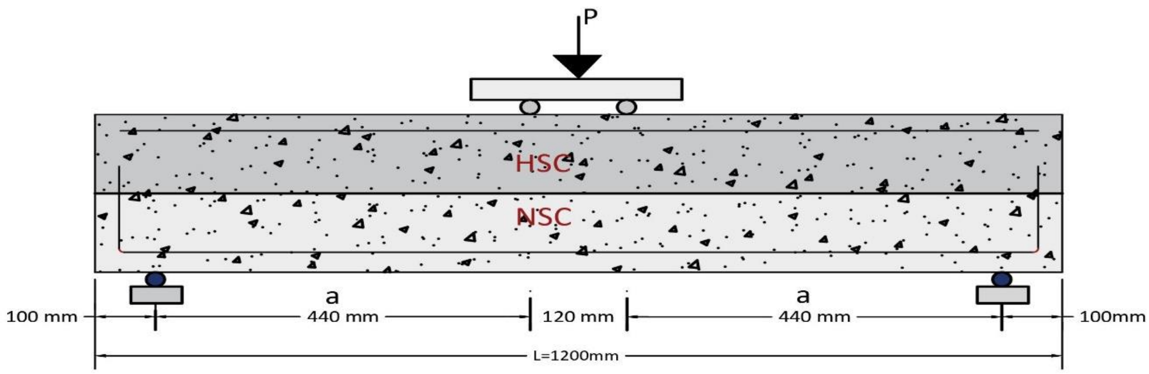

longitudinal section B (14,15,16,and 17)

Fig. 3-16 Details of beams for group (E)

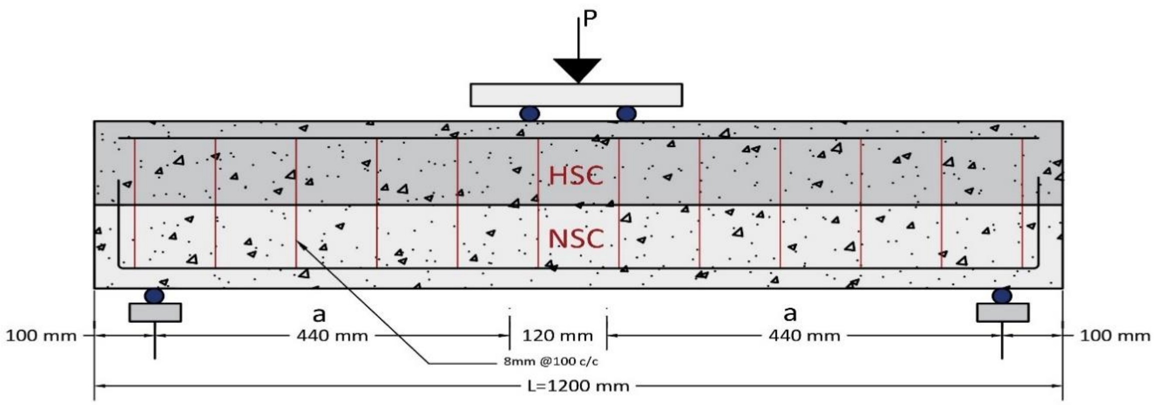

longitudinal section B-18

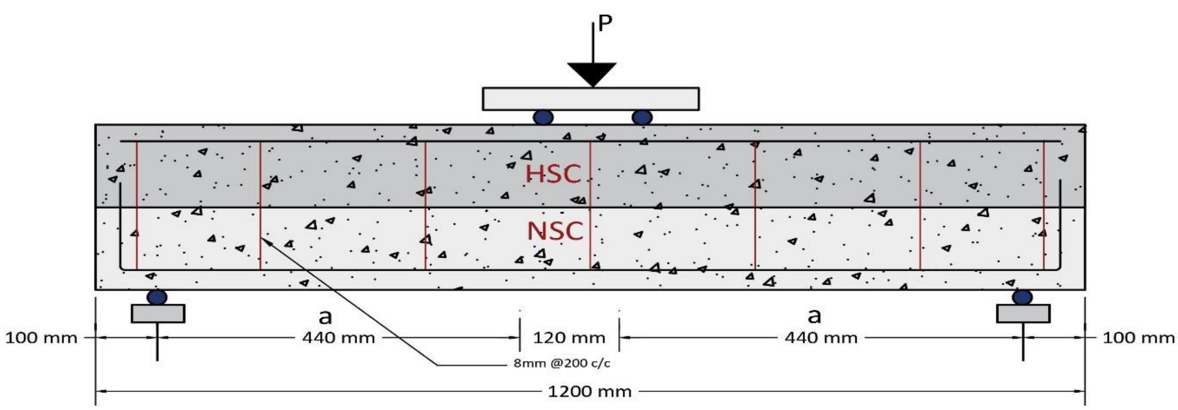

longitudinal section B-19

Fig. 3-17 Details of beams for group (F)

3.12 Loading setup

The beams were tested in the College of Engineering at Salahaddin University (Civil Engineering Laboratory). All the beams were tested at the same age. when curing was completed. The specimens were placed at the laboratory temperature and were painted white with gridlines so that the cracks could be seen quickly and clearly, and the crack pattern could be marked, as shown in Fig. (3-18). The specimens were tested up to failure using a compression-testing machine of 2000 kN capacity and 0.10 kN accuracy. A 2000 kN load cell was used to calibrate the machine. The Load was applied to the center of the distribution steel I-beam which is also divided into two-point loads as shown in Fig. (3-19). The dial gauge had an accurate count of 0.01mm for measuring displacements placed under the center of the beams.

Fig. 3-18 Beam specimens painted with a white color

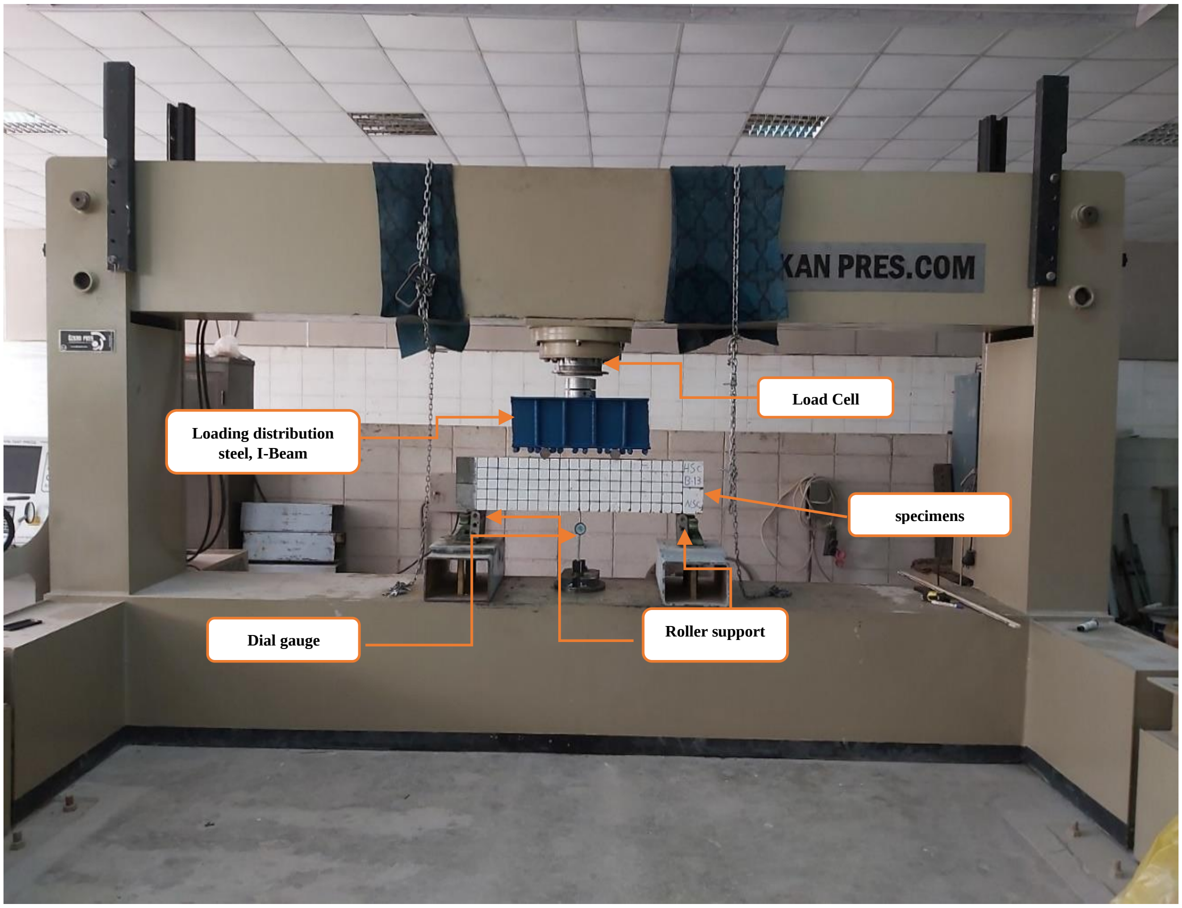

Fig. 3-19 Setup specimens with the loading frame

CHAPTER FOUR

RESULTS AND DISCUSSION

4.1 Introduction

In this chapter, the experimental results of nineteen reinforced concrete beams are included. The beams were subjected to two equal point loads. The primary hypothesis of this study is on the flexural and shear behavior of reinforced concrete beams consisting of two layers with different concrete strengths (grades). First, flexural cracking shear (Vc_1), diagonal shear force (Vc), ultimate shear strength (Vu), bending moment, and maximum deflection at the failure of each beam are described in this chapter.

4.2 Properties of concrete specimens

4.2.1 Concrete Compressive Strength

According to (BS 1881 116 1983 Testing Concrete. Method for Determination of Compressive Strength of Concrete Cubes) three cubes (150 * 150 * 150) mm were tested for each beam and taken an average compressive strength. Table (4-1) shows the result of the concrete compressive strength of all beams.

Table 4-1 Concrete compressive strength of control specimens

Beam No.	Target f_{cu} (MPa)	Average f_{cu} (MPa)	fc' (MPa)
B1 & B15	C45	59.12	47.3
	C30	43.18	34.54
B2 & B16	C60	74.57	63.38
	C30	41.88	33.50

B3 & B17	C75	85.89	73
	C30	44.58	35.66
B4 & B8	C60	71.44	60.73
	C30	42.34	33.87
B5	C60	69.98	59.48
	C30	43.41	34.73
B6 & B14	C60	73.82	62.75
	C30	44.41	35.52
B7 & B11	C60	73.8	62.47
	C30	43.40	34.72
B9 & B10	C60	72.65	61.75
	C30	42.71	34.16
B12 & B13	C60	71.17	60.49
	C30	43.35	34.68
B18 & B19	C60	73.58	62.54
	C30	42.68	34.14

4.2.2 Splitting Tensile Strength

According to ASTM (ASTM-C496), for each beam, three (100×200) mm cylinders were tested to determine tensile splitting strength, the results of the splitting tensile strength of concrete are shown in Table (4-2).

f_{sp}= (2*P)/(πLd) (4.1)

Where: f_{sp} = splitting tensile strength (MPa) P = maximum applied load (kN)

L = length (mm) d = depth (mm)

Table 4-2 Splitting Tensile Strength of control specimens

Beam No.	$f_c^{\backslash}$ (MPa)	Load (kN)	Average Failure load (kN)	L (mm)	D (mm)	f_{sp} (MPa)
B1 & B 15	C 45	110.27	110.27	200	100	3.51
		104.33		200	100	
		116.20		200	100	
	C 30	107.63	100.27	200	100	3.19
		91.70		200	100	
		101.80		200	100	
B2 & B 16	C 60	132.42	122.94	200	100	3.91
		115.75		200	100	
		120.65		1200	100	
	C 30	98.60	105.90	200	100	3.37
		112.35		200	100	
		106.75		200	100	
B3 & B 17	C 75	145.72	145.04	200	100	4.61
		152.30		200	100	
		137.10		200	100	
	C 30	97.30	111.40	200	100	3.54
		121.30		200	100	
		115.6		200	100	
B4 & B 8	C 60	118.22	124.79	200	100	3.97
		125.43		200	100	
		130.73		200	100	
	C 30	110.63	102.56	200	100	3.26
		95.83		200	100	

		101.22		200	100	
B5	C60	118.30	119.82	200	100	3.81
		125.72		200	100	
		115.45		200	100	
	C30	115.80	107.02	200	100	3.40
		99.82		200	100	
		105.46		200	100	
B6 & B14	C60	132.14	125.37	200	100	3.99
		115.85		200	100	
		128.12		200	100	
	C30	112.20	103.85	200	100	3.30
		102.50		200	100	
		96.85		200	100	
B7 & B11	C60	119.20	122.24	200	100	3.89
		113.42		200	100	
		134.12		200	100	
	C30	100.40	101.78	200	100	3.23
		106.20		200	100	
		98.72		200	100	
B9 & B10	C60	117.63	113.05	200	100	3.59
		108.12		200	100	
		113.42		200	100	
	C30	95.68	102	200	100	3.24
		103.12		200	100	
		107.43		200	100	
B12 & B13	C60	119.43	121.87	200	100	3.87
		113.32		200	100	

		132.85		200	100	
	C30	105.42	98.89	200	100	3.14
		98.83		200	100	
		92.42		200	100	
B18 & B19	C60	113.62	115.12	200	100	3.66
		120.42		200	100	
		111.34		200	100	
	C30	91.63	103.52	200	100	3.29
		105.82		200	100	
		113.12		200	100	

4.3 Results and Behavior of Tested Beams

The nineteen specimens were classified into six groups (A, B, C, D, E, and F). A detailed description of the tested beams and testing procedure is given in the Table (3-11) in the previous chapter. Generally, each specimen was tested as a simply supported beam under two equal concentrated loads. The measured loads at failure (Pu), the formation of the first diagonal cracks, and other parametric studies are given in Table (4-3).

Table 4-3 experimental result of all specimens

Groups	**Beam No.**	$\frac{h_{HSC}}{h_{total}}$	**Overlap time (min)**	$\frac{a}{d}$	**fc\`$_{NSC}$ (MPa)**	**fc\`$_{HSC}$ (MPa)**	$\frac{fc`_{HSC}}{fc`_{NSC}}$	**f_{sp} (NSC) (MPa)**	**f_{sp} (HSC) (MPa)**	**P_c (kN)**	**P_u (kN)**	**Vc_1 (kN)**	**V_c (kN)**	**V_u (kN)**	**max δ (mm)**	**Remark**
A	B1	0.5	30	2	34.54	47.3	1.37	3.2	3.51	63.6	136.2	17.8	31.8	68.1	4.01	Effect of $\frac{fc`_{HSC}}{fc`_{NSC}}$
	B2	0.5	30	2	33.5	63.38	1.89	3.37	3.91	72.6	145.3	17.4	36.3	72.65	3.64	
	B3	0.5	30	2	33.14	74.65	2.25	3.54	4.61	75.6	149.4	18.05	37.8	74.7	6.66	
	B8	-	30	2	33.87	-	1	3.26	3.97	55.7	125.7	25.2	27.85	62.85	3.32	Full NSC control beam
B	B8	-	30	2	33.87	-	1	3.26	3.97	55.7	125.7	25.2	27.85	62.85	3.32	Full NSC control beam
	B4	0.5	15	2	33.87	60.73	1.8	3.26	3.97	74.3	145.8	21.5	37.15	72.9	4.68	Effect of overlap time
	B2	0.5	30	2	33.5	63.38	1.89	3.37	3.91	72.6	145.3	17.4	36.3	72.65	3.64	
	B5	0.5	60	2	34.73	59.48	1.72	3.26	3.81	73.4	143.8	18.7	36.7	71.9	3.15	
	B6	0.5	80	2	35.52	62.75	1.77	3.3	3.99	70.5	143	18.55	35.25	71.5	7.54	
	B7	0.5	100	2	34.72	62.47	1.8	3.24	3.89	83.2	142.8	19.7	41.6	71.4	4.93	
C	B8	-	30	2	33.87	-	1	3.26	3.97	55.7	125.7	25.2	27.85	62.85	3.32	Full NSC control beam
	B9	0.25	30	2	34.16	61.75	1.8	3.24	3.59	69.5	127.2	19.3	34.75	63.6	4.03	Effect of layer thickness
	B2	0.5	30	2	33.5	63.38	1.89	3.37	3.91	72.6	145.3	17.4	36.3	72.65	3.64	

	B10	0.75	30	2	34.16	61.75	1.8	3.24	3.59	72.3	139	17.35	36.15	69.5	7.39		
	B11	1	30	2	-	62.47	1	3.24	3.89	82.4	150.4	18.95	41.2	75.2	8.04	Full HSC	
D	B12	0.5	30	1	34.68	60.49	1.75	3.14	3.87	138	289.9	44.7	69	144.95	4.1	Effect of $\frac{a}{d}$	
	B13	0.5	30	1.5	34.68	60.49	1.75	3.14	3.87	117.5	194.6	51.8	58.75	97.3	3.84		
	B2	0.5	30	2	33.5	63.38	1.89	3.37	3.91	72.6	145.3	17.4	36.3	72.65	3.64		
E	B14		30	2	35.52	-	1.77	3.3	3.99	56.7	111.5	16.15	28.35	55.75	3.71	Full NSC control beam	
	B15	0.5	30	2	34.54	47.3	1.37	3.2	3.51	65.4	114	24.8	32.7	57	3.12	Effect of $\frac{fc`_{HSC}}{fc`_{NSC}}$	
	B16	0.5	30	2	33.5	63.38	1.89	3.37	3.91	67.5	115.3	19.6	33.75	57.65	3.82		
	B17	0.5	30	2	33.14	74.65	2.25	3.54	4.61	72.4	118.6	20.2	36.2	59.3	3.32		
																	Ø8 mm stirrups spacing
F	B16	0.5	30	2	33.5	63.38	1.89	3.37	3.91	67.5	115.3	19.6	33.75	57.65	3.82	0	Effect of stirrups spacing
	B18	0.5	30	2	34.14	62.54	1.84	3.29	3.66	79.6	148.5	17.55	39.8	74.25	4.43	100	
	B2	0.5	30	2	33.5	63.38	1.89	3.37	3.91	72.6	145.3	17.4	36.3	72.65	3.64	150	
	B19	0.5	30	2	34.14	62.54	1.84	3.29	3.66	71.2	137.4	19.7	35.6	68.7	5.15	200	

where: - Pc: cracking Load, Pu: ultimate failure load, Vc_1: first flexural shear crack, Vc: shear strength, Vu: ultimate shear strength

4.4 Cracking pattern and failure mode of the specimens

In terms of crack propagation, the behavior of both control and two-layer beams is similar except for crack spacing, compared to the cracks of the control beam, the cracks of the two-layer beams were closer to each other. The longitudinal tension-steel yielded first in all the beams, followed by concrete crushing at moment zone, which is a ductile failure mode.

4.4.1 Effect of compressive strength of layer on the crack pattern

Several crack patterns and failure modes were observed in the experiments. Beams of the group (A) are affected by layer concrete compressive strength. The first flexural crack appeared at the center of the beams at a load level between (17.4 to 25.7 kN) for the specimens, it was followed by the first diagonal shear crack level between (27.85 to 37.8 kN). When the loading was increased, additional diagonal shear and flexural cracks developed, spreading throughout the span. From the internal edge of the supports to the center of the load-bearing plate, the diagonal shear cracks developed gradually. The flexural cracks also spread toward the top of the beam, and a few additional small diagonal cracks were seen. With increasing the layer of the compressive strength, the ultimate failure load increased (8.35%, 15.6%, 18.85%) of beams (B1, B2, and B3) with respect to B8 (control) beam with the full depth normal concrete. All beams in this group failed in flexural at the load level (125.7, 136.2, 145.3, 149.4 kN). The final crack pattern of the beams was shown in Fig. (4-1).

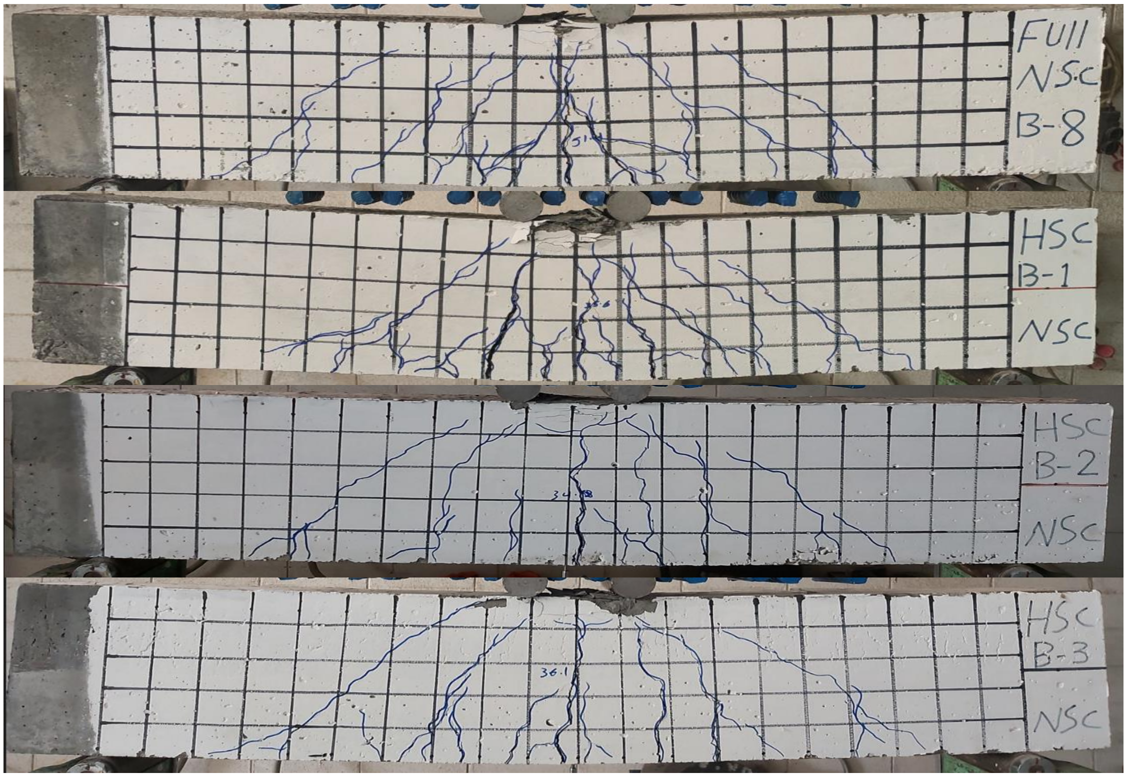

Fig. 4 -1 Group (A) Cracking pattern of the test specimens (B1, B2, B3, and B8)

4.4.2 Effect of overlap time casting between layers on the crack pattern

The specimens of this group were affected by the overlap time of layer casting. During the testing of the specimens, several crack patterns and failure modes were observed. The first flexural crack appeared at the mid-span at a load level of between (17.4 to 25.7 kN), while the first diagonal shear crack appeared close to the left support at a load level of between (27.85 to 41.6 kN). When the loading was increased, additional diagonal shear and flexural cracks developed, spreading throughout the span. From the internal edge of the supports to the center of the load-bearing plate, the diagonal shear cracks developed gradually. The flexural cracks also spread toward the top of the beam, and a few additional small diagonal cracks were seen. The flexural cracks grew corresponding to the yielding of steel bars with the increase of loads. Up to (15 min) ultimate load greater than the (60 to 100 min). all specimens in this group failed in flexural at the level of load (125.7, 145.8, 145.3, 143.8, 143, 142.8 kN) for beams (B8, B4, B2, B5, B6, and B7) respectively. The ultimate load increased by (16%, 15.6%, 14.4%, 13.8%, and 13.6%) for beams (B4, B2, B5, B6, and B7) with respect to the control beam with full depth normal concrete (B8). The final crack of the specimens was given in Fig. (4-2).

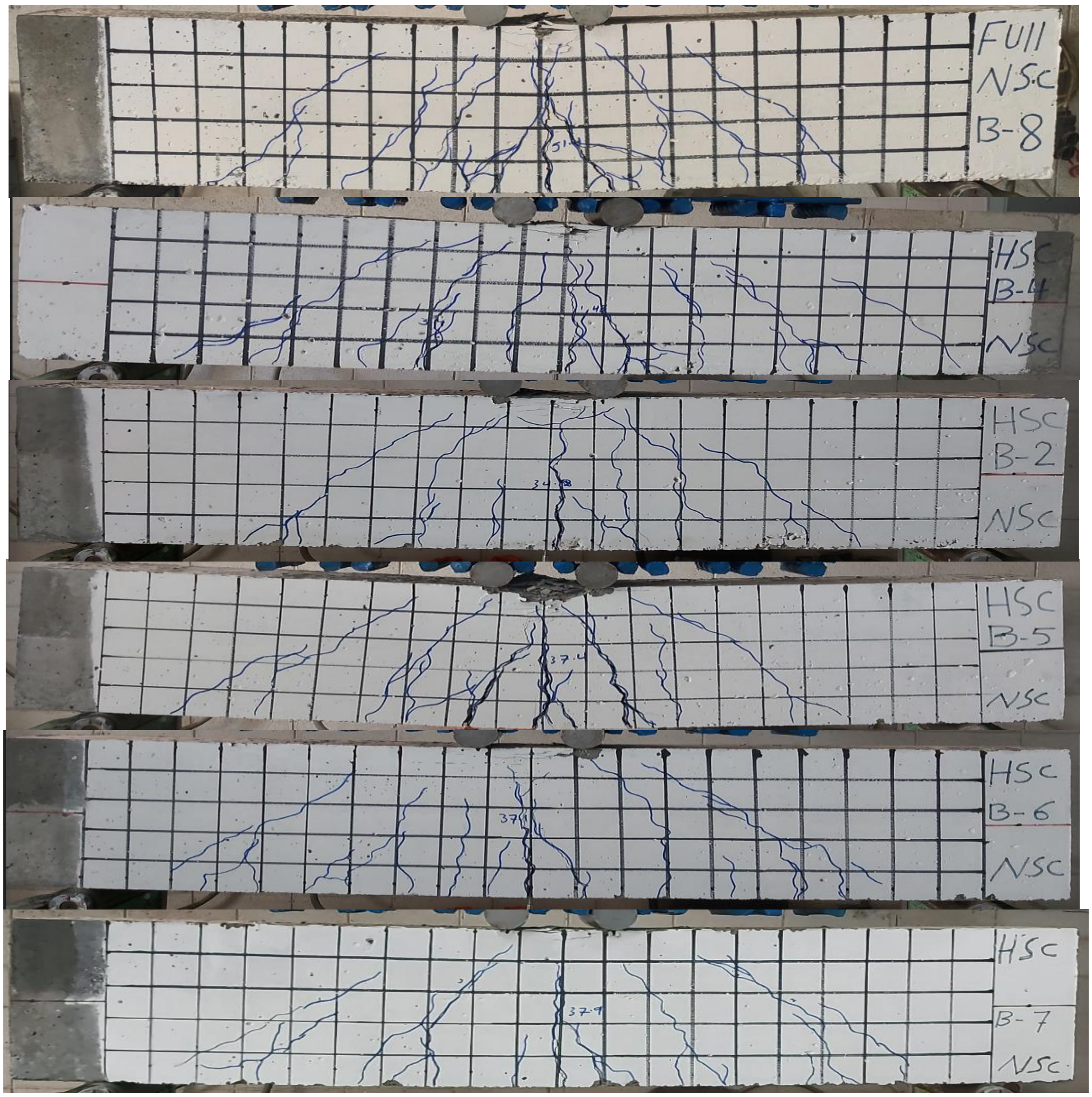

Fig. 4-2 Group (B) Cracking pattern of the test specimens (B2, B4, B5, B6, B7, and B8)

4.4.3 Effect of high-strength layer thickness on crack pattern

This group was subjected to a different layer thickness of NSC and HSC. Several crack patterns and failure modes were observed in the experiments. It was observed that the first flexural crack appeared at the center of the specimens. Specimen (B2) consists of (50%) of HSC and had an earlier appearance of flexural crack at (17.4 kN), and in other specimens (B8, B9, B2, B10, B11) the flexural crack seen at level load of (25.2, 19.3, 17,4, 17.35, 18.95 kN) respectively, the diagonal shear crack occurred at (27.85, 34.75, 36.3, 36.15, 41.2 kN) respectively. When the loading was increased, additional diagonal shear and flexural cracks developed, spreading throughout the span. From the internal edge of the supports to the center of the load-bearing plate, the diagonal shear cracks developed gradually. The flexural cracks also spread toward the top of the beam, and a few additional small diagonal cracks were seen. With increasing loads, the flexural cracks increased in proportion to the yielding of steel bars. The ultimate load for specimens was (125.7, 127.2, 145.3, 139, and 150.4 kN) for (B8, B9, B2, B10, and B11) respectively. The ultimate load increased by (1.6%, 15.6%, 10.6%, and 19.65%) with respect to control beam (B8). All beams in this group failed in flexural. The final crack pattern is shown in Fig. (4-3).

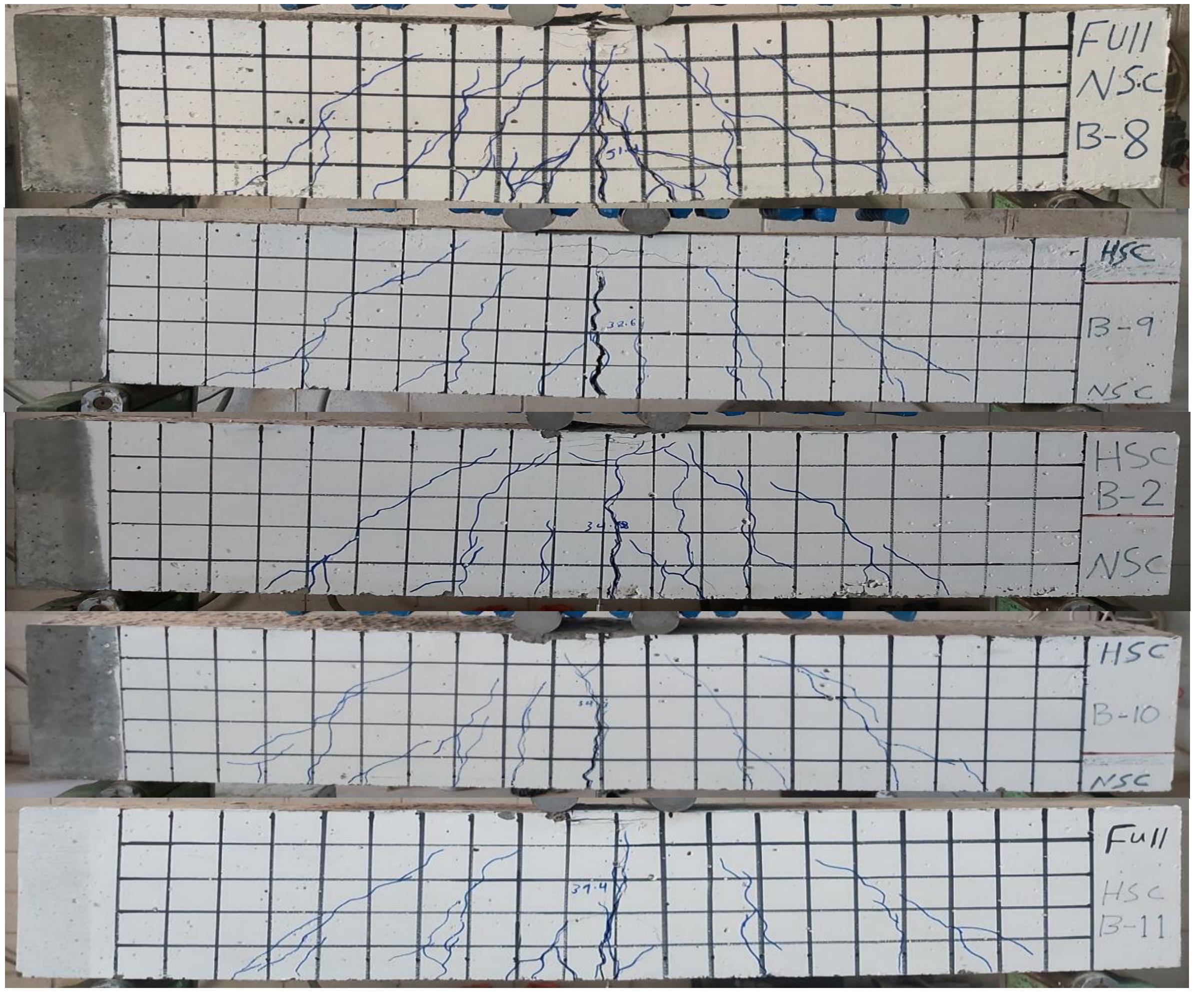

Fig. 4-3 Group (C) Cracking pattern of the test specimens (B2, B8, B9, Band B11)

4.4.4 Effect of shear span ratio (a/d) on crack pattern

In this group the difference in the shear span ratio was study span ratio (a/d), several cracks, and modes of failure was recorded for all specimens. the first flexural crack appeared at the mid-span at load levels of (44.7, 51.8, and 17.4 kN) followed by the first diagonal shear crack at a load level of (69, 58.75, and 36.3 kN) for (B12, B13, and B2) respectively. With the increase of loading, more diagonal shear and flexural cracks were propagated over the whole span of the beams, also It was found that the cracks developed an angle of (40°-50°) near the ends of both specimens (B12, and B13). These cracks dispersed throughout both sides of the beam. The flexural cracks grew corresponding to the yielding of steel bars with the increase of loads. With decreasing the shear span ratio (a/d) from (2 to 1.5 and 1) the ultimate load failure increased by (99% and 34%) for beams (B12, and B13) with respect to (B2) All specimens failed in flexural at load (289.9, 194.6, 145.3 kN) respectively. The final crack pattern was given in Fig. (3-4).

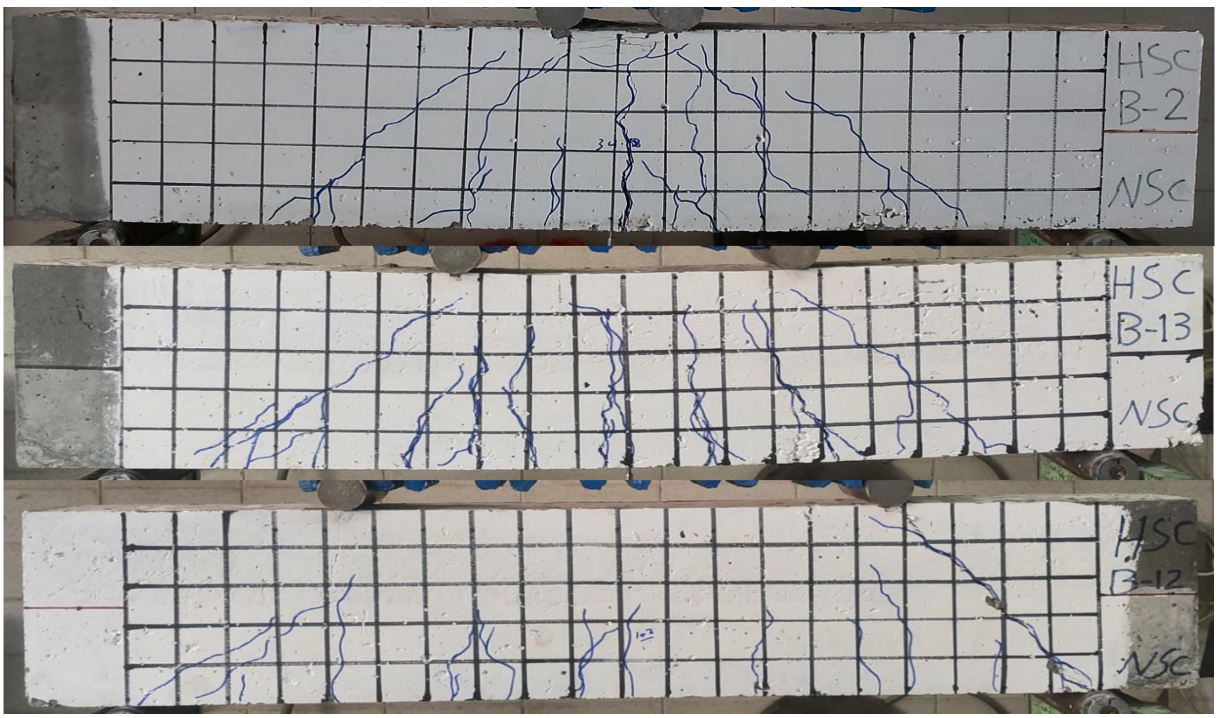

Fig. 4-4 Group (D) Cracking pattern of the test specimens (B12, B13, and B2)

4.4.5 Effect of compressive strength of layer without stirrups on the crack pattern

This group is like group (A) different compressive strength layers were use while no stirrups were used for the beams. This group had more diagonal shear cracks. The flexural cracks also spread but don’t toward the top of the beam for all specimens in this group as shown in Fig. (4-5). The first flexural crack was seen at load (16.15, 24.8, 19.6, and 20.2 kN). Also, the first diagonal shear appeared at load (28.35, 32.7, 33.75, and 36.2) for specimens (B14, B15, B16, and B17) respectively. With applying more load, the cracks diagonally start at the interior face of the support and propagate approximately (45) degrees toward the neutral axis of the beam. By increasing the layer of HSC ratio, the ultimate load was raised by (2.24%, 3.4%, and 6.37%) for beams (B15, B16, and B17) with respect to beam (B14) consisting full depth normal concrete without stirrups respectively. The ultimate load failure of the specimens was (111.5, 114, 115.3, and 118.6 kN).

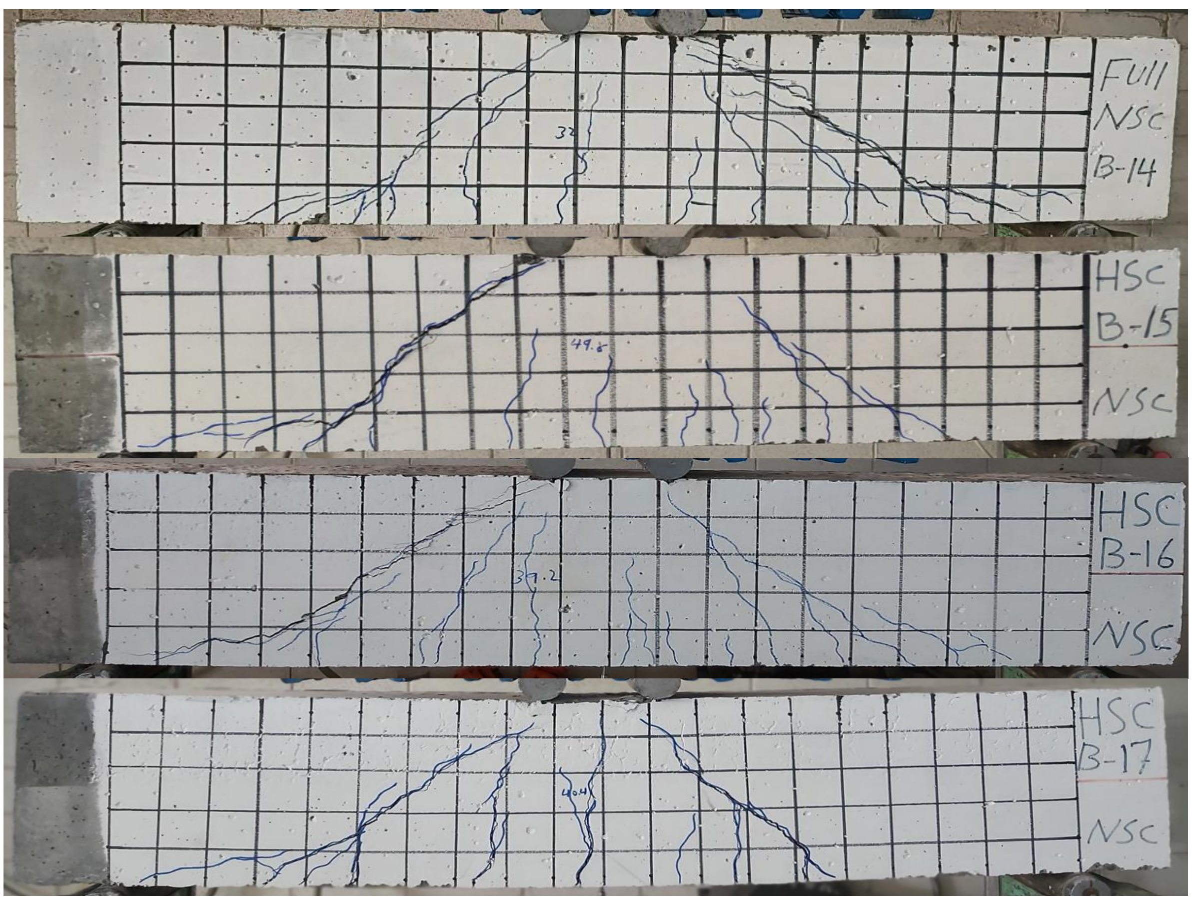

Fig. 4-5 Group (E) Cracking pattern of the test specimens (B14, B15, B16, and B17)

4.4.6 Effect of stirrup spacing on the crack pattern

In this group, the effect of spacing between stirrups was study. The first flexural crack was noticed at the mid-span at a load level of (19.6, 17.55, 17.4, and 19.7 kN) and complied with the first diagonal shear crack at a load level of (33.75, 39.8, 36.3, and 35.6 kN) also, the failure load is recorded at a load level of (115.3, 148.4, 145.3 137.4 kN) for beams (B16, B18, B2, and B19). The mode of failure depended on the stirrup spacing, with decreasing the space between stirrups of the two-layer reinforced concrete the ultimate failure load was increase by (28.7, 26, and 19.17%), for beams (B18, B2, and B19) with respect to (B16) without stirrups, respectively. as shown in Fig. (4-6).

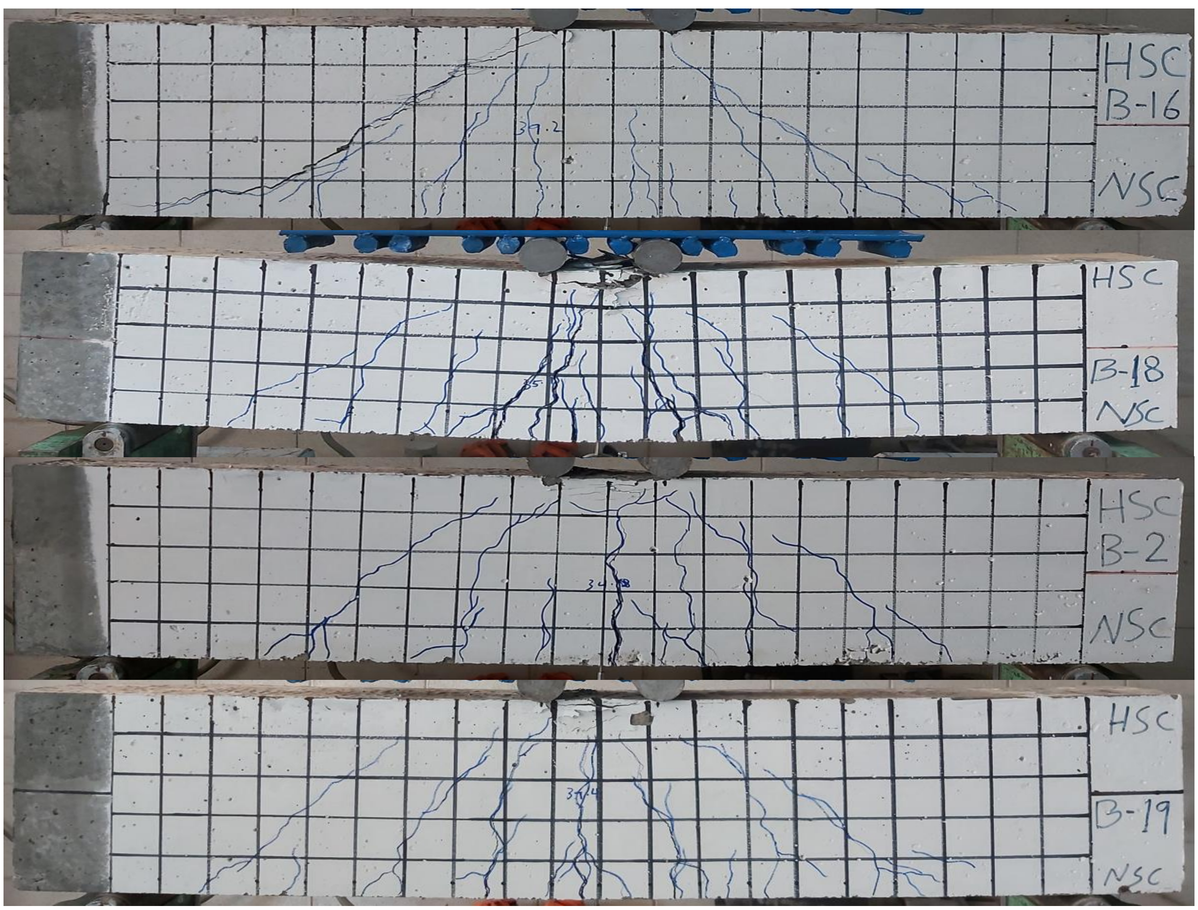

Fig. 4-6 Group (F) Cracking pattern of the test specimens (B2, B16, B18, and B19)

4.5 Measured Load-Deflection Curves

For all specimens, were displacements measured in the experiment at the span's mid-location of the beam. When the load increased gradually, the mid-span deflection of each beam showed a similar crack pattern. The deformation of deflection of all the specimens shows with the previous figures of the crack pattern.

Group (A) is affected by the layer concrete compressive strength ratio, Figure (4.7) shows the measured load-deflection curves for beams (B1, B2, B3, and B8). The elastic region was represented by the linear rising limb which has a greater angle until it reaches the linear limit value of (130, 140, 120, and 125.7 kN) with a corresponding deflection of (3.08, 3.38, 2.97, and 3.32 mm) respectively but (B2, and B8) has a small plastic region range. By increasing the layer compressive strength, the ultimate load was increase, and the maximum applied load over the plastic region was (136.2, 145.3, 149.94, and 125.7 kN) with a maximum deflection at the mid-span of specimens (4.01, 3.64, 6.66, and 3.32 mm) respectively.

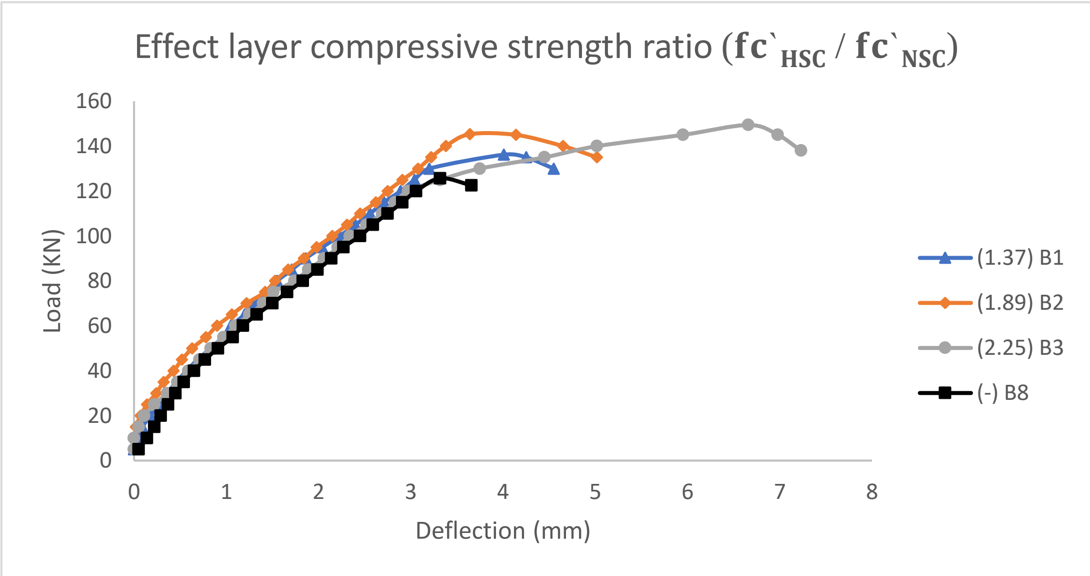

Fig. 4-7 Deflection at mid-span group (A)

Group (B) was affected by the overlap time of the casting of two layers of specimens. The elastic region is represented by the linear rising limb which has a greater angle until it reaches the linear limit value of (125.7, 125, 140, 140, 125, and 135 kN) with a corresponding deflection of (3.32, 2.79, 3.38, 2.89, 3.44, and 3.88mm) for specimens (B8, B4, B2, B5, B6, and B7) respectively. The maximum applied load over the plastic region was (125.7, 145.8, 145.3, 143, and 142.8 kN) with a maximum deflection at the mid-span of specimens (3.32, 4.68, 3.15, 7.54, and 4.93 mm). this is given in Fig. (4-8).

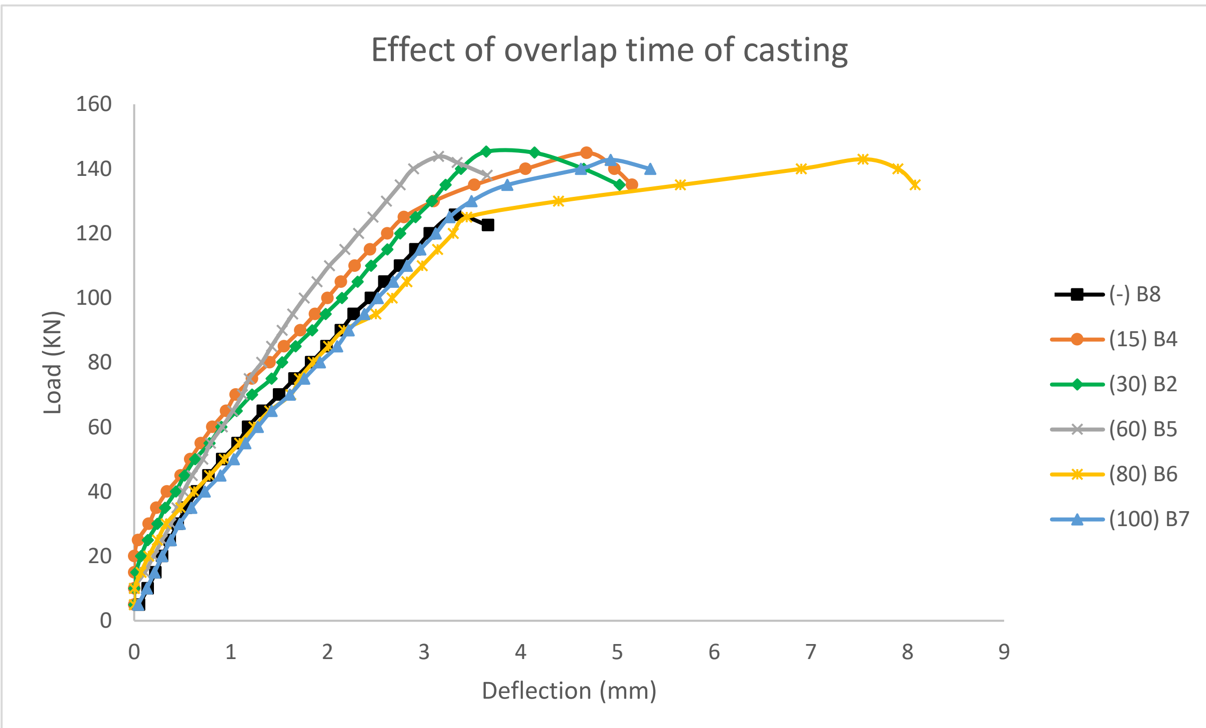

Fig. 4-8 Deflection at mid-span group (B)

Group (C) was affected by the concrete layer thickness, the measured deflection was increased linearly until the applied load reached (125.7, 120, 140, 115, and 135 kN) with a corresponding deflection of (3.32, 3.44, 3.38, 3.15, and 3.69 mm) for specimens of (B8, B9, B2, B10, and B11) respectively. The maximum applied load over the plastic region was (125.7, 127.2, 145.3,139, and 150.4 kN) with the deflection at the mid-span of specimens (3.32, 4.03, 3.64, 7.39, and 8.04 mm). this is illustrated in Fig. (4-9).

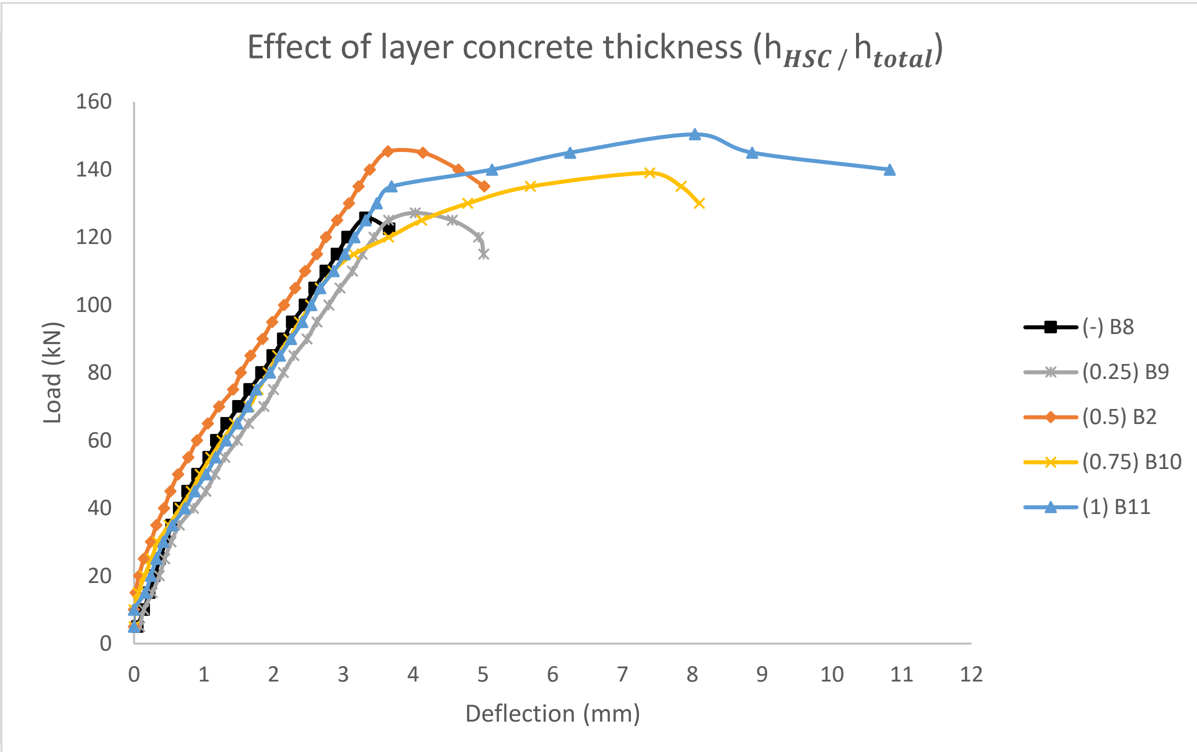

Fig. 4-9 Deflection at mid-span group (C)

Group (D) is affected by shear span ratio (a/d). The elastic region was represented by the linear rising limb which has a greater angle until it reaches a peak value of (280, 190, and 140 KN) with a corresponding deflection of (3.72, 3.69, and 3.38 mm) for specimens of (B12, B13, and B2) respectively. By decreasing the ratio of (a/d) from (2 to 1.5, and 1) the measured deflection at mid-span was increase by (5, and 12%) for specimens (B13 and, B12). The maximum applied load over the plastic region was (289.9, 194.5, and 145.3 kN) with a maximum deflection at the mid-span of the specimens (4.1, 3.84, and 3.64 mm), as shown in Fig. (4-10).

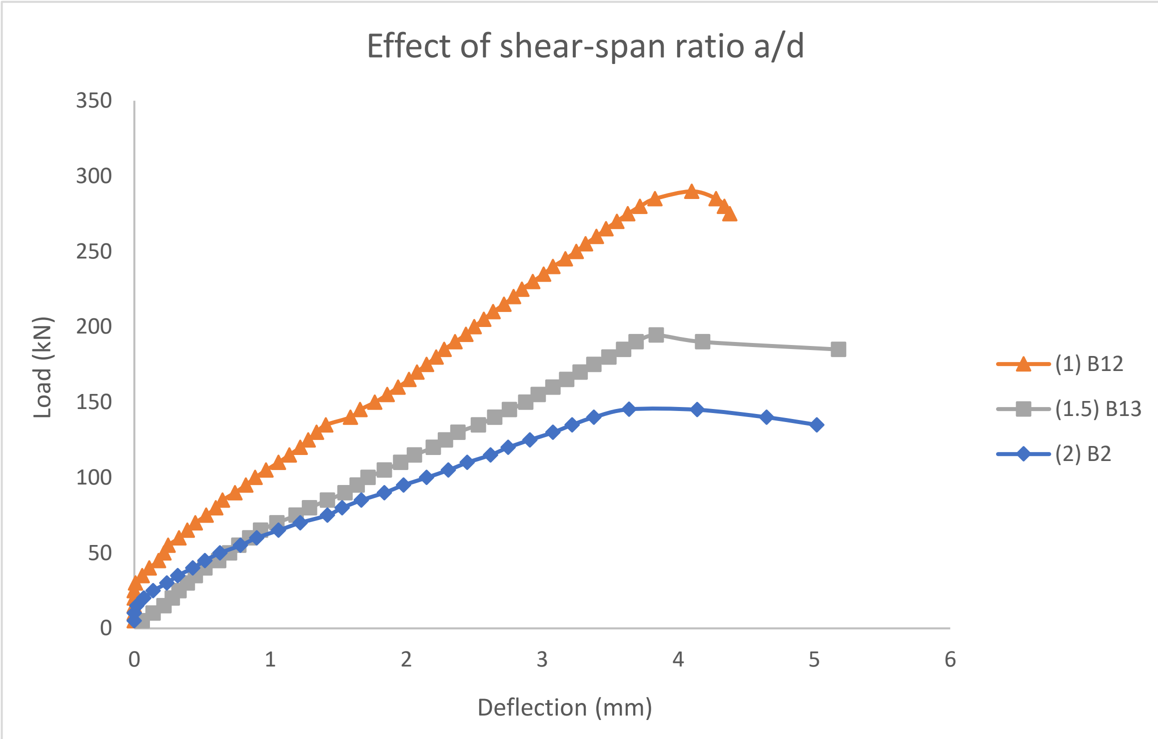

Fig. 4-10 Deflection at mid-span group (D)

Group (E) is affected by layer compressive strength without stirrups, the deflection of the control beam with full normal strength greater than other beams consisting of two layers. The elastic region was represented by the linear rising limb which has a greater angle until it reaches a peak value of (110, 115, 115,3, and 118.6 kN) with a corresponding maximum deflection at mid-span (3.71, 3.12, 3.82, and 3.32 mm). for specimens of (B14, B15, B16, and B17). The ultimate load was (111.5, 115, 115.3, and 118.6 kN). The applied load was discontinuous at the plastic region because the beams were without stirrups. It is given in Fig. (4-11).

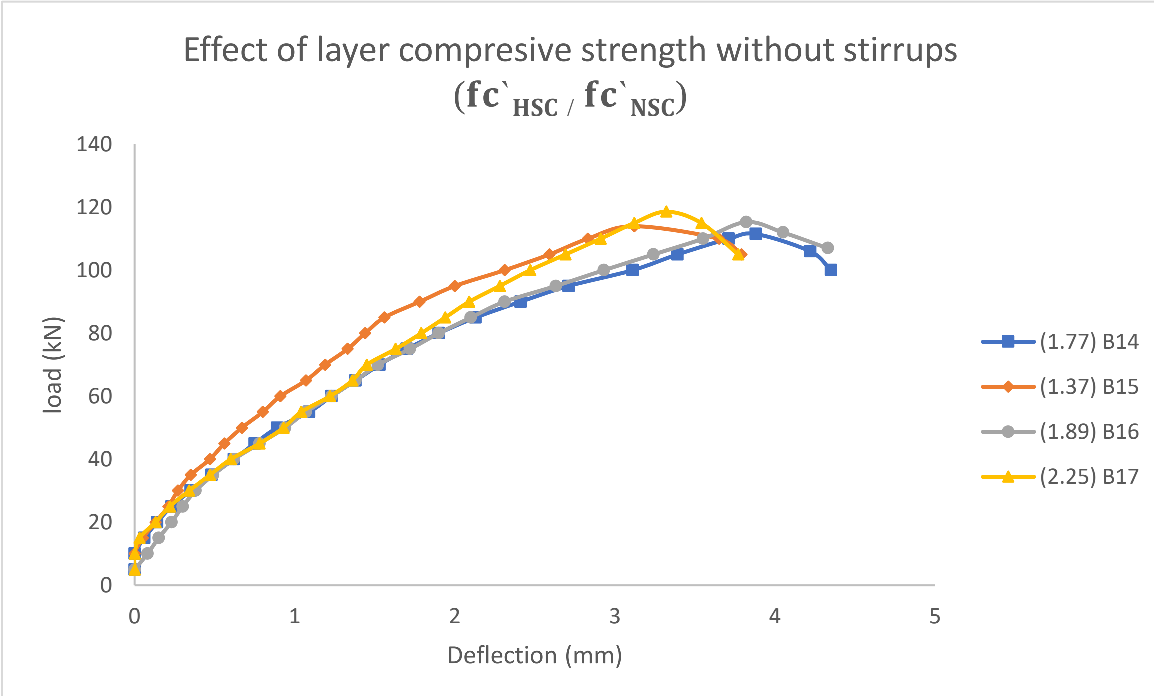

Fig. 4-11 Deflection at mid-span group (E)

Group (F) is affected by stirrup spacings. The elastic region is represented by the linear rising limb which has a greater angle until it reaches a peak value of (115,3, 135, 140, and 125 kN) with a corresponding deflection of (3.82, 3.52, 3.38, and 3.58 mm) for specimens of (B16, B18, B2, and B19) respectively. The maximum applied load over the plastic region was (148.4, 145.3, and 137.2 kN) with a maximum deflection at the mid-span of the specimens (4.43, 3.64, and 5.15mm) for beams (B18, B2, and B19), as illustrated in Fig. (4-12).

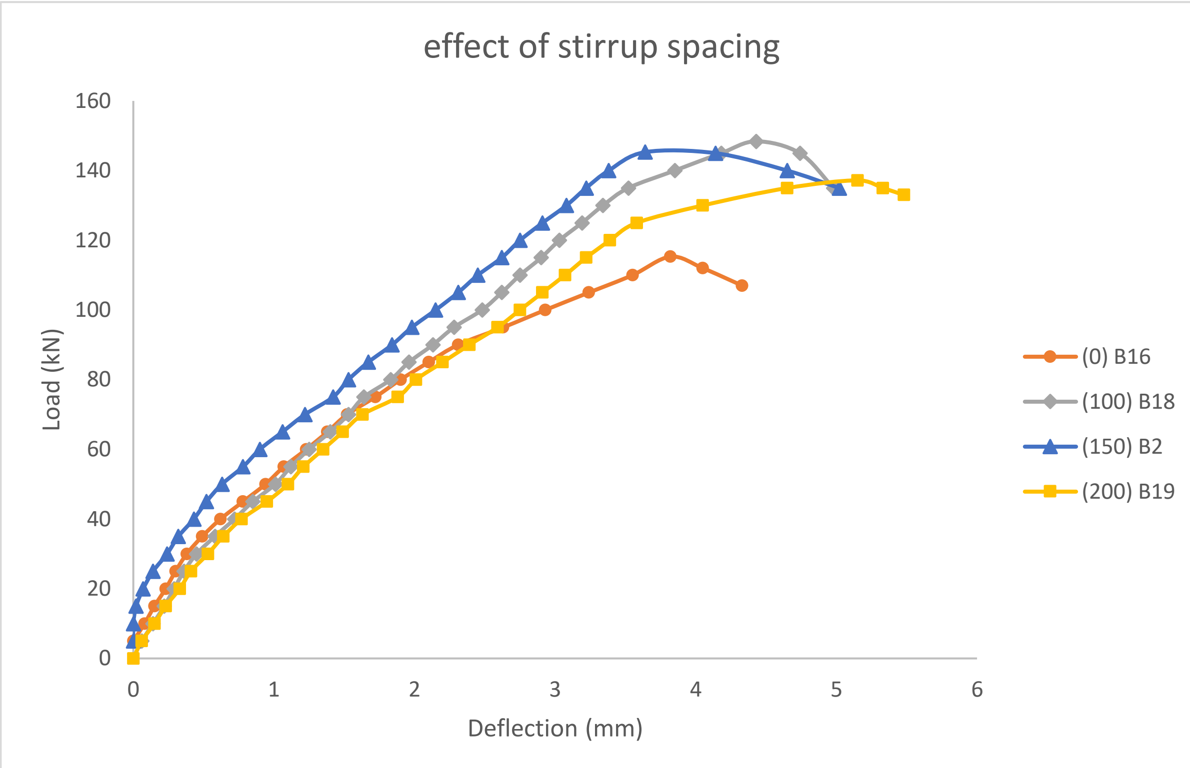

Fig. 4-12 Deflection at mid-span group (F)

4.6 Effect of the layer compressive strength on the shear capacity of the beams.

Table (4-4) shows the experimental value of shear strength (Vc) and ultimate shear strength (Vu) of the specimens with different compressive strength ratios.

Table 4-4 Experimental data of (Vc & Vu) group (A)

Group	Beam No.	$fc`_{NSC}$	$fc`_{HSC}$	$(fc`_{HSC})/(fc`_{NSC})$	Vc (kN)	% Increase	Vu (kN)	% Increase
A	8	33.87		1	27.85	-	62.85	-
	1	34.54	47.3	1.37	31.8	14.2	68.1	8.4
	2	33.5	63.38	1.89	36.3	30.3	72.65	15.6
	3	33.14	74.65	2.25	37.8	35.7	74.2	18.9

The cracking shear force (Vc) and ultimate shear strength (Vu) of the two-layer beams increased linearly with an increasing compressive strength ratio between the two layers (37%, 89%, 125%), the value of shear strength (Vc) increased by (14.2%, 30.3%, and 35.7%) respectively also the value of ultimate shear strength (Vu) increased by (8.4%, 15.6%, and 18.9%) respectively with respect to the control beam (B8) as shown in Fig. (4-13). The effect of the layer compressive strength ratio $(fc`_{HSC})/(fc`_{NSC})$ on (Vc) is greater than (Vu) by (50 to 70%). So, the compressive strength of concrete layers has a direct effect on the shear strength of concrete.

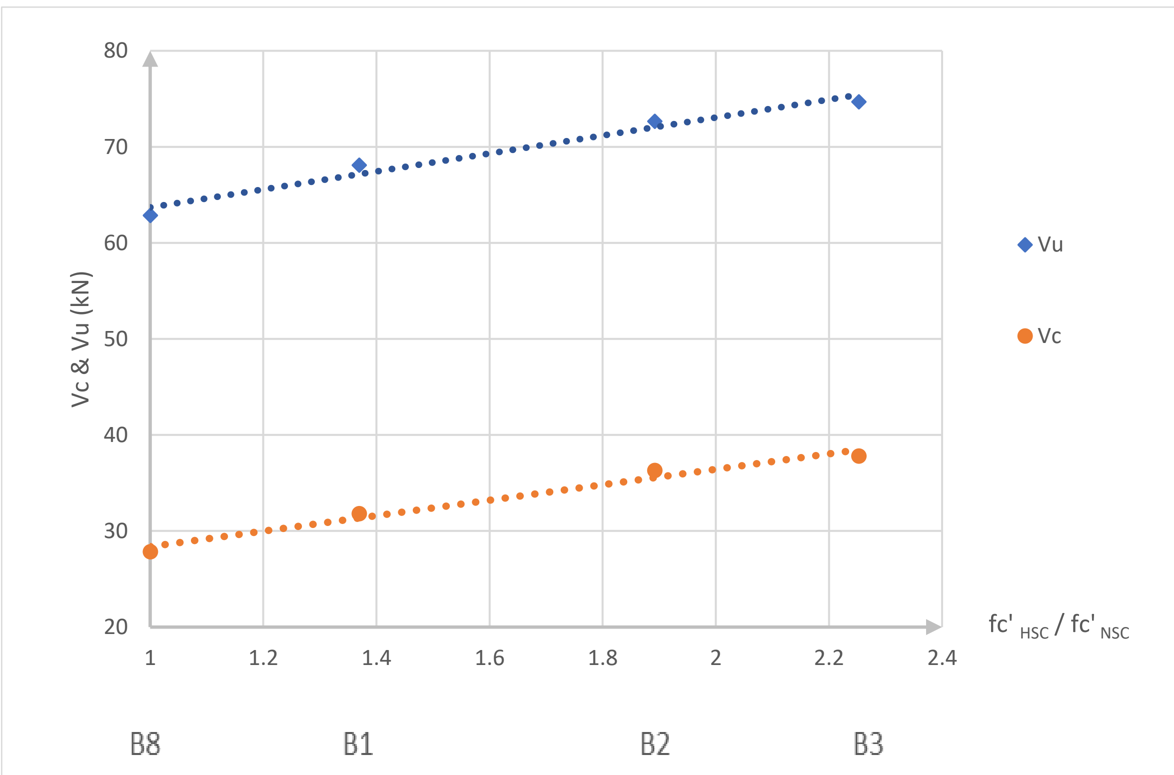

Fig. 4-13 Effect of concrete compressive strength ratio on (Vc & Vu)

4.7 Effect of the overlap casting time on the shear capacity of the beams

Table (4-5) present the experimental value of shear strength (Vc) and ultimate strength of shear of the specimens at different time of casting two-layer of concrete.

Table 4-5 Experimental data of (Vc & Vu) group (B)

Group	Beam No.	Overlap time (min)	Vc (kN)	% Increase	Vu (kN)	% Increase
B	8	0	27.85	-	62.85	-
	4	15	37.15	33.4	72.9	0.16
	2	30	36.3	30.3	72.65	0.156
	5	60	36.7	31.8	71.9	14.4
	6	80	35.25	26.6	71.5	13.8
	7	100	41.6	49.4	71.4	13.6

According to Table (4-5) when the overlap time is zero the value of the shear strength (Vc) and ultimate shear strength (Vu) control beam is lower than other beams consisting of two-layer reinforced concrete beams with different overlap times. Up to 30 overlap time concrete shear strength (Vc) increases (33 %). Likewise, ultimate shear strength (Vu) rises by (15.6%) up to 30 min then the strength decreased by (13.6%) at an overlap time of 100 min, as shown in Fig. (4.14). It can be concluded that the casting overlap time of up to (15 min) can be used for casting two-layered reinforced concrete beams, which is recommended, beyond this time the strength of the beam (Vc &Vu) decreases.

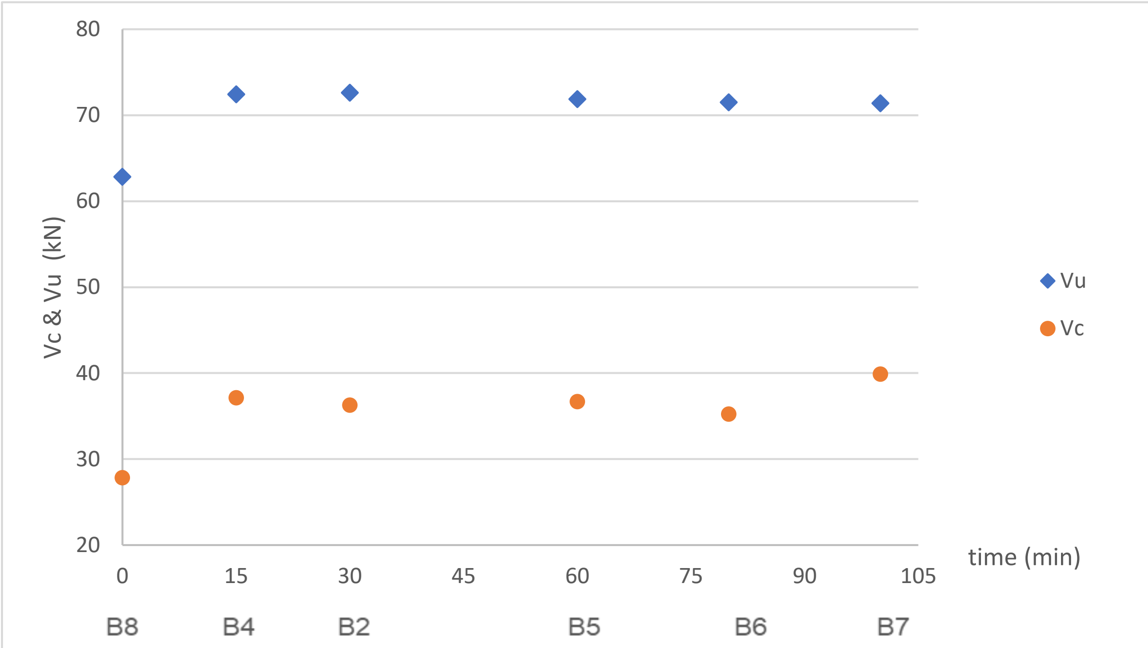

Fig. 4-14 Value of (Vc & Vu) with different overlap time

4.8 Effect of concrete layer thickness on the shear capacity of the specimens

Table (4-6) shows the experimental results of shear strength (Vc) and ultimate shear strength (Vu) of the beams with a different layer thickness of concrete.

Table 4-6 Experimental data of (Vc & Vu) group (C)

Group	Beam No.	h_{HSC} (mm)	h_{total} (mm)	$\frac{h_{HSC}}{h_{total}}$	Vc (kN)	% Increase	Vu (kN)	% Increase
C	8	0	250	0	27.85	-	62.85	-
	9	62.5	250	0.25	34.75	24.8	63.6	1.2
	2	125	250	0.5	36.3	30.3	72.65	15.6
	10	187.5	250	0.75	36.15	29.8	69.5	10.6
	11	250	250	1	41.2	41.2	75.2	19.65

The shear strength and the ultimate strength of the control beam are lower than the beams consisting of two-layer with a different layer thickness of high-strength concrete, for the beam consisting of (0.25h) of high strength layer ratio, the concrete shear strength increased by (24.2%), and ultimate shear strength (Vu) increased by (1.2%). When the high strength layer rises to (0.5h), (Vc) and (Vu) increase by (30.3 and 15.6%) respectively. For the high strength layer of (0.75h), (Vc) increased by (29.8%) and (Vu) by (10.6%). When the high strength layer ratio reaches (1), means the beam consisting of full high strength concrete (Vc) increased by (48%), and (Vu) by (19.65%). This means that by increasing the high strength layer ratio the value of (Vc and Vu) increased linearly as demonstrated in Fig. (4.15). Also, the effect of the high strength concrete layer thickness on (Vc) is greater than (Vu).

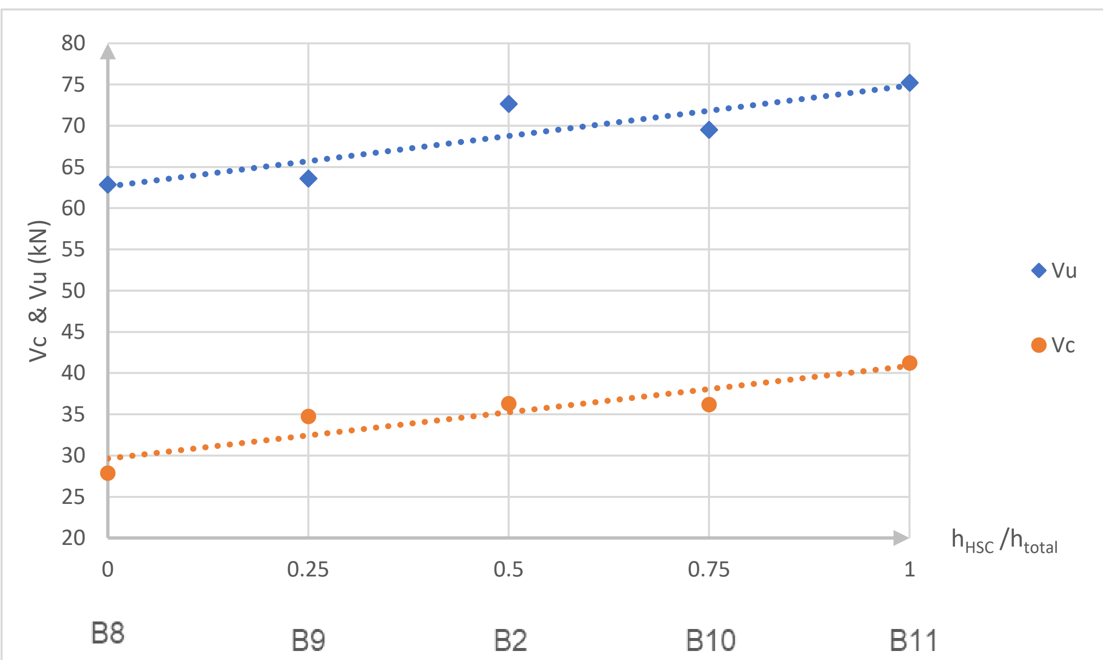

Fig. 4-15 Effect of the different HSC layer ratios on (Vc & Vu)

4.9 Effect of shear span ratio ($\frac{\mathbf{a}}{\mathbf{d}}$) on the shear capacity of the beams

Table (4-7) shows the experimental results of shear strength (Vc) and ultimate shear strength (Vu) of the beams with different shear span ratios a/d.

Table 4-7 Experimental data of (Vc & Vu) group (D)

Group	Beam No.	a (mm)	d (mm)	$\frac{a}{d}$	Vc (KN)	% Reduction	Vu (KN)	% Reduction
D	12	220	220	1	69	-	144.95	-
	13	330	220	1.5	58.75	%15	97.3	33%
	2	440	220	2	36.3	47.4	72.65	50%

Table (4-7) presented the value of (Vc & Vu) by affecting the shear span ratio (a/d). With increased the shear span ratio (a/d), the shear capacity of the two-layer concrete beams decreases gradually. Fig. (4-16) shows the influence of the shear span– ratio (a/d) on the shear capacity. With a smaller shear span ratio, the amount of (Vc & Vu) is increased, for (a/d = 1.5) (Vc) decreased by (15%), and (Vu) by (33%). While (a/d = 2) (Vc) decreased by (47.4%) and (Vu) decreased by (50%). The effect of (a/d) on the ultimate shear strength (Vu) is greater than (Vc).

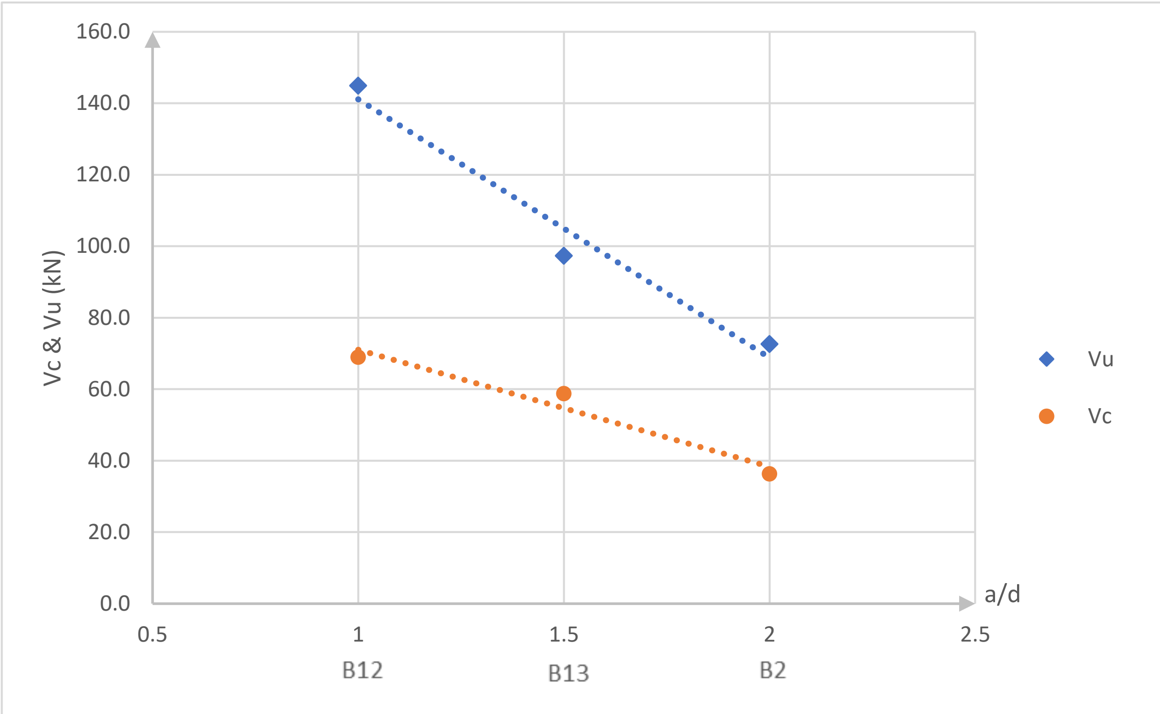

Fig. 4-16 Effect of shear span ratio (a/d) on (Vc & Vu)

4.10 Effect of the layer compressive strength on the shear capacity of the beams without stirrups.

Table (4-8) shows the experimental value of shear strength (Vc) and ultimate shear strength of the specimens with different compressive strength ratios of the beams without stirrups.

Table 4-8 Experimental data of (Vc & Vu) group(E)

Group	Beam No.	$fc`_{NSC}$	$fc`_{HSC}$	$(fc`_{HSC})/(fc`_{NSC})$	Vc (kN)	% Increase	Vu (kN)	% Increase
E	14	35.52	62.75	1.77	28.35	-	55.75	-
	15	34.54	47.3	1.37	32.7	15.3	57	2.24
	16	33.5	63.38	1.89	33.75	19	57.65	3.4
	17	33.14	74.65	2.25	36.2	27.7	59.3	6.4

The above table presented the experimental value of (Vc & Vu) two-layer reinforced concrete beams without stirrups. The capacity of shear strength and ultimate shear strength of the control beam is less than the other beam consisting of two-layer of concrete beams. The beams have a concrete compressive strength ratio (1.37) the amount of (Vc and Vu) is increased by (15.3 and 2.24%) respectively. When the compressive strength ratio is (1.89) the value of (Vc & Vu) rises to (19 and 3.4%). For the last beam which is the compressive strength ratio is (2.25) also, the value of (Vc) is rising to (27.7%) and (Vu) to (6.4%). With increasing the layer of high compressive strength ratio, the value of (Vc and Vu) is increased as shown in Fig. (4.17), the effect of strength ratio ($fc`_{HSC}$ /$fc`_{NSC}$) on (Vc) is much greater than the (Vu). The behavior of the beams without stirrups are same as the beams with stirrups.

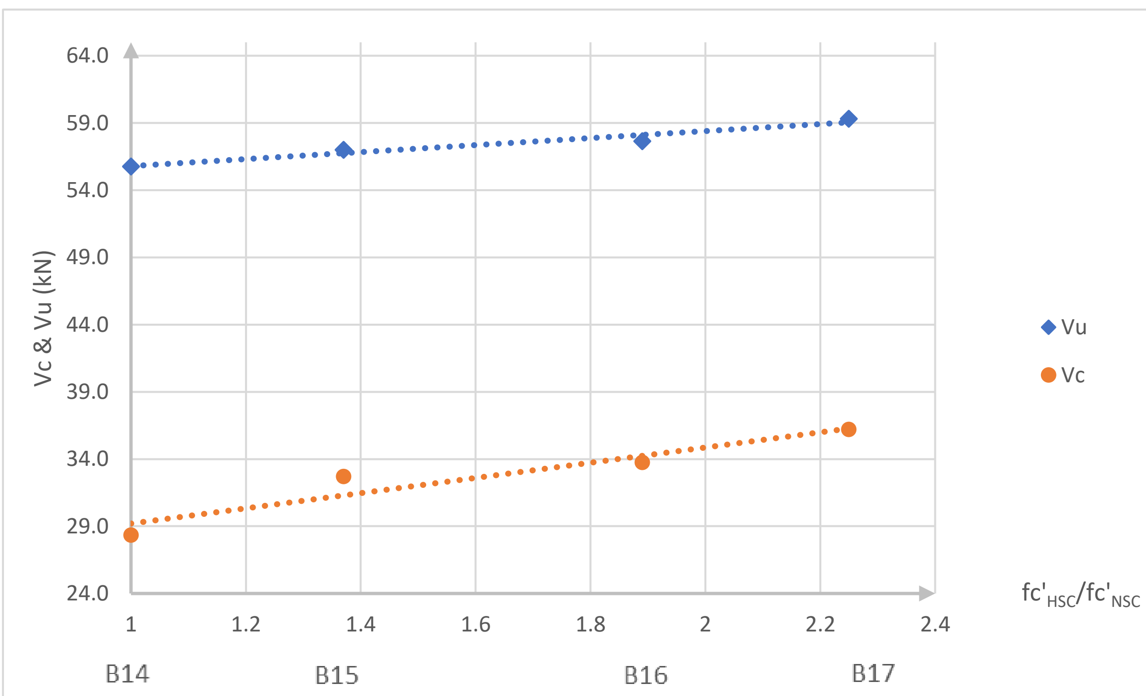

Fig. 4-17 Effect of ($fc`_{HSC}$)/($fc`_{NSC}$) without stirrups on (Vc & Vu)

4.11 Effect of stirrup spacing (amount of reinforcement) on the shear capacity of the beams

Table (4-9) present the experimental value of shear strength (Vc) and ultimate shear strength of the specimens with different amount of transverse reinforcement (spacing of stirrups).

Table 4-9 Experimental data of (Vc & Vu) group (F)

Group	Beam No.	S (mm)	Vc (kN)	% Increase	Vu (kN)	% Increase
F	16	0	33.75	-	57.65	-
	18	100	39.8	18	74.75	29.7
	2	150	36.3	7.56	72.65	26
	19	200	35.6	5.5	68.7	19.2

Table (4-9) demonstrates the influence of different stirrup spacing on the result of cracking shear and ultimate shear force (Vc & Vu) in the group (F). stirrup spacing has played a significant role in the capacity of shear strength. When the stirrup spacing is (200 mm) the amount of (Vc) increased by (5.5%) and (Vu) by (19.2%). For beams with stirrup, spacing is (150 mm) the value of (Vc &Vu) again rises to (7.56 and 26%) respectively. When reducing the space of stirrups to (100 mm) the amount of (Vc) is going up to (18 %) and (Vu) to (29.7%). With decreasing the spacing of stirrups, the capacity of shear strength is increased and that is illustrated in Fig. (4.18). Also, the effect of stirrup spacing on (Vu) is much greater than on (Vc).

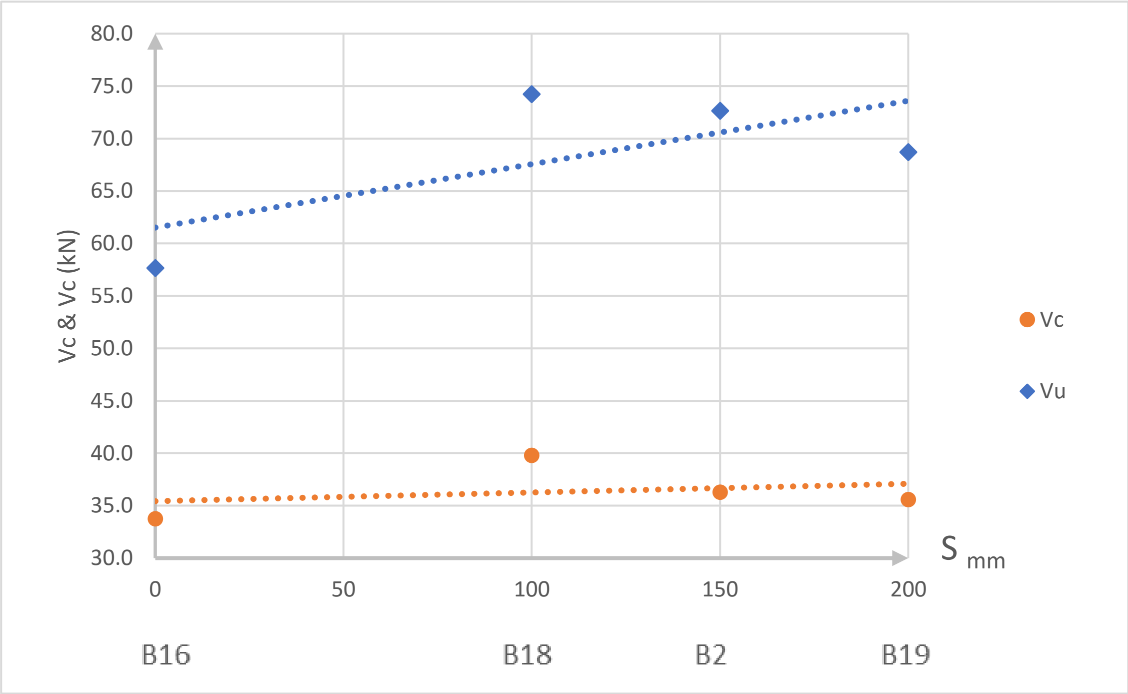

Fig. 4-18 Effect of stirrup spacing on (Vc & Vu)

CHAPTER FIVE

THEORETICAL CALCULATION

5.1 Shear strength calculation

The shear strength was calculated using theoretical and empirical methods found in codes and literature. For the two-layer beam shown in Fig. (5.1), the total shear strength is the sum of the shear strength of two layers. The methods used to calculate the shear strength of concrete beams are described below:

5.1.1 ACI Code 318-19 ACI (American Concrete Institute) (2019)

$$Vc = \frac{\lambda}{6}\sqrt{fc'}\ b_w d \tag{5.1}$$

For two-layer beam equation (5.1) can be written as:

$$Vc_{layer1} = \frac{\lambda}{6}\left[\sqrt{fc'_{HSC}}\ \times b_w h_{HSC}\right] \tag{5.2}$$

$$Vc_{layer2} = \frac{\lambda}{6}\left[\sqrt{fc'_{NSC}}\ \times b_w (d - h_{HSC})\right] \tag{5.3}$$

$$Vc = Vc_{layer1} + Vc_{layer2} \tag{5.4}$$

Where:

Vc = Shear strength of the beam (N), fc' = Cylinder compressive strength of the beam (MPa), b_w = Width of the beam (mm), d = effective depth of the beam (mm), h_{HSC} = depth of the layer (top layer) mm.

λ = lightweight concrete modification factor

λ = 1   for normal concrete

λ = 0.85 for the concrete with sand's weight is light

λ= 0.75 for all types of concrete that has light weight

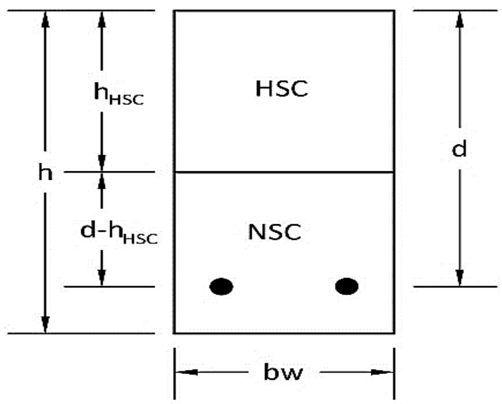

Fig. 5- 1 Beam section

5.1.2 EC2 Code CEN Eurocode (2004)

$$Vc = \left[\frac{0.18}{\gamma_c}\left(1+\sqrt{\frac{200}{d}}\right)(100\,\rho_l\,fc')^{\frac{1}{3}}\right]b_w d \qquad (5.5)$$

For two-layer beam equation (5.5) can be written as:

$$Vc_{layer1} = \frac{0.18}{\gamma_c}\left(1+\sqrt{\frac{200}{d}}\right)(100\,\rho_l\,fc'_{HSC})^{\frac{1}{3}}\,b_w\,h_{HSC} \qquad (5.6)$$

$$Vc_{layer2} = \frac{0.18}{\gamma_c}\left(1+\sqrt{\frac{200}{d}}\right)(100\,\rho_l\,fc'_{NSC})^{\frac{1}{3}}\,b_w\,(d-h_{HSC}) \qquad (5.7)$$

$$Vc = Vc_{layer1} + Vc_{layer2} \qquad (5.8)$$

ρ_l = Percentage of longitudinal reinforcement

γ_c = coefficient of material = 1.4

5.1.3 BS 8110-1: British Standards Institution. (1985)

$$\mathrm{Vc} = \left[\frac{0.79}{\gamma_m}\left(100\,\frac{As}{b_w d}\right)^{\frac{1}{3}}\left(\frac{400}{d}\right)^{\frac{1}{4}}\times\left(\frac{f_{cu}}{25}\right)^{\frac{1}{3}}\right]b_w d \qquad (5.9)$$

For two-layer beam equation (5.9) can be written as:

$$Vc_{layer1} = \frac{0.79}{\gamma_m}\left(100\ \frac{As}{b_w d}\right)^{\frac{1}{3}}\left(\frac{400}{d}\right)^{\frac{1}{4}} \times \left(\frac{fcu}{25}\right)^{\frac{1}{3}}_{\text{HSC}} b_w h_{HSC} \tag{5.10}$$

$$Vc_{layer2} = \frac{0.79}{\gamma_m}\left(100\ \frac{As}{b_w d}\right)^{\frac{1}{3}}\left(\frac{400}{d}\right)^{\frac{1}{4}} \times \left(\frac{fcu}{25}\right)^{\frac{1}{3}}_{\text{NSC}} b_w (d - h_{HSC}) \tag{5.11}$$

$$Vc = Vc_{layer1} + Vc_{layer2} \tag{5.12}$$

Where:

γ_m = concrete partial factor of safety = 1.25, As = Area of the longitudinal reinforcement (mm^2), f_{cu} = cube compressive strength of concrete (MPa).

5.1.4 Canadian Code CSA Committee A23.3 (2004)

$$Vc = 0.2\sqrt{fc'}\ b_w d \tag{5.13}$$

For two-layer beam equation (5.13) can be written as:

$$Vc_{layer1} = 0.2\sqrt{fc'_{HSC}}\ b_w\ h_{HSC} \tag{5.14}$$

$$Vc_{layer2} = 0.2\sqrt{fc'_{NSC}}\ b_w\ (d - h_{HSC}) \tag{5.15}$$

$$Vc = Vc_{layer1} + Vc_{layer2} \tag{5.16}$$

The available models and theoretical equations (5.1 to 5.16) are applied on the tested beams of this study (19 beams), the theoretical results of the shear force are compared with the experimental results. Moreover, Statistical parameters are calculated and displayed in the Table (5-1), such as the average ratio of (R) experimental shear force divided by theoretical shear force, standard deviation, (σ), varians, and coefficient of correlation between the experimental and theoretical results.

Table 5-1 The experimental shear force and that calculated from the available code

Beam No.	Vc_{exp} (kN)	Vc ACI	Vc EC2	Vc BS8110	Vc CAN	$\frac{Vc_{exp}}{Vc_{ACI}}$	$\frac{Vc_{exp}}{Vc_{Ec2}}$	$\frac{Vc_{exp}}{Vc_{BS}}$	$\frac{Vc_{exp}}{Vc_{CAN}}$
1	31.8	29.54	22.398	23.824	35.450	1.077	1.420	1.335	0.897
2	36.3	32.19	23.668	25.162	38.624	1.128	1.534	1.443	0.940
3	37.8	33.89	24.457	25.994	40.672	1.115	1.546	1.454	0.929
4	37.15	31.81	23.494	24.979	38.175	1.168	1.581	1.487	0.973
5	36.7	31.75	23.470	24.955	38.097	1.156	1.564	1.471	0.963
6	35.25	32.42	23.797	25.302	38.909	1.087	1.481	1.393	0.906
7	41.6	32.24	23.705	25.204	38.693	1.290	1.755	1.651	1.075
8	27.85	26.674	20.937	22.538	32.008	1.044	1.330	1.236	0.870
9	34.75	29.41	22.298	23.847	35.291	1.182	1.558	1.457	0.985
10	36.15	34.65	24.901	26.336	41.583	1.043	1.452	1.373	0.869
11	41.2	36.23	25.677	27.087	43.470	1.137	1.605	1.521	0.948
12	69	31.91	23.546	25.036	38.291	2.162	2.930	2.756	1.802
13	58.75	31.91	23.546	25.036	38.291	1.841	2.495	2.347	1.534
14	28.35	27.316	21.272	22.638	32.779	1.038	1.333	1.252	0.865
15	32.7	29.54	22.398	23.824	35.450	1.107	1.460	1.373	0.922
16	33.75	32.187	23.668	25.162	38.624	1.049	1.426	1.341	0.874
17	36.2	33.89	24.457	25.994	40.672	1.068	1.480	1.393	0.890
18	39.8	32.16	23.660	25.155	38.590	1.238	1.682	1.582	1.031
19	35.6	32.16	23.660	25.155	38.590	1.107	1.505	1.415	0.923
R_{Min}						1.038	1.330	1.236	0.865
R_{Max}						2.162	2.930	2.756	1.802
R_{avg}						1.212	1.639	1.541	1.010
S. D						0.290	0.399	0.376	0.242
Var						0.84	0.159	0.141	0.059
Corr.(r)						0.332	0.335	0.338	0.331
r^2						0.110	0.112	0.114	0.110

As shown in Table (5-1) the correlation between the experimental and theoretical results obtained from the available codes, EC2 and BS8110 equation give underestimate results, the main ratio of (R= Vc_{exp}/Vc_{cal}) are 1.639 and 1.541 respectively, ACI code equation gives more reasonable results and still underestimate results, the mean ratio (R) is (1.212). Figs. (5-2, 5-16) show that all the plotted points are over the unity line, underestimate, while the results obtained from the Canadian Code (CAN Code) most of points under the unity line, overestimate, and mean value of (R) is (1.01) as shown in Figs.(5-17, 5-21). Because there is a low correlation between the experimental data and theoretical results that calculated from the available Code equations, new equations are proposed to calculate shear strength for two-layer beams including the variables of this study (the compressive strength ratio ($\frac{fc'_{HSC}}{fc'_{NSC}}$) of the two layers for beams with and without stirrups, overlap casting time as a ratio to the cement initial setting time ($\frac{t}{t_o}$), layer thickness ratio ($\frac{fc'_{HSC}}{fc'_{total}}$), shear span ratio ($\frac{a}{d}$), and spacing of stirrups which is represented by the ratio of transverse reinforcement index divided by the longitudinal index $\left(\frac{\rho_t}{\rho_l}\right)$).

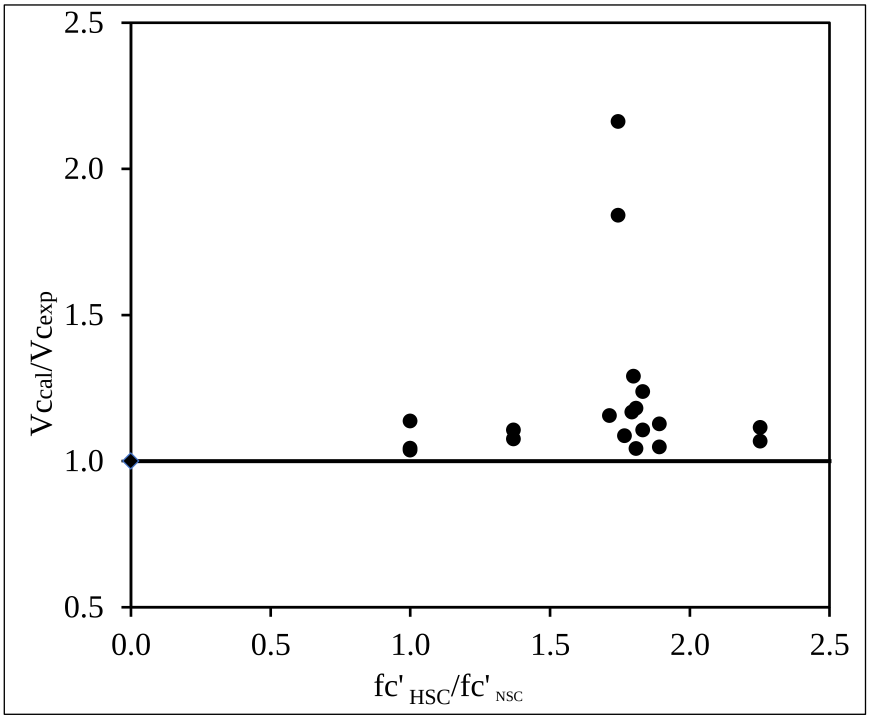

Fig. 5-2 Experimental/calculated shear force ACI Code (2019)

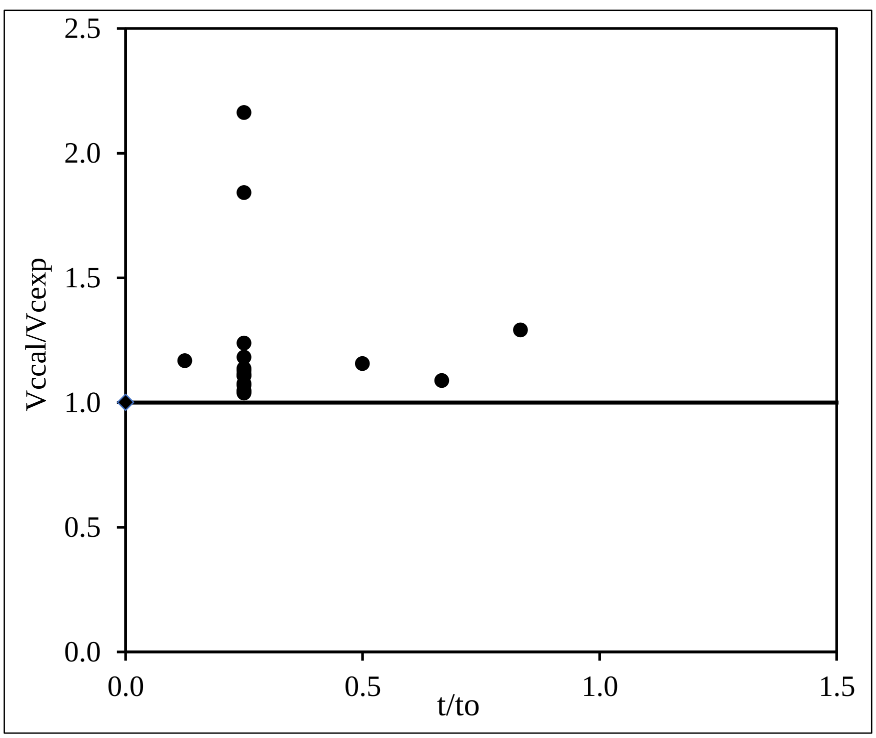

Fig. 5-3 Experimental/calculated shear force ACI Code (2019)

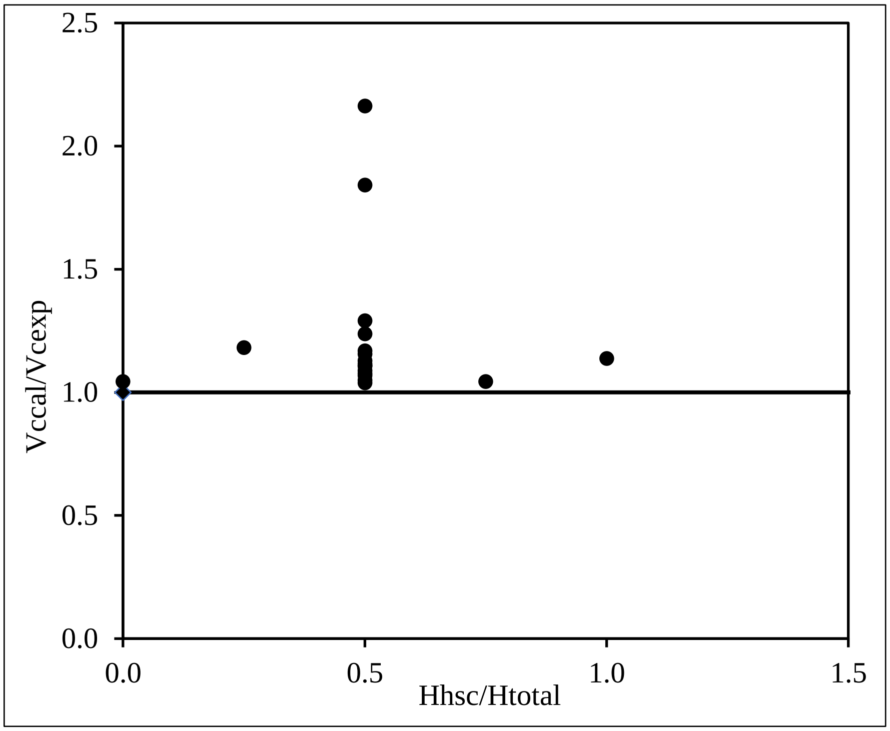

Fig. 5-4 Experimental/calculated shear force ACI Code (2019)

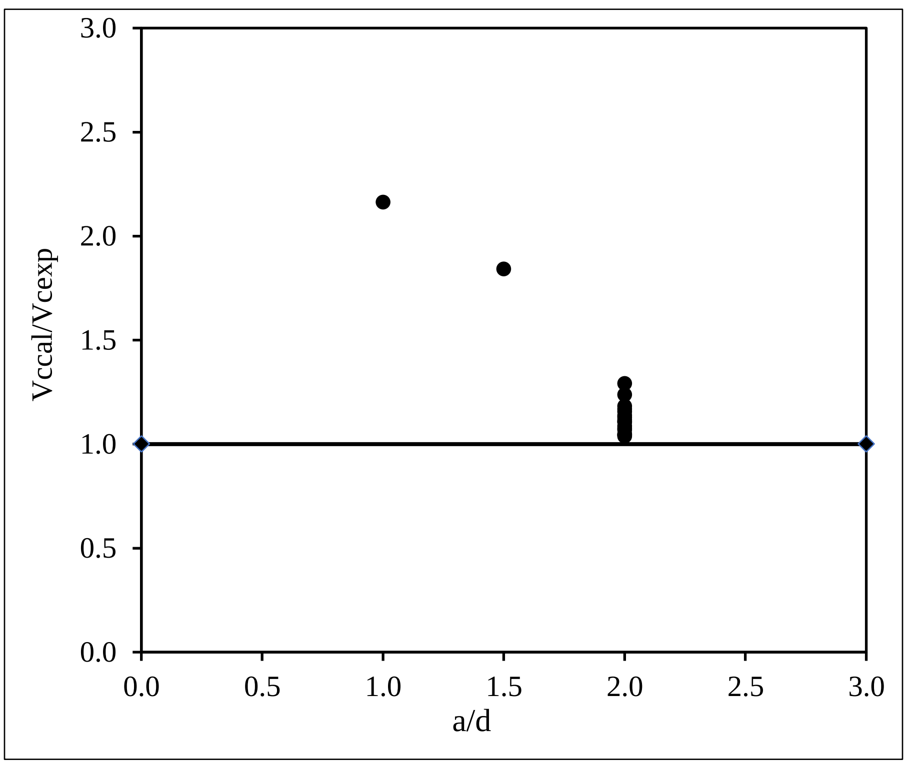

Fig. 5-5 Experimental/calculated shear force ACI Code (2019)

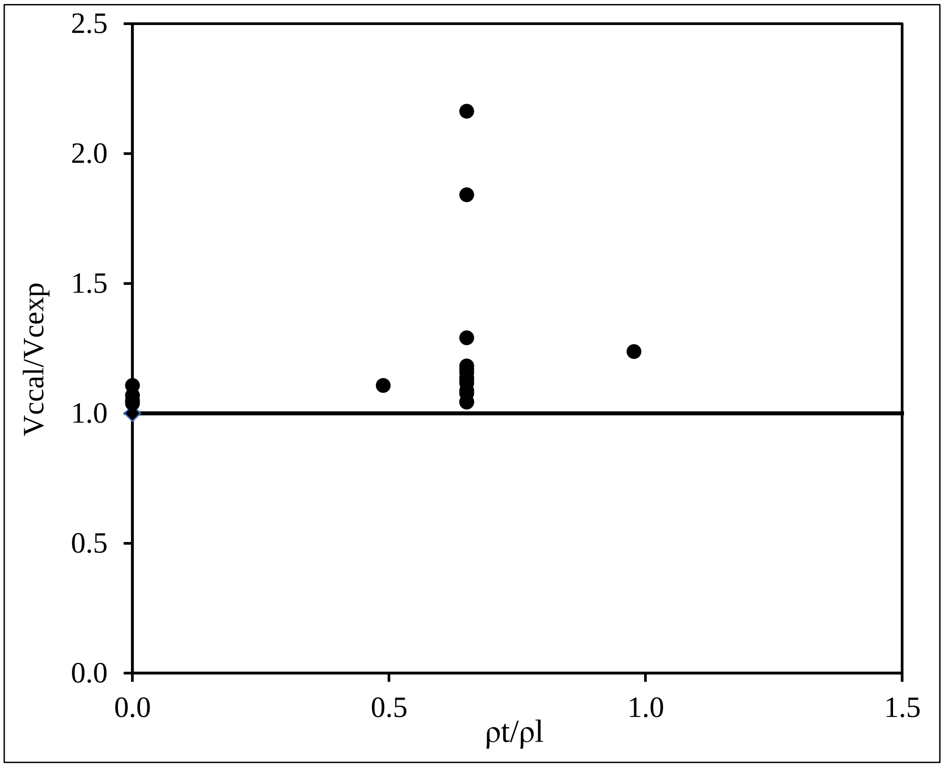

Fig. 5-6 Experimental/calculated shear force ACI Code (2019)

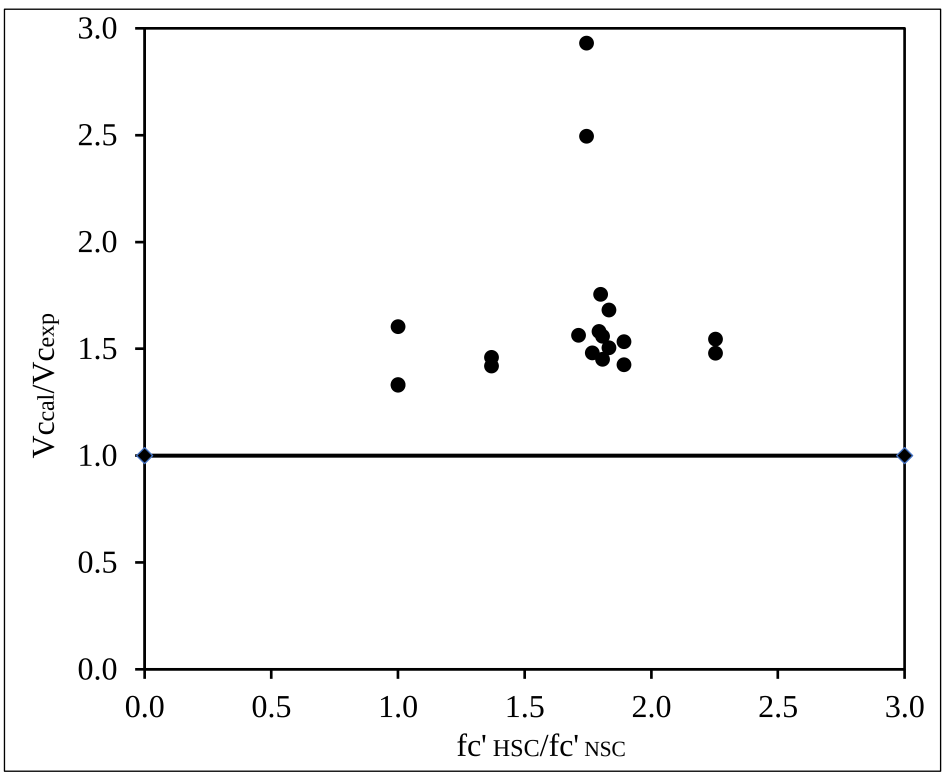

Fig. 5-7 Experimental/calculated shear force EC2 (2004)

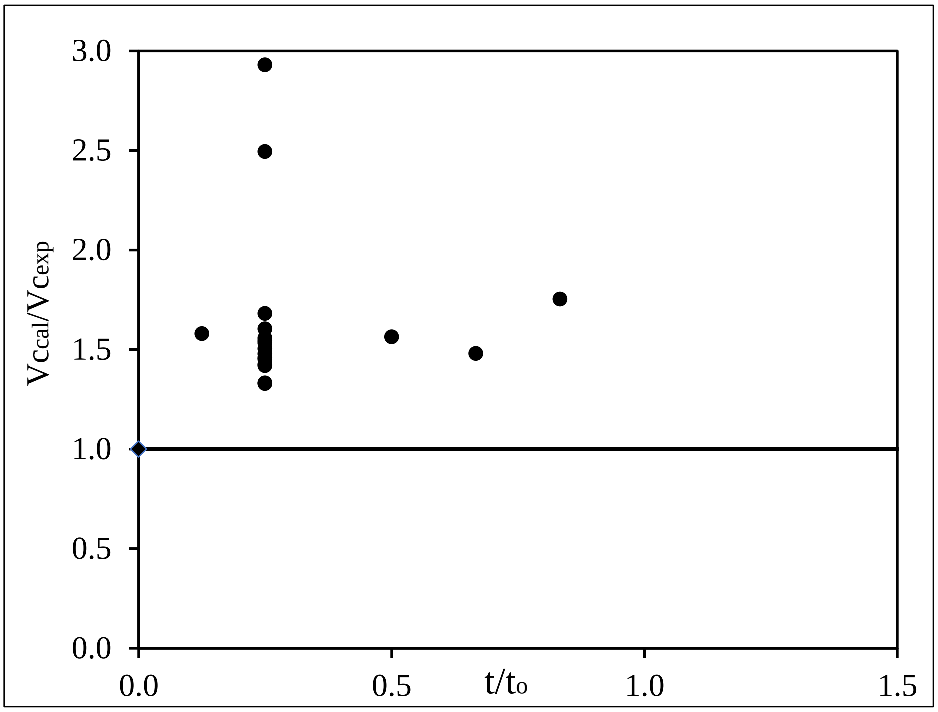

Fig. 5-8 Experimental/calculated shear force EC2 (2004)

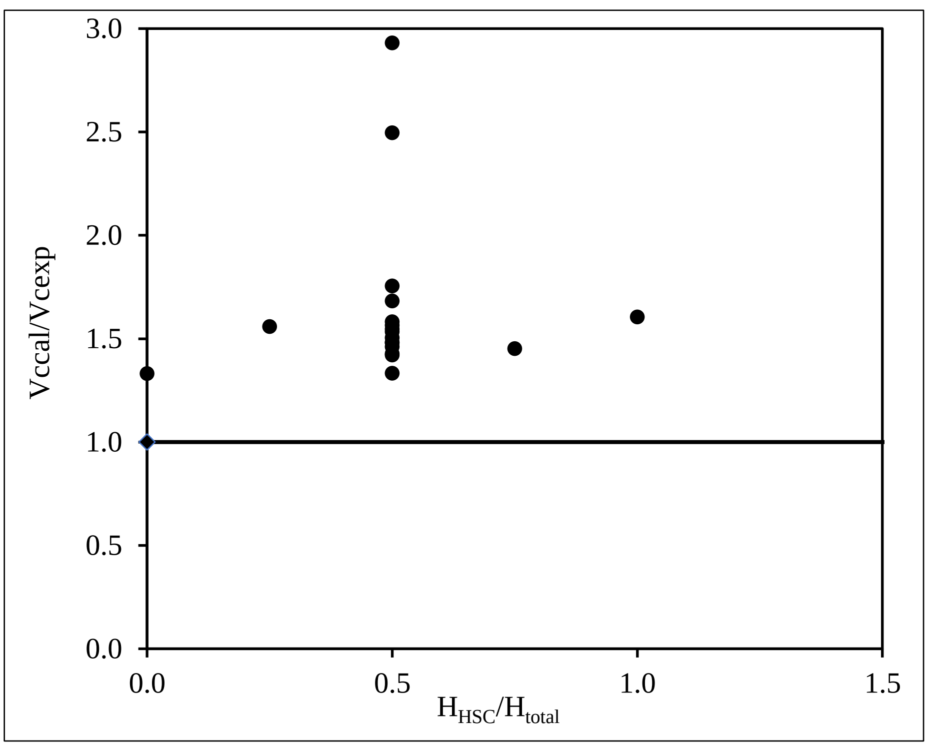

Fig. 5-9 Experimental/calculated shear force EC2 (2004)

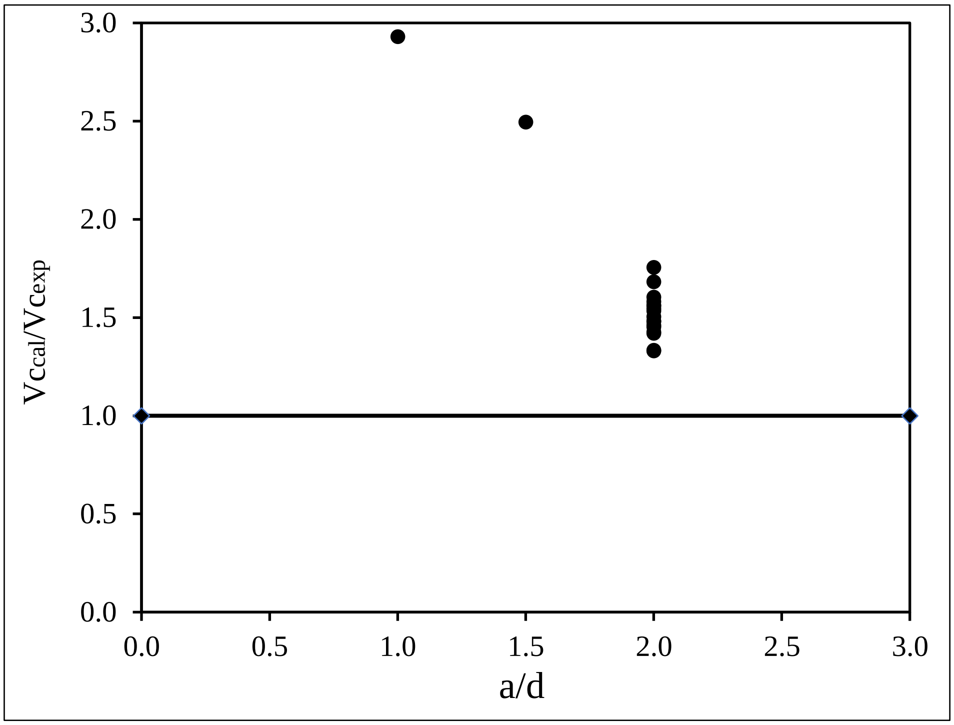

Fig. 5-10 Experimental/calculated shear force EC2 (2004)

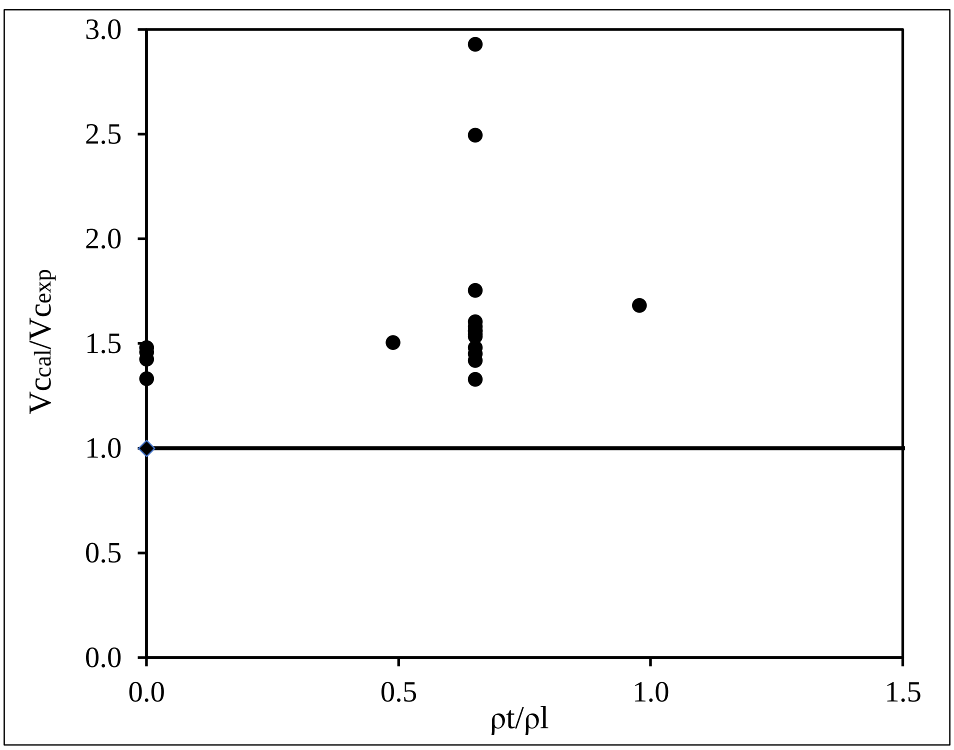

Fig. 5-11 Experimental/calculated shear force (EC2 (2004)

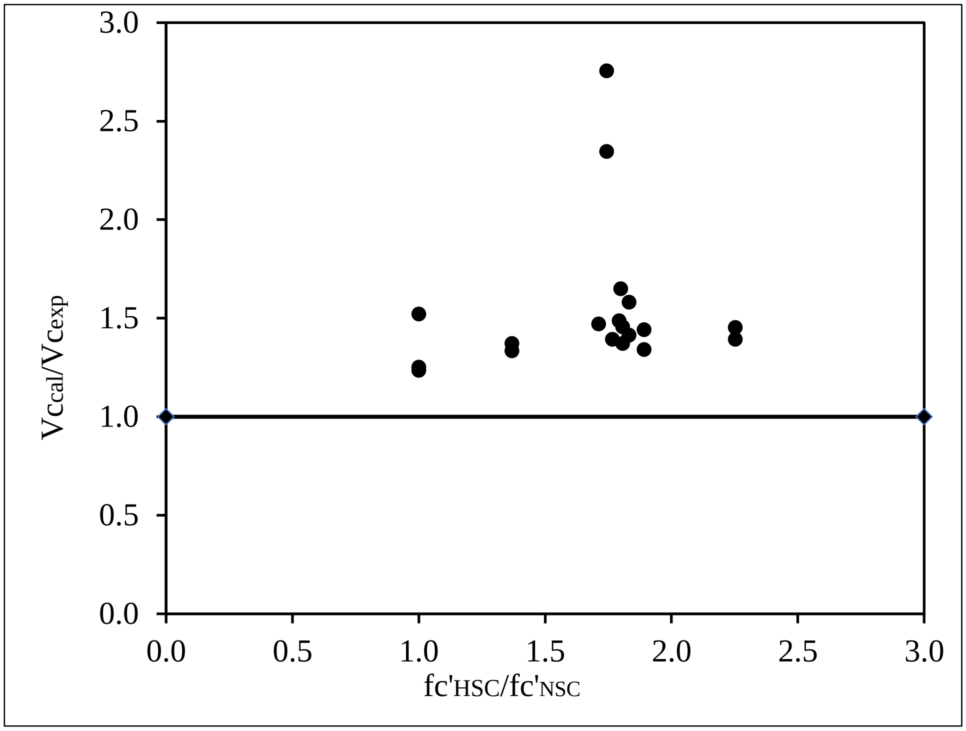

Fig. 5-12 Experimental/calculated shear force BS8110-(1985)

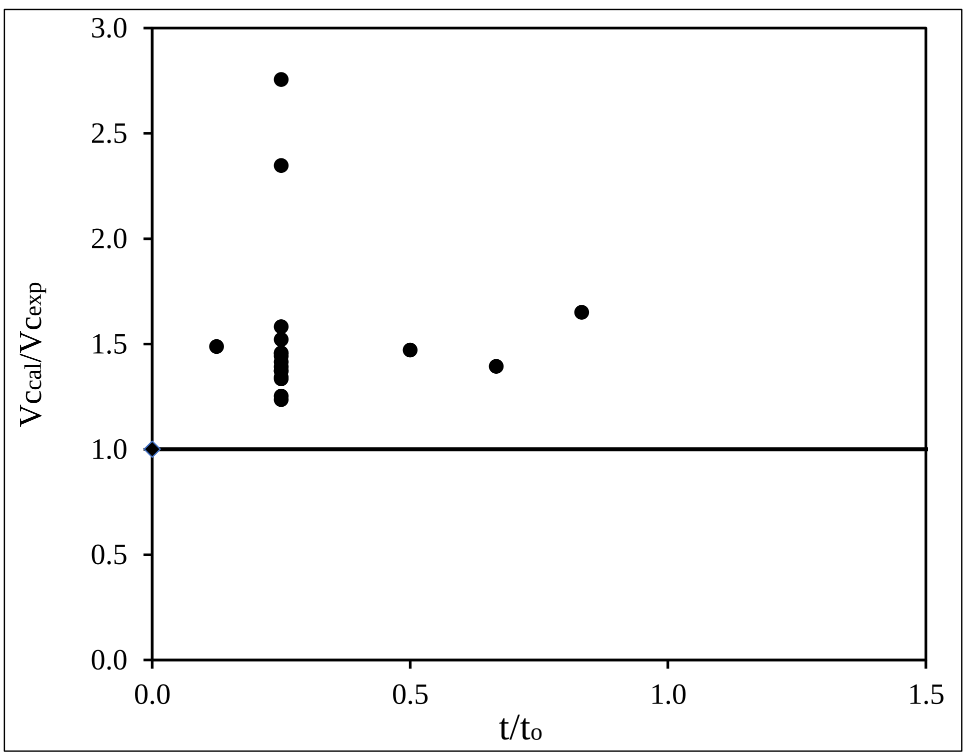

Fig. 5-13 Experimental/calculated shear force BS8110-(1985)

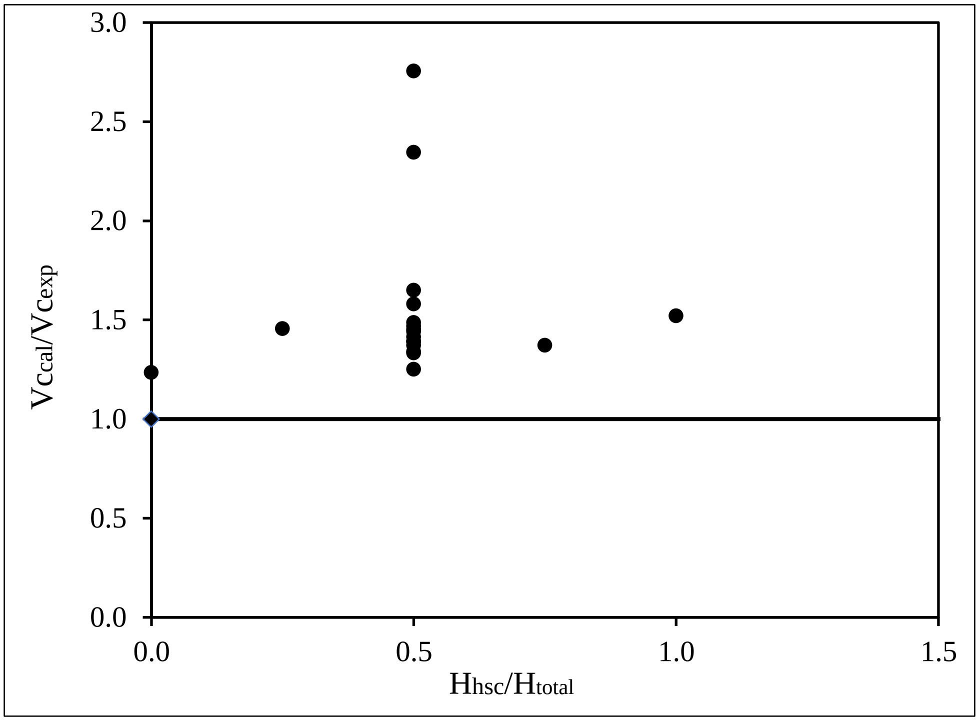

Fig. 5-14 Experimental/calculated shear force BS8110-(1985)

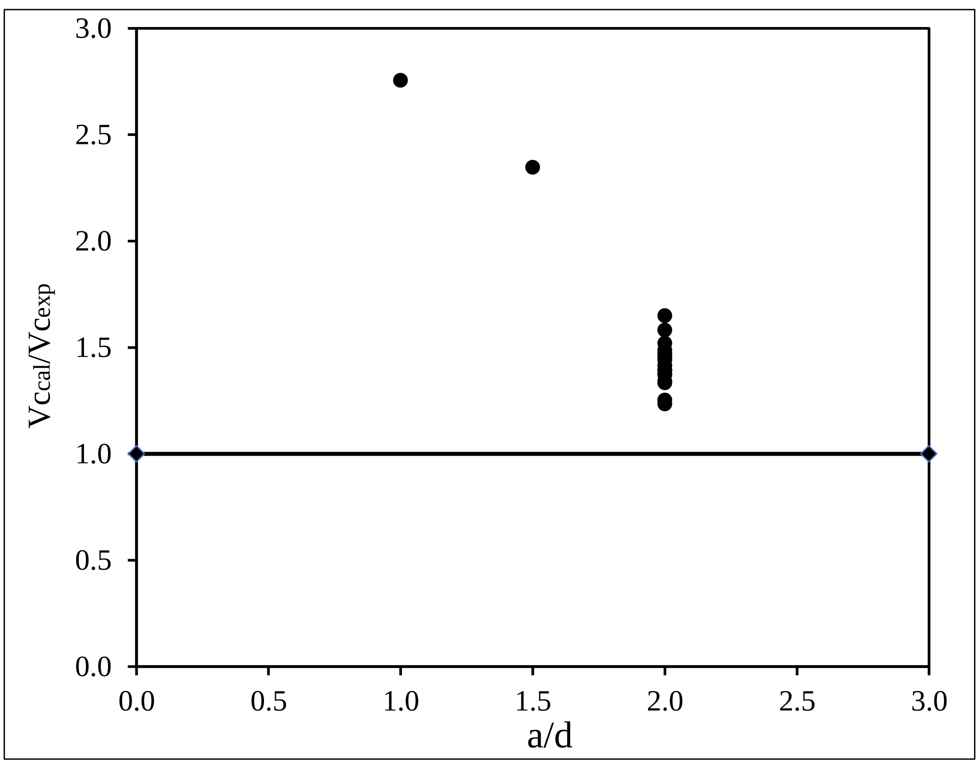

Fig. 5-15 Experimental/calculated shear force BS8110-(1985)

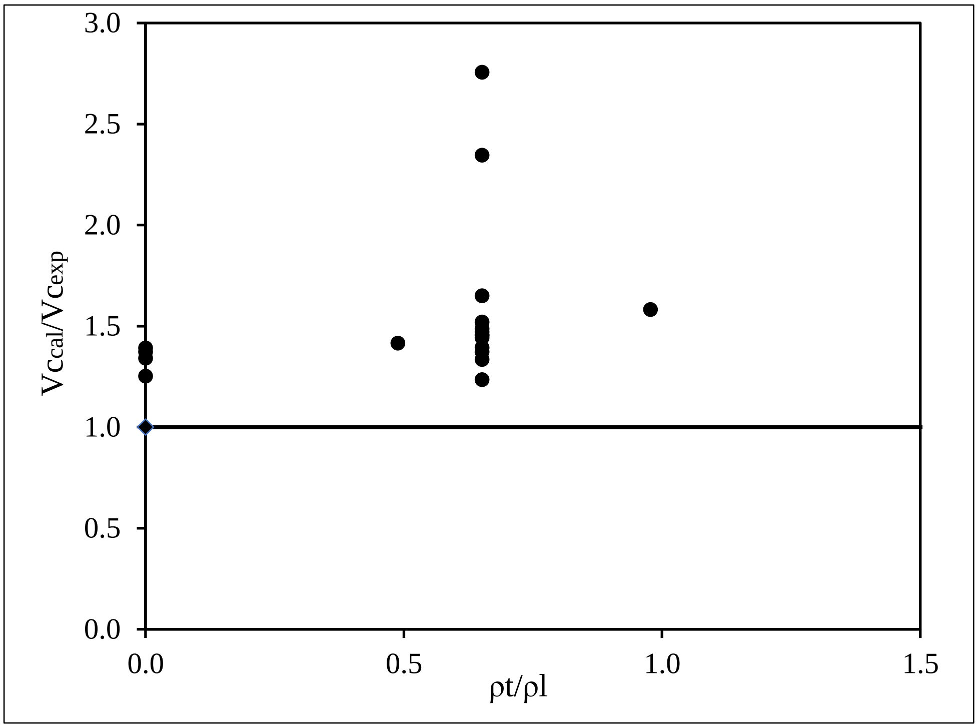

Fig. 5-16 Experimental/calculated shear force BS8110-(1985)

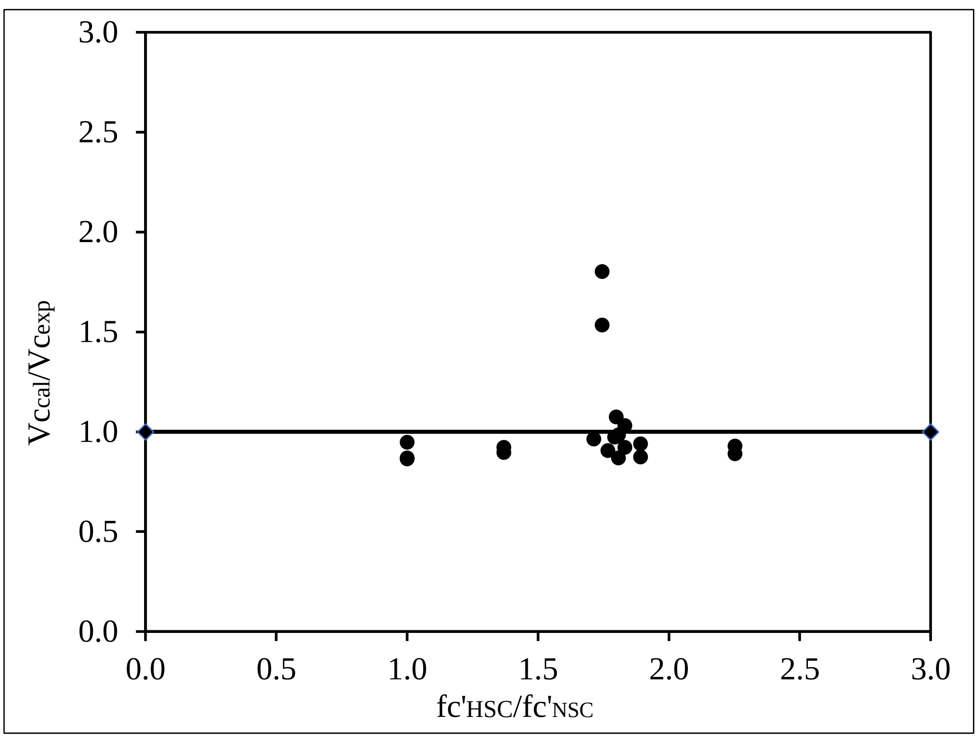

Fig. 5-17 Experimental/calculated shear force CSA Committee A23.3 (2004)

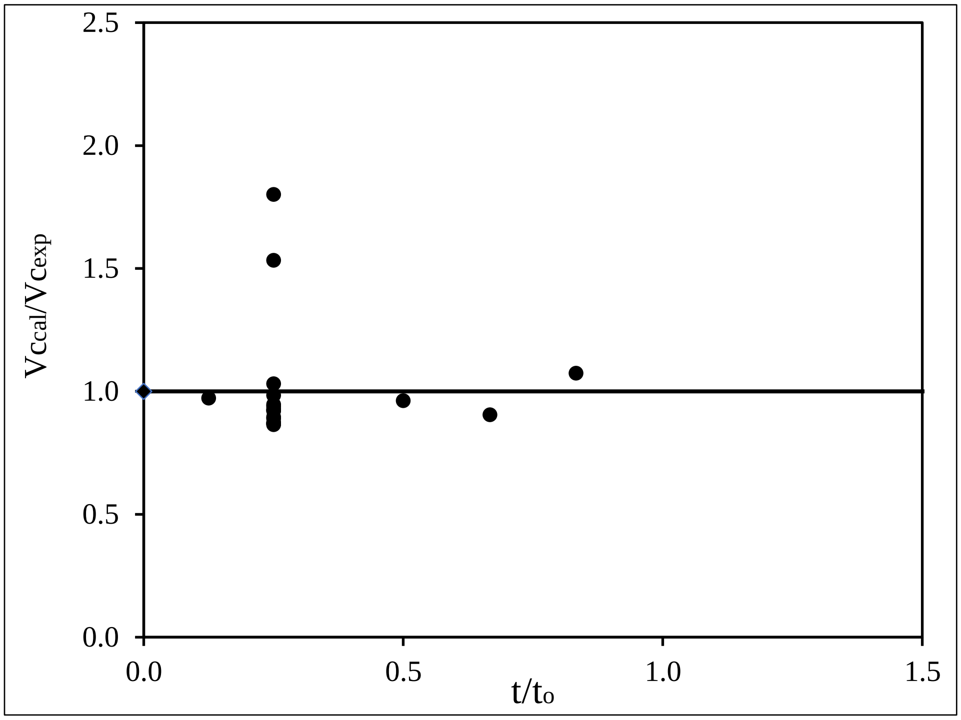

Fig. 5-18 Experimental/calculated shear force CSA Committee A23.3 (2004)

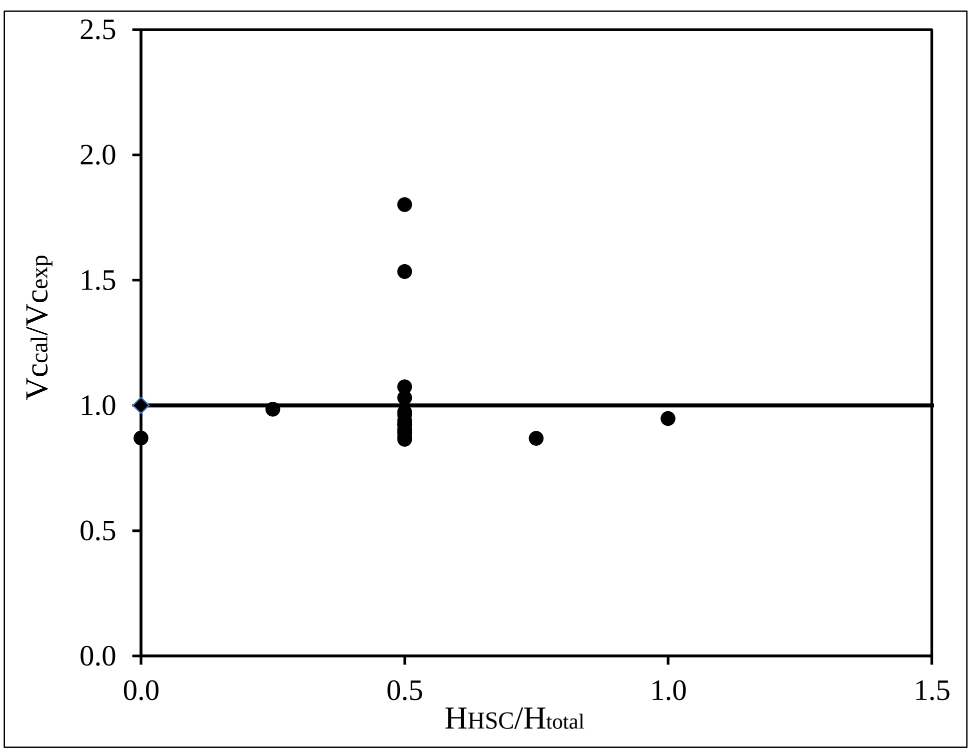

Fig. 5-19 Experimental/calculated shear force CSA Committee A23.3 (2004)

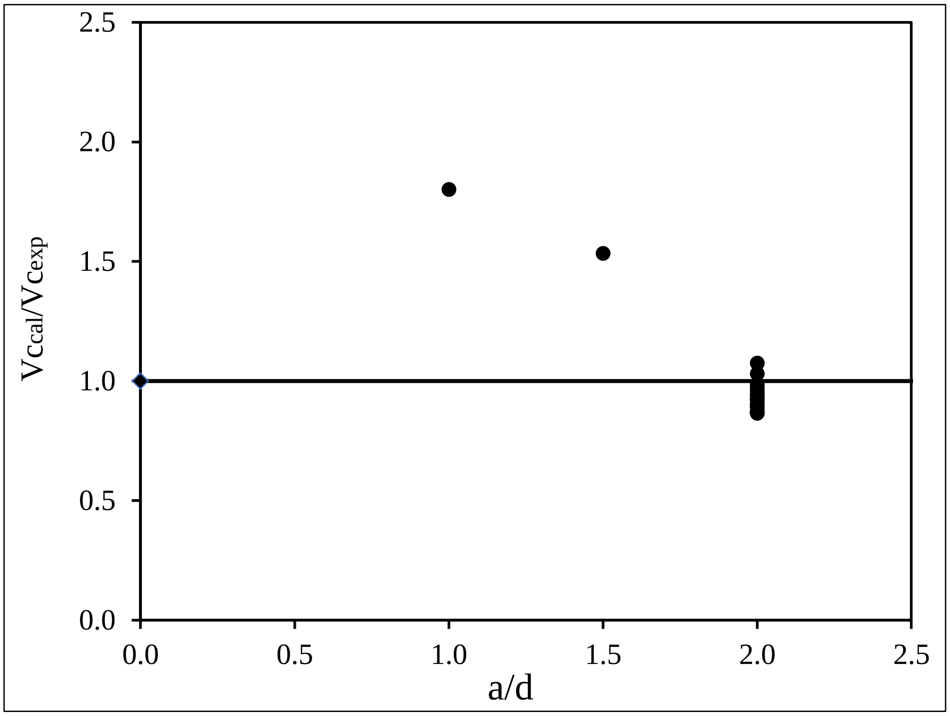

Fig. 5-20 Experimental/calculated shear force CSA Committee A23.3 (2004)

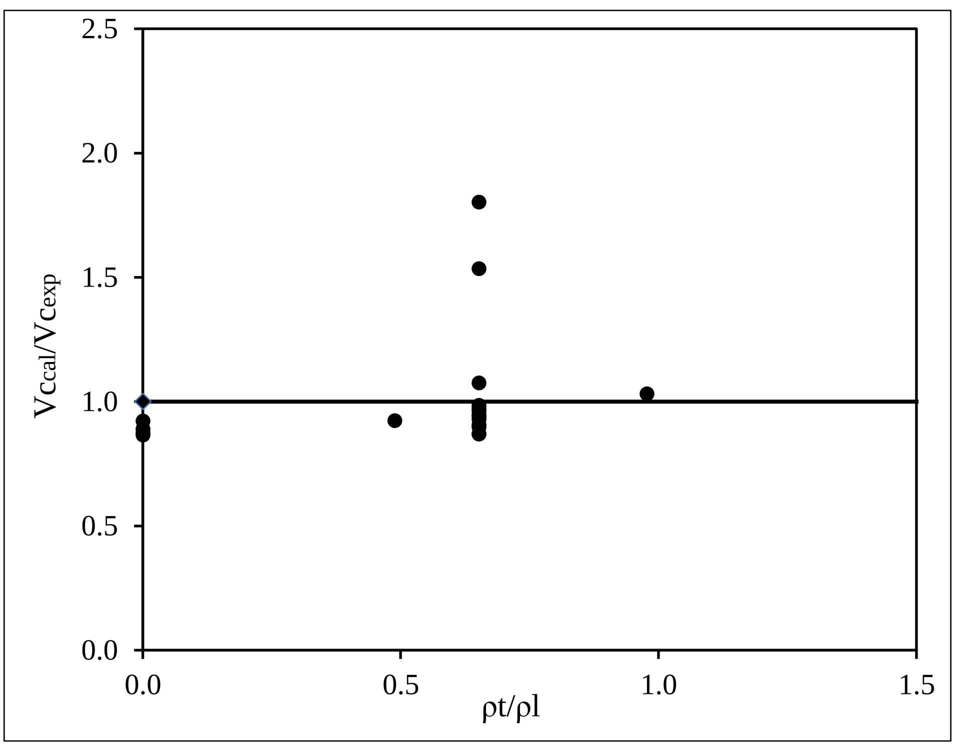

Fig. 5-21 Experimental/calculated shear force CSA Committee A23.3 (2004)

5.2 Modified shear strength equations

The ACI code-19 equation (5.1) for beams with one layer is modified for two layer beams as a function of the variables taken into consideration in this study: The compressive strength ratio $(\frac{fc'_{HSC}}{fc'_{NSC}})$ of the two layers for beams with and without stirrups, overlap casting time as a ratio to the cement initial setting time $(\frac{t}{t_o})$, layer thickness ratio $(\frac{fc'_{HSC}}{fc'_{total}})$, shear span ratio $(\frac{a}{d})$, and spacing of stirrups which is represented by the ratio of transverse reinforcement index divided by the longitudinal index $(\frac{\rho_t}{\rho_l})$. The best fit curve is determined using linear regression analysis and applied to the experimental data, the following equations are proposed to predict the shear strength of the two-layer beams in terms of different variables:

$$Vc = \left(1 + 0.063\ \frac{fc'_{HSC}}{fc'_{NSC}}\right)\left[\frac{\sqrt{fc'}}{6} b_w d\right] \tag{5.17}$$

For beams without stirrups:

$$Vc = \left(1.06 + 0.004\ \frac{fc'_{HSC}}{fc'_{NSC}}\right)\left[\frac{\sqrt{fc'}}{6} b_w d\right] \tag{5.18}$$

$$Vc = \left(1.08 + 0.162\ \frac{t}{t_o}\right)\left[\frac{\sqrt{fc'}}{6} b_w d\right] \tag{5.19}$$

Where: t = overlap casting time (min) t_o = initial setting time of cement

$$Vc = \left(1.097 + 0.02\frac{h_{HSC}}{h_{total}}\right)\left[\frac{\sqrt{fc'}}{6} b_w d\right] \tag{5.20}$$

$$Vc = \left(3.263 - 1.035\ \frac{a}{d}\right)\left[\frac{\sqrt{fc'}}{6} b_w d\right] \tag{5.21}$$

$$Vc = \left(0.92 + 0.3038\ \frac{\rho_t}{\rho_l}\right)\left[\frac{\sqrt{fc'}}{6} b_w d\right] \tag{5.22}$$

Figs. (5-22, 5-27) shows the plot of the shear force ratio ($Vc/Vc_{ACI,}$) and the variables.

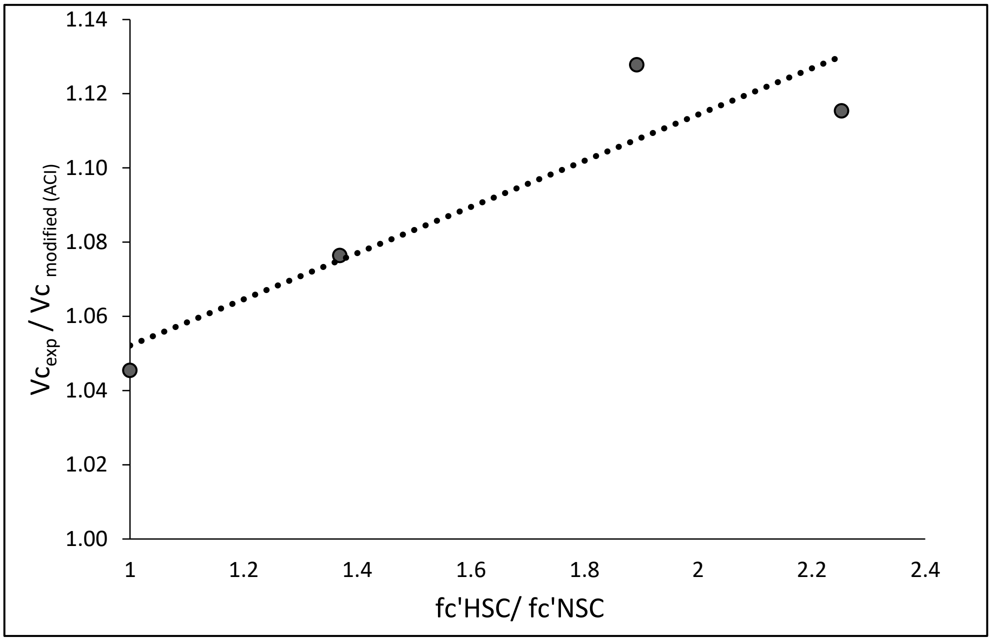

Fig. 5-22 plot of (fc'_{HSC}/fc'_{NSC}) versus (Vc_{exp}/Vc_{ACI}) for beams with stirrups and the best fit Eq. (5.17) (group A)

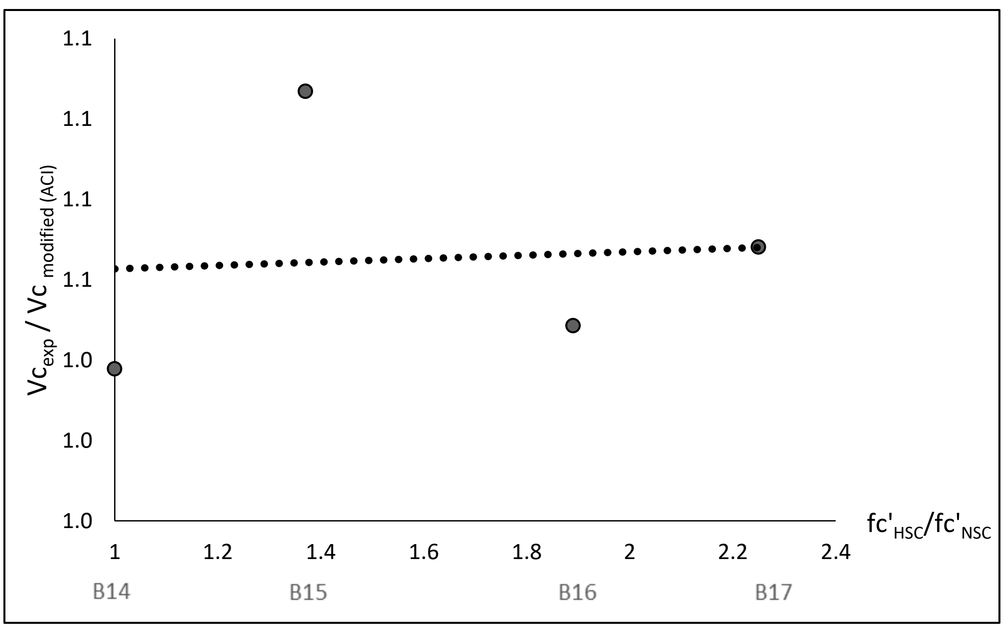

Fig. 5-23 Plot of (fc'_{HSC}/fc'_{NSC}) versus (Vc_{exp}/Vc_{ACI}) for beams without stirrups and the best fit Eq. (5.18) (group E)

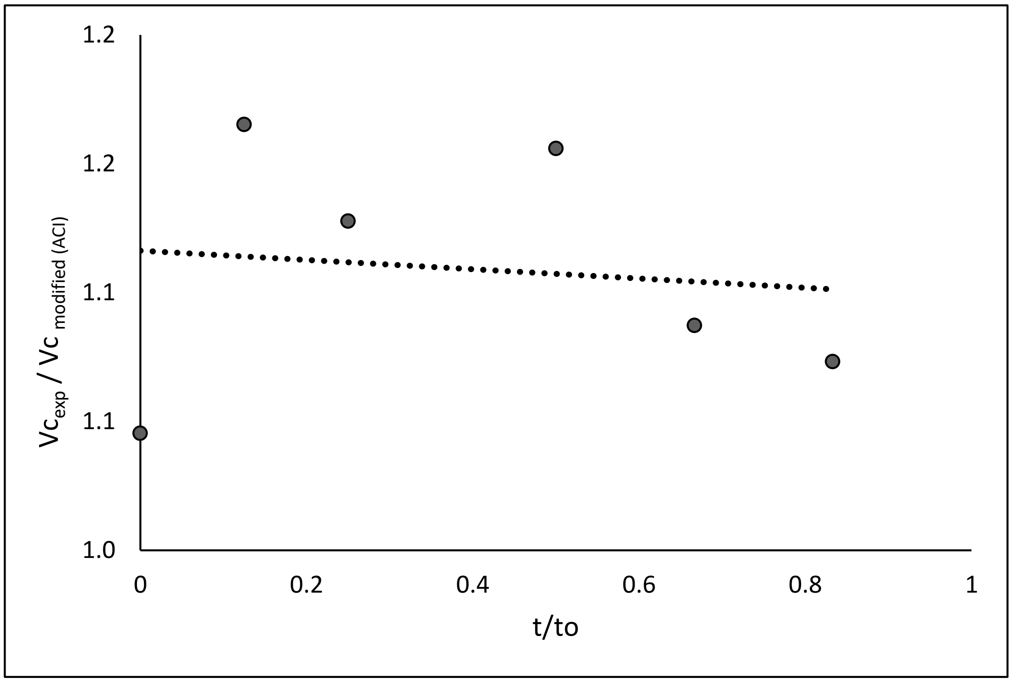

Fig. 5-24 Plot of (t/to) versus (Vc_{exp}/Vc_{ACI}) and the best fit Eq. (5.19) (group B)

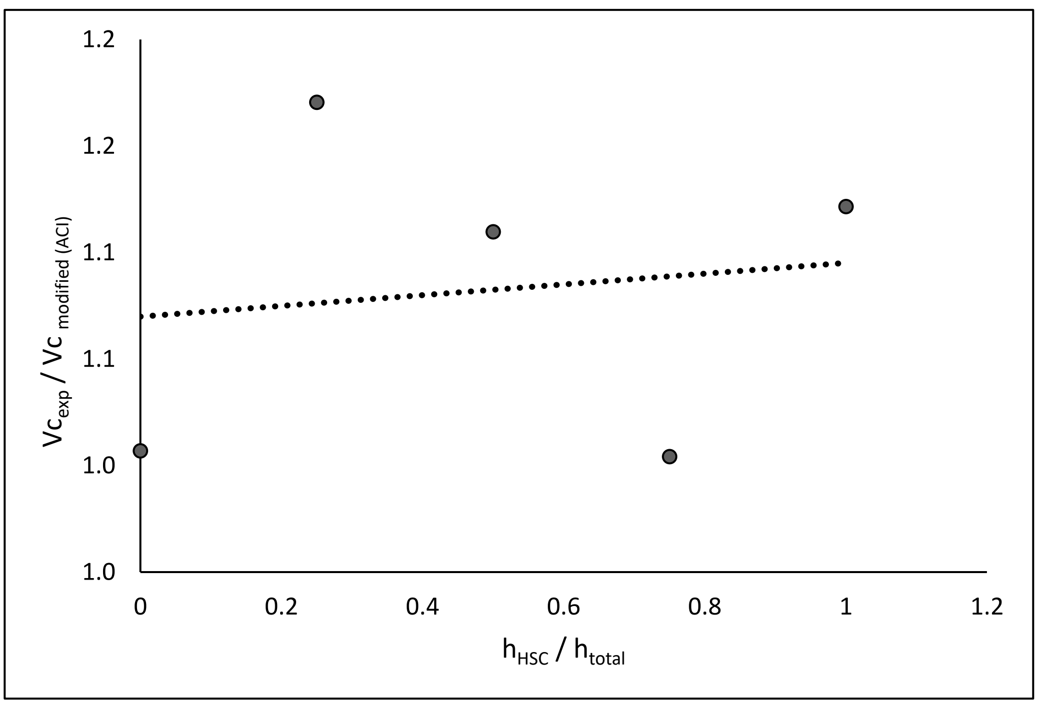

Fig. 5- 25 Plot of (h_{HSC}/h_{total}) versus (Vc_{exp}/Vc_{ACI}) and the best fit Eq. (5.20) (group C)

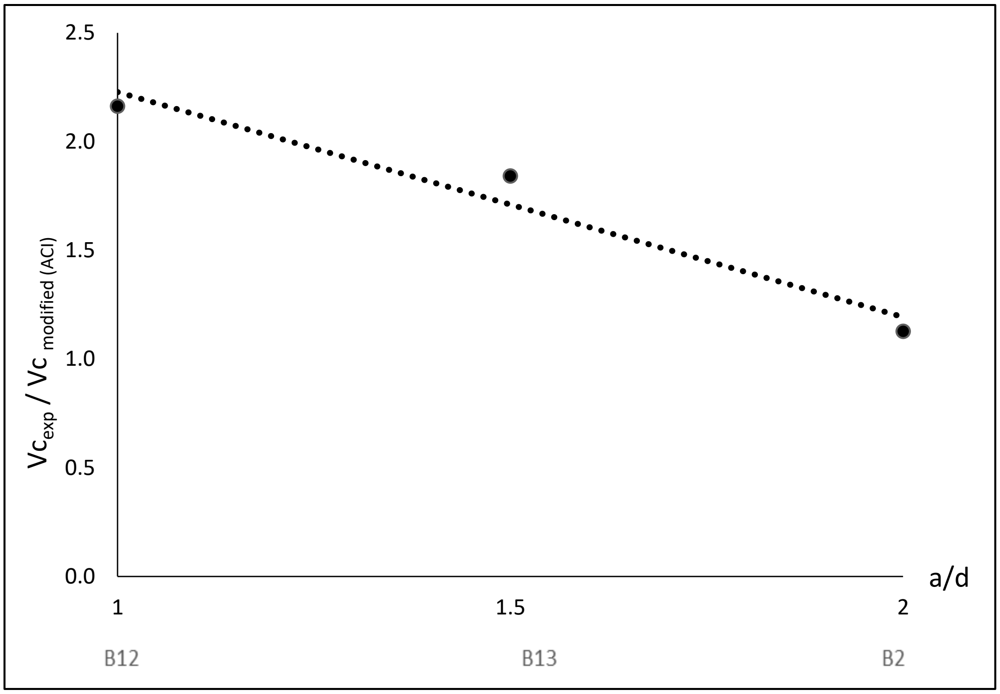

Fig. 5-26 Plot of (a/d) versus (Vc_{exp}/Vc_{ACI}) and the best fit Eq. (5.21) (group D)

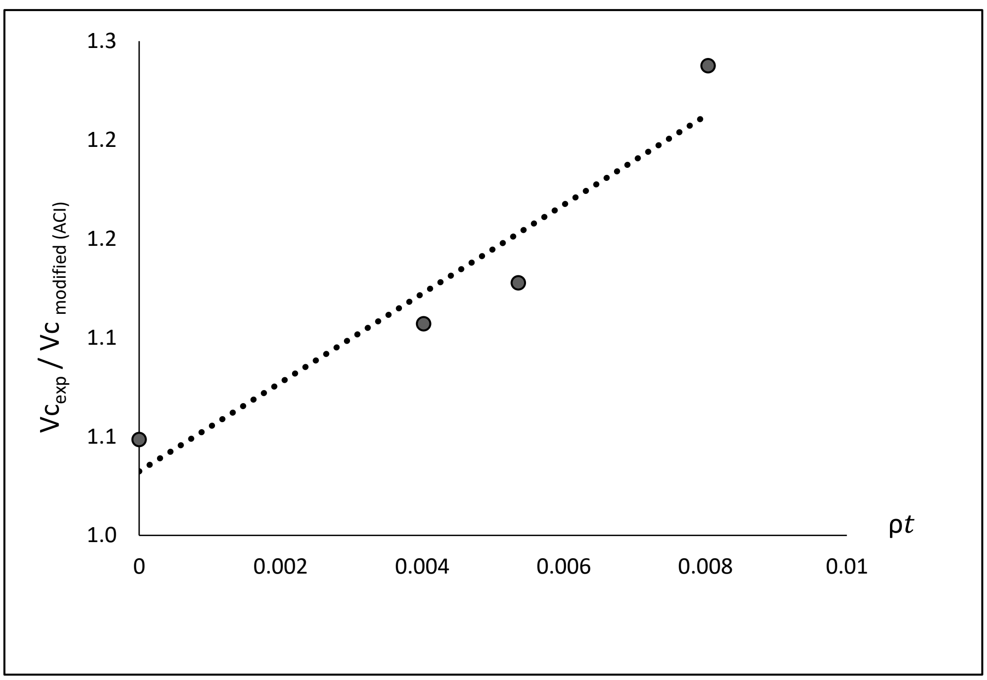

Fig. 5-27 Plot of (ρt) versus (Vc_{exp}/Vc_{ACI}) and the best fit Eq. (5.22) (group F)

As shown the first term of the modified equations represent the modification factor on the ACI 318-19 equation for two-layer beams. The predicted shear strength of the beams from these equations shows excellent correlation with the experimental data, because the maximum and minimum average ratio close to each other and the average ratio (Vc_{exp}/Vc_{cal}) of all these equations are near unity and the coefficient of correction values are acceptable, all statistical data are shown in Table (5-2).

Table 5-2 Summary of the statistical data and proposed equations values of (Vc exp/Vc cal)

Groups	No Eq.	Improved Equation	Avg. R	Max. R	Min. R	St. Dev. (σ)	Varia.	Coeff. of correlation (r)
A	5.17	with stirrups $Vc = \left(1 + 0.063\,\frac{fc'_{HSC}}{fc'_{NSC}}\right)\left[\frac{\sqrt{fc'}}{6} b_w d\right]$	0.989	1.007	0.976	0.0134	0.00018	0.994
E	5.18	without stirrups $Vc = \left(1.06 + 0.004\,\frac{fc'_{HSC}}{fc'_{NSC}}\right)\left[\frac{\sqrt{fc'}}{6} b_w d\right]$	0.999	1.038	0.975	0.028	0.00081	0.962
B	5.19	$Vc = \left(1.08 + 0.162\,\frac{t}{t_o}\right)\left[\frac{\sqrt{fc'}}{6} b_w d\right]$	1	1.060	0.914	0.0564	0.00319	0.883
C	5.20	$Vc = \left(1.097 + 0.02\frac{h_{HSC}}{h_{total}}\right)\left[\frac{\sqrt{fc'}}{6} b_w d\right]$	0.997	1.069	0.935	0.0547	0.00299	0.92
D	5.21	$Vc = \left(3.263 - 1.035\,\frac{a}{d}\right)\left[\frac{\sqrt{fc'}}{6} b_w d\right]$	0.998	1.076	0.945	0.069	0.00484	0.976
F	5.22	$Vc = \left(0.92 + 0.3038\,\frac{\rho_t}{\rho_l}\right)\left[\frac{\sqrt{fc'}}{6} b_w d\right]$	1	1.036	0.937	0.0428	0.00184	0.795

The plot of calculated shear strength from these proposed equations versus the experimental shear strength is shown in Fig. (5.28 – 5.33).

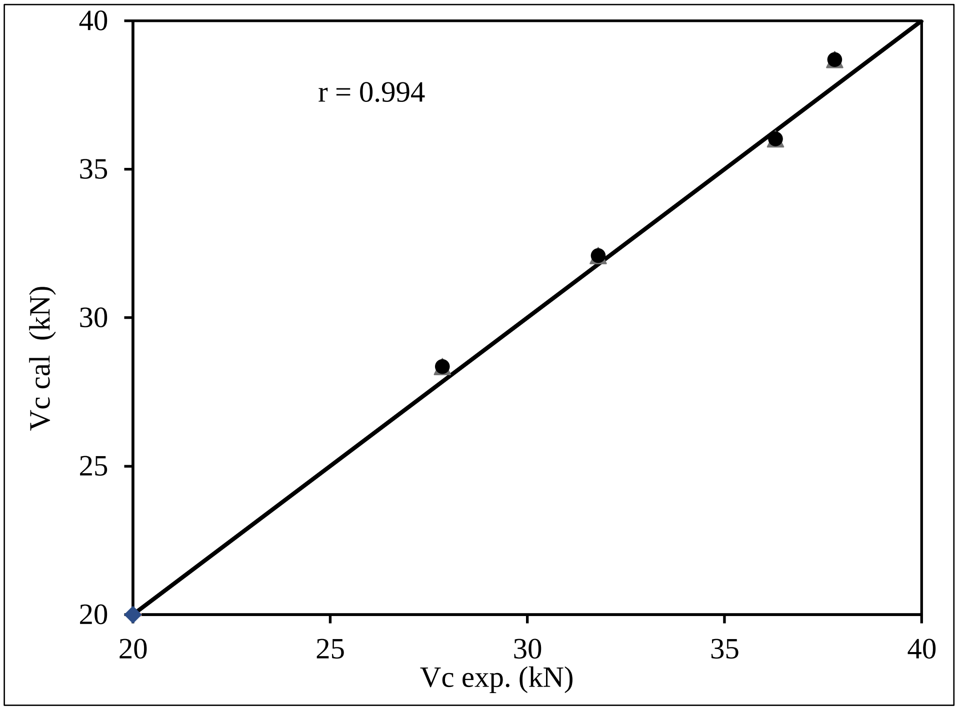

Fig. 5-28 Calculated shear force versus experimental shear force (group A) from proposed eq. (5.17)

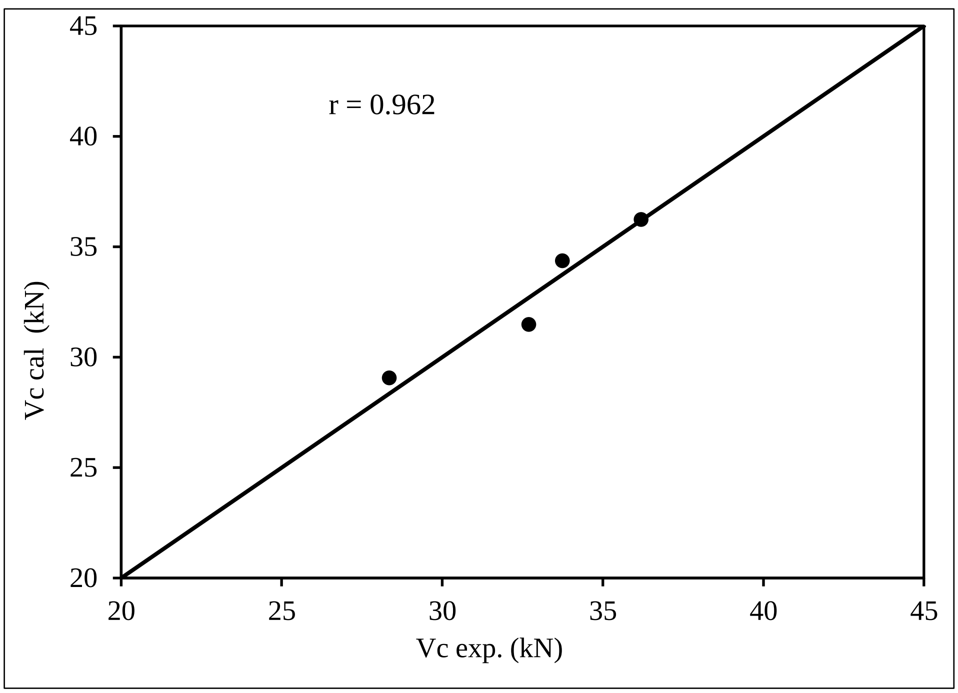

Fig. 5-29 Calculated shear force versus experimental shear force (group E) from proposed eq. (5.18)

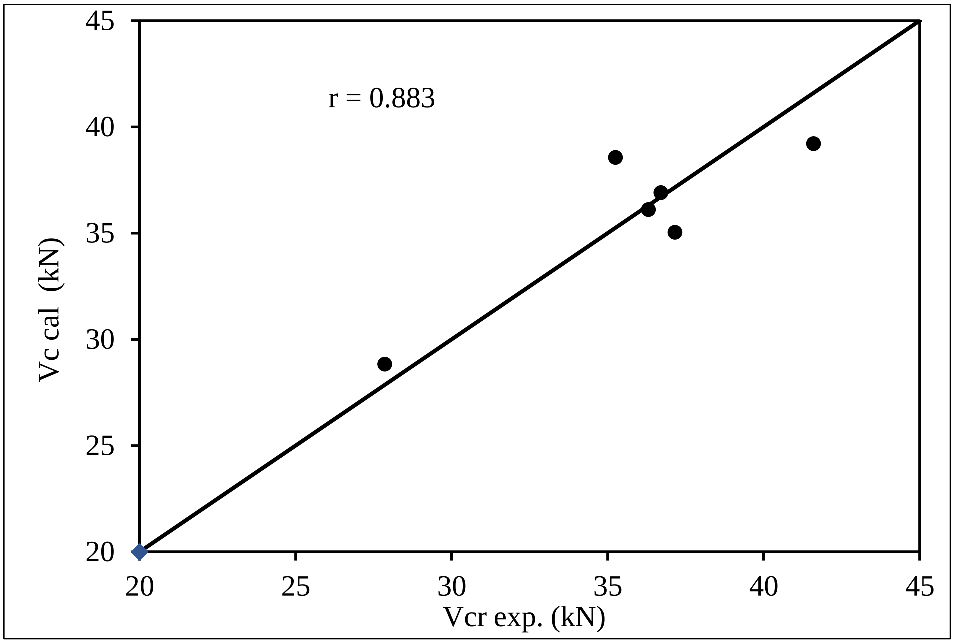

Fig. 5-30 Calculated shear force versus experimental shear force (group B) from proposed eq. (5.19)

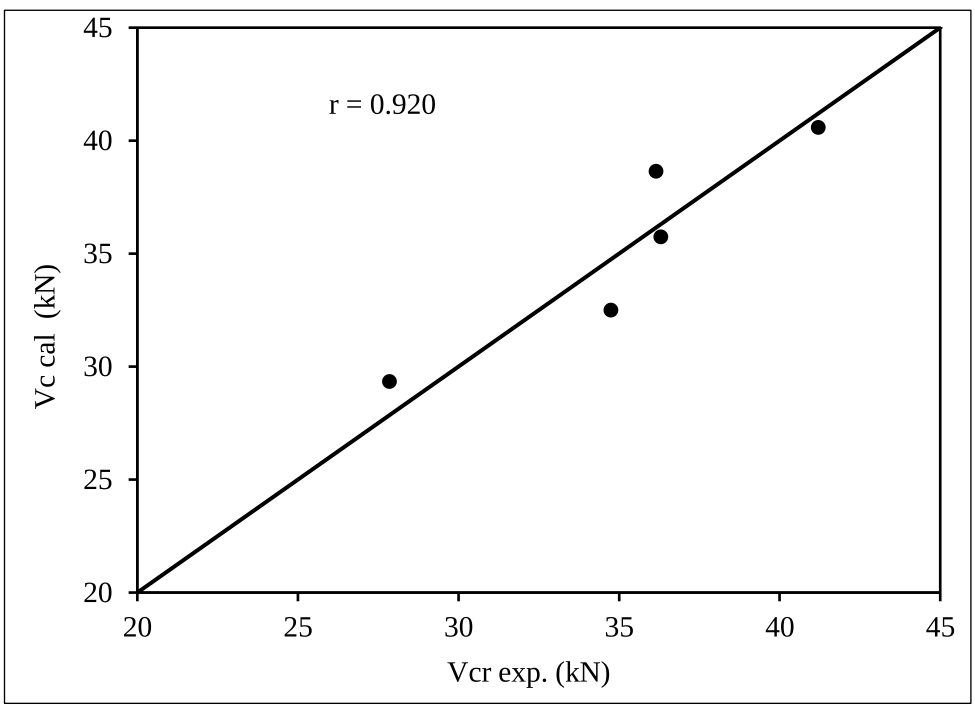

Fig. 5-31 Calculated shear force versus experimental shear force (group C) from proposed eq. (5.20)

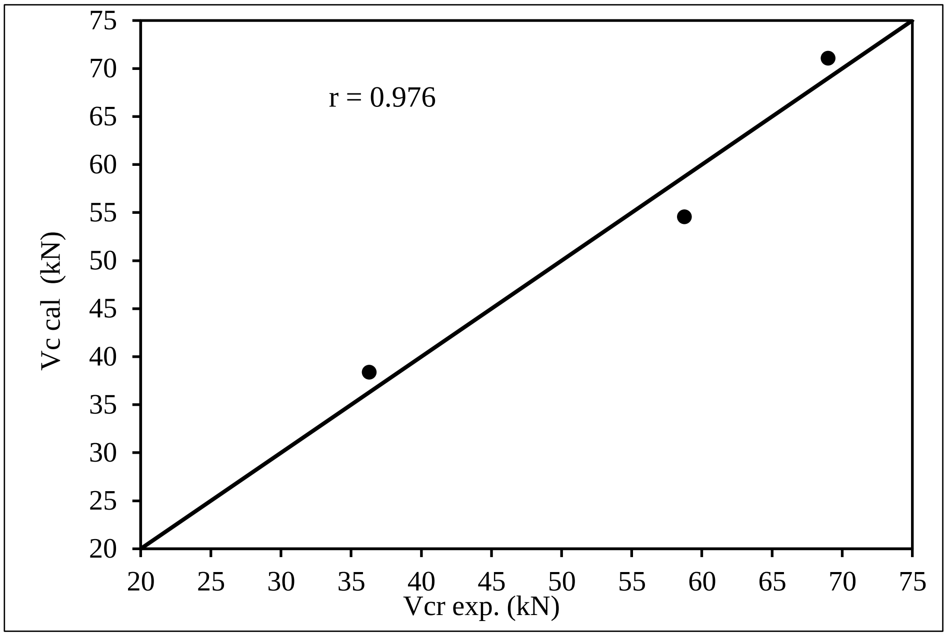

Fig. 5-32 Calculated shear force versus experimental shear force (group D) from proposed eq. (5.21)

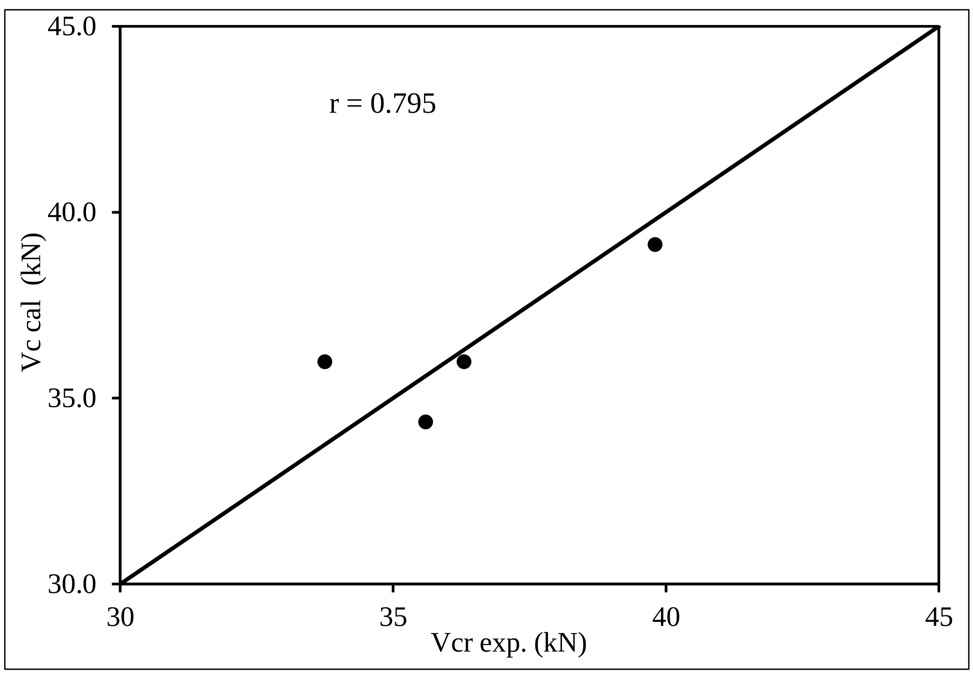

Fig. 5-33 Calculated shear force versus experimental shear force (group F) from proposed eq. (5.22)

Finally, the multi-linear regression analysis method is used to propose a general equation to predict the shear strength of two-layer beams in terms of the variables of this study: the compressive strength ratio ($\frac{fc'_{HSC}}{fc'_{NSC}}$) of the two layers of beams with and without stirrups, overlap casting time as a ratio to the cement setting time ($\frac{t}{t_o}$), layer thickness ratio ($\frac{h_{HSC}}{h_{total}}$), shear span ratio ($\frac{a}{d}$), and spacing of stirrups which are represented by the ratio of transverse reinforcement index divided by the longitudinal index ($\frac{\rho_t}{\rho_l}$).

$$Vc = \left[1.77 + 0.072\left(\frac{fc'_{HSC}}{fc'_{NSC}}\right) + 0.035\left(\frac{t}{t_o}\right) + 0.0188\left(\frac{h_{HSC}}{h_{total}}\right) - 0.4384\left(\frac{a}{d}\right) + 0.2173\left(\frac{\rho_t}{\rho_l}\right)\right]\left[\frac{\sqrt{fc'}}{6} b_w d\right] \quad (5.23)$$

Where:

ρ_t = Percentage of transverse reinforcement

ρ_l = Percentage of longitudinal reinforcement

The average ratio of ($R = Vc_{exp}/Vc_{cal}$) is (1.017) and coefficient of correlation (r = 0.965). The plot of calculated shear strength verse experimental data is shown in Fig. (5-34).

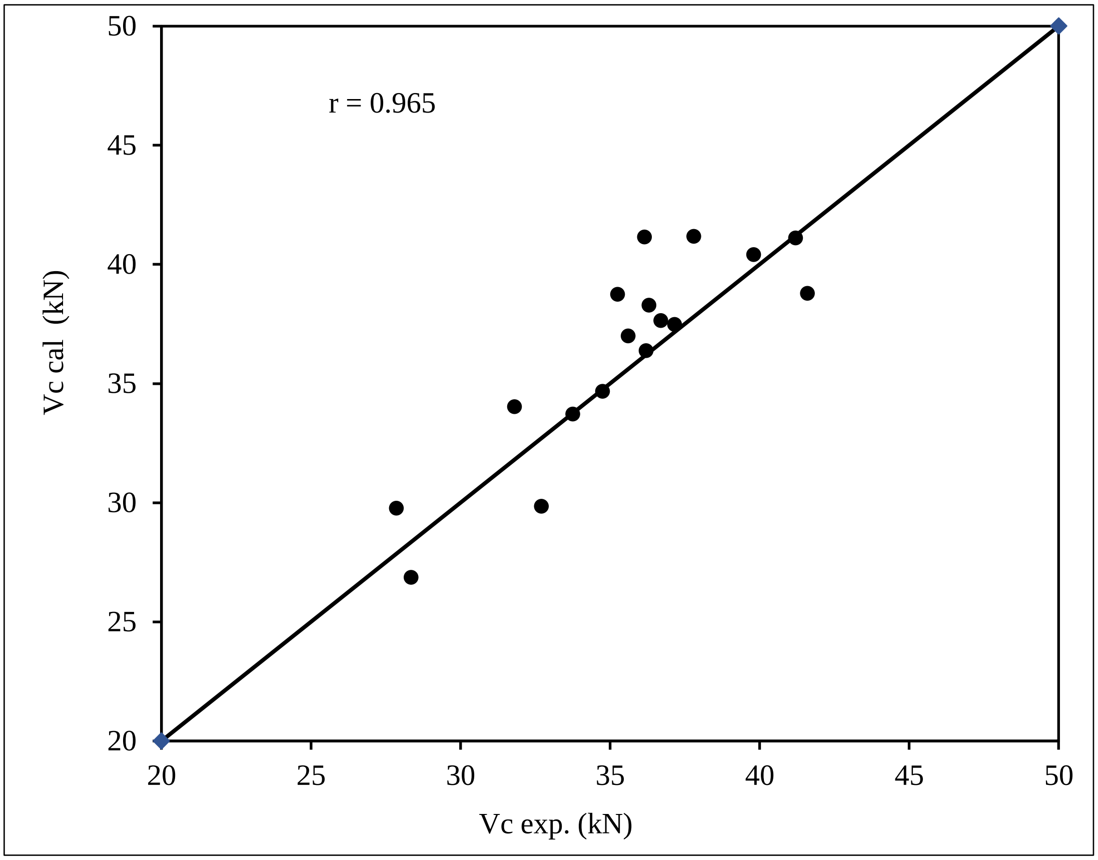

Fig. 5-34 Experimental versus calculated shear force from proposed eq. (5.23)

5.3 Flexural calculations

Nominal bending moment of rectangular section shown in Fig. (5-35), can be calculated from the following equation for under reinforcement concrete beam

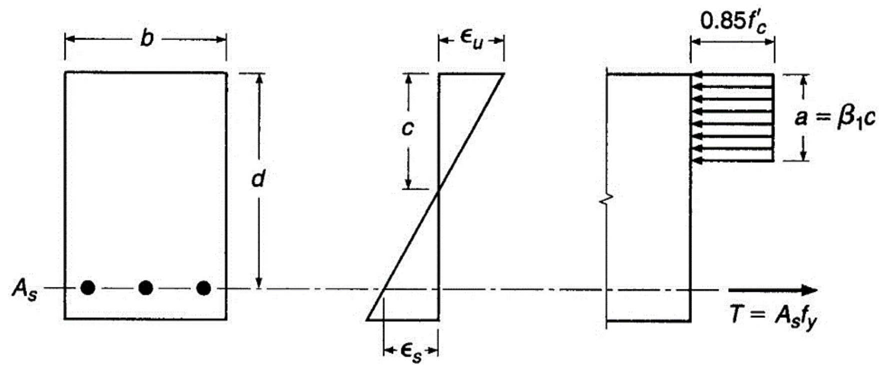

Fig. 5-35 Singly reinforced concrete beam (Nilson et al., 2009)

$Mn = As\, fy(d - \frac{a}{2})$ (Nilson et al., 2009) (5.24)

$a = \frac{As\, fy}{0.85\, fc'_{HSC} b_w}$ (5.25)

If $a < h_{HSC}$

$Mn = \rho b d^2 fy \left(1 - 0.59 \frac{fy}{fc'_{HSC}}\right)$ (Nilson et al., 2009) (5.26)

If $a > h_{HSC}$

$c_1 = 0.85 fc'_{HSC}(h_{HSC} \times b_w)$ (5.27)

$c_2 = 0.85\, fc'_{NSC}(a - h_{HSC}) b_w$ (5.28)

$T = A_s fy$ (5.29)

$C = C_1 + C_2$ (5.30)

Where: -

$$a = \frac{A_s fy - 0.85 fc'_{HSC}(h_{HSC} \times b_w)}{0.85\ fc'_{NSC} \times b_w} + h_{HSC} \tag{5.31}$$

$$Mn_1 = 0.85 fc'_{HSC}\ h_{HSC}\ b_w \left(d - \frac{h_{HSC}}{2}\right) \tag{5.32}$$

$$Mn_2 = 0.85 fc'_{NSC}(a - h_{HSC}) b_w \left[d - \left(\frac{a + h_{HSC}}{2}\right)\right] \tag{5.33}$$

$$Mn = Mn_1 + Mn_2 \tag{5.34}$$

Experimental bending moment for beam subjected to two equal point loads can be determined as the following:

$$Mu_{exp} = \frac{Pu_{exp}}{2} \times a \tag{5.35}$$

Where:

Pu = ultimate failure load (N)

a = Shear span (mm)

Also cracking bending moment is:

$$M_{cr} = \frac{P_{cr}}{2} \times a \tag{5.36}$$

Where:

$P_{cr} =$ Cracking load (N)

The theoretical and experimental cracking and ultimate bending moments of all beams are shown in Table (5-3), generally the experimental ultimate bending moment is greater than theoretical values, and the ratio of (Mu_{exp} /Mu_{cal}) of all beams is greater than one, the average ratio (1.2364).

Table 5-3 Experimental and calculated moment ratio with cracking moment

Groups	Beam No.	a (m)	Mcr (kN.m)	Mu_{exp} (kN.m)	Mu_{cal} (kN.m)	Mu_{exp}/Mu_{cal}
A	1	0.44	5.492	29.964	23.966	1.2503
	2	0.44	5.391	31.966	24.342	1.3132
	3	0.44	5.351	32.868	24.51	1.3410
B	4	0.44	5.421	32.076	24.294	1.3203
	5	0.44	5.483	31.636	24.27	1.3035
	6	0.44	5.533	31.46	24.33	1.2931
	7	0.44	5.478	31.416	24.326	1.2915
C	8	0.44	5.481	27.641	23.278	1.1874
	9	0.44	5.440	27.984	24.313	1.1510
	10	0.44	5.440	30.58	24.313	1.2578
	11	0.44	7.134	33.088	24.326	1.3602
D	12	0.22	5.478	31.889	24.29	1.3128
	13	0.33	5.478	32.109	24.29	1.3219
E	14	0.44	5.592	24.53	23.474	1.0450
	15	0.44	5.492	25.08	23.966	1.0465
	16	0.44	5.391	25.366	24.342	1.0421
	17	0.44	5.351	26.092	24.51	1.0645
F	18	0.44	5.437	32.76	24.328	1.3466
	19	0.44	5.437	30.228	24.328	1.2425
Average						1.2364

The first flexural cracking shear force occurred before the diagonal cracking shear force, the experimental flexural first cracking load (Vc_1) and the diagonal shear force (Vc) of all beams are shown in Table (5-4), the ratio of (Vc_1/Vc) of all beams is less than one, and the average ratio is about (0.578), that is the flexural first cracking shear is about (57.8 %) of the diagonal cracking shear, and the diagonal cracking shear is greater than the flexural first cracking shear by about (73%).

The flexural first cracking shear force can be calculated from the transformed uncracked section of two-layer reinforced concrete beam shown in Fig. (5-36).

$$y' = \frac{\frac{b_w h^2}{2} + (n-1)As\, d + (n'-1)As' d'}{b_w d + (n-1)As + (n'-1)As'} \qquad (5.37)$$

Where:

$$n = \frac{Es}{Ec_{NSC}}$$

$$n' = \frac{Es}{Ec_{HSC}}$$

$$Ec = 4730\sqrt{fc'}$$

Where:

As = area of reinforcement in tension zone (NSC) mm^2

As' = area of reinforcement in compression zone (HSC) mm^2

Moment of inertia of the transformed section (Ig)

$$I_g = \frac{b_w h^3}{12} + b_w h\,(y' - \frac{h}{2})^2 + (n-1)As\,(d - y')^2 + (n'-1)As'(y' - d')^2 \qquad (5.38)$$

$$M_{cr} = \frac{f_r\, I_g}{y_t} \qquad (5.39)$$

Where: f_r = modulus of rupture of the concrete = $0.625\sqrt{fc'}$ (MPa)

$y_t = h - y'$ distance from the neutral axes to the tension face (mm)

$$Vc_1 = \frac{M_{cr}}{a} \tag{5.40}$$

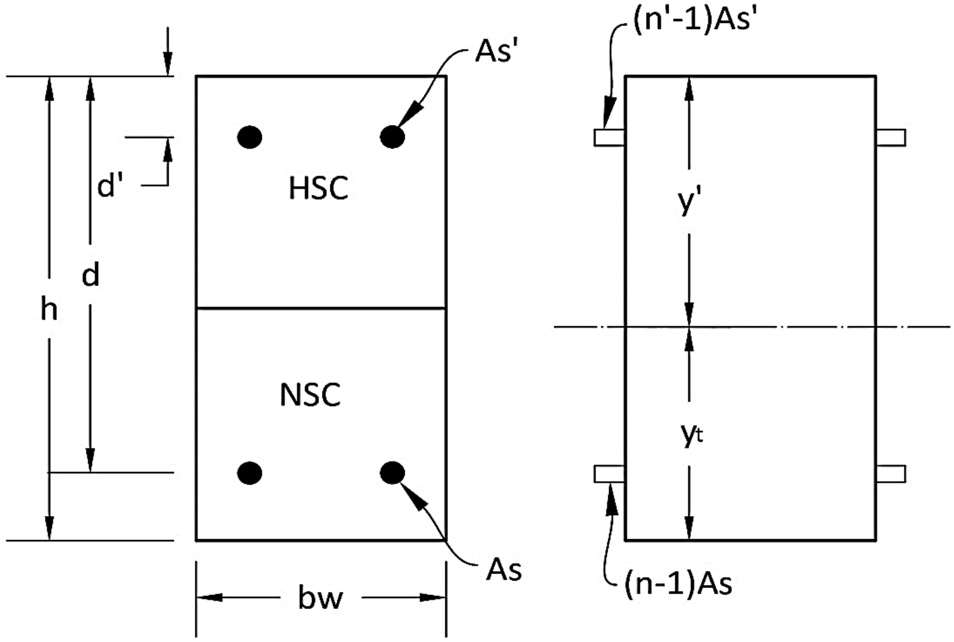

Fig. 5-36 Uncracked transformed beam section

The theoretical results of the flexural first cracking shear for all beams are less than the experimental values as shown in Table (5-4), the ratio of experimental cracking shear to predicted value ($Vc_{1\,exp}/Vc_{1\,cal}$) is greater than one for all beams and the average value is (1.644).

Table 5-4 Relation between first flexural and diagonal shear crack

Groups	Beam No.	$Vc_{1\ Exp}$	$Vc_{1\ cal}$	Vc_{Exp} (kN)	Vc_{1Exp}/Vc_{cal}	$Vc_{1\ exp}/Vc_{exp}$
A	1	17.8	12.482	31.8	1.4261	0.5597
	2	17.4	12.252	36.3	1.4202	0.4793
	3	18.05	12.162	37.8	1.4841	0.4775
B	4	21.5	12.320	37.15	1.7451	0.5787
	5	18.7	12.462	36.7	1.5006	0.5095
	6	18.55	12.576	35.25	1.4751	0.5262
	7	19.7	12.450	41.6	1.5823	0.4736
C	8	25.2	12.456	27.85	2.0232	0.9048
	9	19.3	12.363	34.75	1.5611	0.5554
	10	17.35	12.363	36.15	1.4034	0.4799
	11	18.95	16.214	41.2	1.1688	0.4600
D	12	44.7	24.901	69	1.7951	0.6478
	13	51.8	16.601	58.75	3.1204	0.8817
E	14	16.15	12.708	28.35	1.2708	0.5697
	15	24.8	12.482	32.7	1.9869	0.7584
	16	19.6	12.252	33.75	1.5998	0.5807
	17	20.2	12.162	36.2	1.6609	0.5580
F	18	17.55	12.357	39.8	1.4202	0.4410
	19	19.7	12.357	35.6	1.5942	0.5534
Average					1.644	0.578

Depending on the experimental data of the flexural first cracking shear (Vc_1) and the variables taken in this study, equation (5.40) is modified using multi-linear regression analysis to predict flexural first cracking shear in terms of the variables of the study.

The proposed equation:

$$Vc_1 = [1.55 + 0.076\frac{fc'_{HSC}}{fc'_{NSC}} - 0.27\frac{t}{t_o} + 0.73\frac{h_{HSC}}{h_{total}} - 0.17\frac{a}{d} + 0.024\frac{\rho t}{\rho l}](\frac{f_r\, I_g}{y_t.a}) \quad (5.41)$$

The average ratio of experimental flexural first cracking shear divided by the calculated value ($Vc_{1\ exp}/Vc_{1\ cal}$) is (1.011) and the coefficient of correlation is (0.67). The plot of calculated versus experimental flexural first cracking shear data shown in Fig. (5-37).

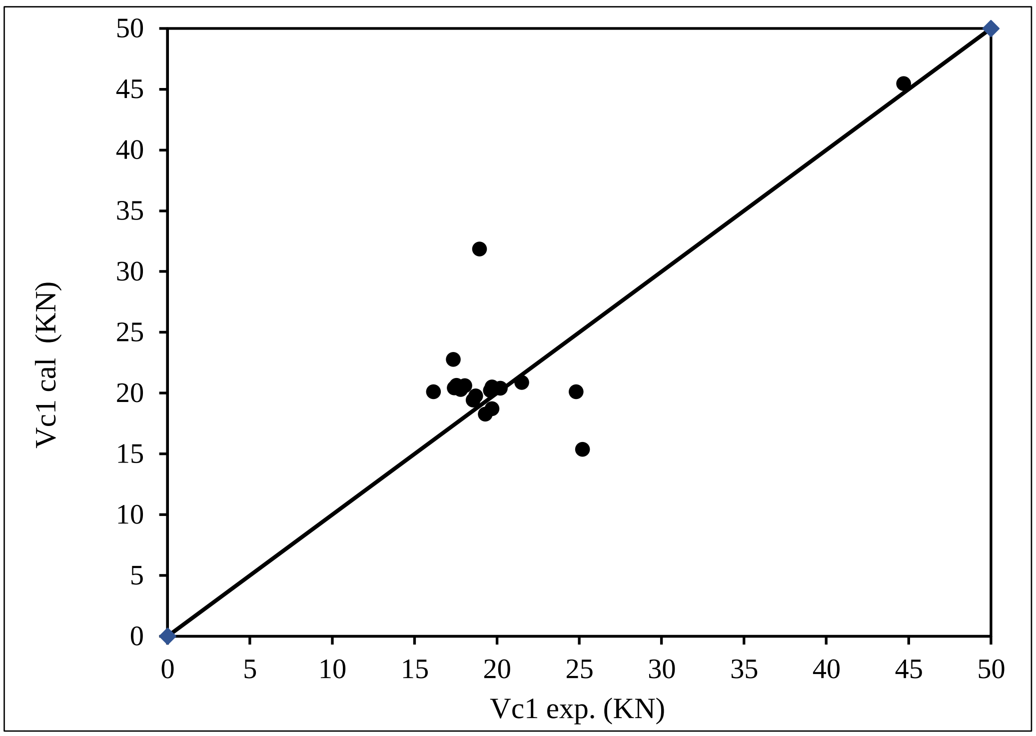

Fig. 5-37 Experimental versus calculated first shear force from proposed eq. (5.41)

CHAPTER SIX

CONCLUSIONS AND RECOMMENDATIONS

6.1 Conclusions

The following conclusions can be drawn from the experimental results obtained from the tested beams:

1. The mid-span deflection and the crack pattern of the two-layer reinforced concrete beams are similar and closer to the crack pattern and behavior of the control beam (one layer of normal strength concrete)

2. Increasing the compressive strength of the top layer, the ultimate failure load increased by (8.35%, 15.6%, and 18.85%), with respect to the (control beam) which has a full depth of normal concrete.

3. In general, the cracking and the value of ultimate shear strength increased when the waiting time (overlap time) was 15 minutes between the casting of the two layers. This value decreased when the waiting time was extended to 100 minutes. Therefore 30 minutes or less of waiting time (overlap time) between the layers is recommended.

4. The increase in the depth of the layer high strength concrete (top layer), resulted in the increase of ultimate load by (1.2%, 15.6%, 10.6%, and 19.65%) comparing the control beam, with the thickness ratio of each layer (0.25, 0.5, 0.75, and 1) respectively.

5. Changing the shear span ratio (a/d) from (1 to 1.5) and from (1 to 2), lowered the ultimate load to reach the failure to (33%) and (50%) respectively.

6. The effect of the layer compressive strength ratio ($fc`_{HSC}$)/($fc`_{NSC}$) on shear strength (Vc) is greater than ultimate shear strength (Vu) within the range of (50 to 70%).

7. Increasing the high strength layer ratio ($h_{HSC}\backslash h_{total}$), the value of shear strength (Vc) and ultimate shear strength (Vu) increases linearly.

8. By increasing stirrup spacing the capacity of shear strength is decreasing for two-layer beams.

9. Different available equation (ACI 318-19, EC2, BS8110, and Canadian Code) are used to predict the shear strength (Vc), EC2 and BS8110 equations give lower values of the results, but ACI 318-19 equations gives more reasonable results and still lower values of the results, while the equations of the Canadian Code results are more conservative.

10. Different new equations are proposed to modify the ACI 318-2019 for two-layer beams to predict the shear strength of the beams in terms of the variables (the compressive strength ratio ($\frac{fc'_{HSC}}{fc'_{NSC}}$) of the two layers for beams with and without stirrups, waiting time for casting (overlap casting time) as a ratio to the cement initial setting time ($\frac{t}{t_o}$), layer thickness ratio ($\frac{h_{HSC}}{h_{total}}$), shear span ratio ($\frac{a}{d}$), and amount of transverse reinforcement (spacing of stirrups) which is represented by the ratio of transverse reinforcement index divided by the longitudinal index ($\frac{\rho_t}{\rho_l}$)). The predicted results are very close to the experimental results and shows an acceptable correlation.

11. General equations are proposed using multi-linear analysis regression to predict cracking shear and flexural first cracking shear of two-layer beams in terms of the variables of this study, the average ratio of (($\frac{Vc_{exp}}{Vc_{cal}}$)are (1.017 and 1.011) respectively.

6.2 Recommendations

The following studies are recommended for future project works:

1. Study on the flexural behavior of two-layer reinforced concrete beams using lightweight concrete.
2. Study on the behavior of torsion using two-layer reinforced concrete beams.
3. Study on the flexural behavior of two-layer reinforced concrete beams using recycle aggregate.

Reference

ACI 318M-19 (2019). Building Code Requirements for Structural Concrete. American Concrete Institute, Farmington Hills, MI 48331.

Adnan, O., Adai Al-Farttoosi, H., Al Bremani, H., (2021). Flexural behavior of two-layer beams made with normal and lightweight concrete layers. Period. Eng. Nat. Sci. PEN 9, 1124–1140. https://doi.org/10.21533/ pen. v9i2.1952.

Adnan, T., (2018). Project & Thesis BECM 4000 STUDY ON FLEXURAL BEHAVIOR OF REINFORCED CONCRETE BEAM IN UNDER, BALANCED, AND OVER REINFORCED CONDITION USING ANSYS.

ASTM C150-(2007) - Standard Specification for Portland Cement, American Society for Testing and Materia.

ASTM-C33 (2007). Standard Specification for Concrete Aggregates. American Society for Testing and Material.

ASTM International - ASTM C1611/C1611M-18 (2007). Standard Test Method for Slump Flow of Self-Consolidating Concrete.

ASTM-C1240 (2007). silica-fume-in-cementitious-mixture. American Society for Testing and Material.

ASTM-C494 (2007). Classification of admixtures. American Society for Testing and Material.

ASTM-C31 (2007). Standard Specification for Concrete Aggregates. American Society for Testing and Material.

ASTM-C469 (2007). Standard Specification for Concrete Aggregates. American Society for Testing and Material.

Ataria, R.B., Wang, Y.C., (2019). Bending and shear behavior of two-layer beams with one layer of rubber recycled aggregate concrete in tension. Structures 20, 214–225. https://doi.org/10.1016/j.istruc.2019.03.014

Bekem Kara, İ., (2021). Experimental Investigation of the Effect of Cold Joint on Strength and Durability of Concrete. Arab. J. Sci. Eng. 46, 10397–10408. https://doi.org/10.1007/s13369-021-05400-5

BS 1881 116 (1983) Testing Concrete. Method for Determination of Compressive Strength of Concrete Cubes [WWW Document], pdfcoffee.com. URL https://pdfcoffee.com/bs-1881-116-1983-testing-concrete-method-for-determination-of-compressive-strength-of-concrete-cubes-pdf-free.html (accessed 6.5.22).

British Standards Institution. (1985), Code of Practice Design and construction (BS 8110: Part 1:1985), British Standards Institution, London.

Butean, C., Heghes, B., (2020). Flexure Behavior of a Two Layer Reinforced Concrete Beam. Procedia Manuf., 13th International Conference Interdisciplinarity in Engineering, INTER-ENG 2019, 3–4 October 2019, Targu Mures, Romania 46, 110–115. https://doi.org/10.1016/j.promfg.2020.03.017

CEN (2004) EuroCode2: "Design of concrete structures, part 1-1: General rules for buildings", CEN, Brusels,EN 1992-1-1:2004.

CSA Committee A23.3 (2004). Design of Concrete Structures, Canadian Standards Association, Mississauga, Ontario, Canada, 214 pp.

Choi, S.-J., Kang, S.-P., Kim, S.-C., Kwon, S.-J., (2015). Analysis Technique on Water Permeability in Concrete with Cold Joint considering Micro Pore Structure and Mineral Admixture. https://doi.org/10.1155/2015/610428.

Classification of admixtures according to ASTM C-494., (2007). [WWW Document], ResearchGate. URL https://www.researchgate.net/figure/ Classification-of-admixtures-according-to-ASTM-C-494_tbl1_329892744 (accessed 5.5.22).

Committee 363, A.C.I., (2005). High-Strength Concrete (ACI 363R). Spec. Publ. 228, 79–80. https://doi.org/10.14359/14461

Dybeł, P., Wałach, D., (2017). Evaluation of the Development of Bond Strength between Two Concrete Layers. IOP Conf. Ser. Mater. Sci. Eng. 245, 032056. https://doi.org/10.1088/1757-899X/245/3/032056.

Elwell, D.J., Fu, G., (1995). Compression Testing of Concrete: Cylinders versus Cubes (No. FHWA/NY/SR-95/119).

Ge, W.-J., Ashour, A.F., Ji, X., Cai, C., Cao, D.-F., (2018). Flexural behavior of ECC-concrete composite beams reinforced with steel bars. Constr. Build. Mater. 159, 175–188. https://doi.org/10.1016/j.conbuildmat.2017.10.101

Introducing ACI 318-(2019): Building code requirements for structural concrete, ICC. URL https://www.iccsafe.org/building-safety-journal/bsj-technical/introducing-aci-318-19-building-code-requirements-for-structural-concrete/ (accessed 7.30.22).

Iskhakov, I., Ribakov, Y., Holschemacher, K., (2017). Experimental investigation of continuous two-layer reinforced concrete beams. Struct. Concr. 18, 205–215. https://doi.org/10.1002/suco.201600027

Iskhakov, I., Ribakov, Y., Holschemacher, K., Mueller, T., (2014). Experimental Investigation of Full Scale Two-Layer Reinforced Concrete Beams. Mech. Adv. Mater. Struct. 21, 27-28https://doi.org/10.1080/15376494.2012.680.

Jamal, Z., Lateef, A., Saleem, A., (2019). Mechanical behaviour of simple supported two layers reinforced concrete (LWC-NSC) beam. Int. J. Civ. Eng. Technol. 10, 1122–1132.

Korol, E., Vu, T., (2020). Bond strength between concrete layers of three-layer concrete structures. IOP Conf. Ser. Mater. Sci. Eng. 775, 012115. https://doi.org/10.1088/1757-899X/775/1/012115

Krishnaraja, A.R., Kandasamy, S., (2018). Flexural Performance of Hybrid Engineered Cementitious Composite Layered Reinforced Concrete Beams. Period. Polytech. Civ. Eng. https://doi.org/10.3311/PPCI.11748

Li, C., Zhu, H., Niu, G., Cheng, S., Gu, Z., Yang, L., (2022). Flexural behavior and a new model for flexural design of concrete beams hybridly reinforced by continuous FRP bars and discrete steel fibers. Structures 38, 949–960. https://doi.org/10.1016/j.istruc.2022.02.037

Martínez-Pérez, I., Valivonis, J., Šalna, R., Cobo-Escamilla, A., (2017). Experimental study of flexural behavior of layered steel fiber reinforced concrete beams. J. Civ. Eng. Manag. 23, 806–813. https://doi.org/10.3846/13923730.2017.1319413

Nes, L., Overli, J., (2015). Structural behavior of layered beams with fibre reinforced LWAC and normal density concrete. Mater. Struct. 49. https://doi.org/10.1617/s11527-015-0530-9

Nilson, A., Darwin, D., Dolan, C., (2009). Design of Concrete Structures, 14th edition. ed. McGraw-Hill Education, Boston.

Nilson, A.H., (1985). Design Implications of Current Research on High-Strength Concrete. https://doi.org/10.14359/6526

Polak, M., Dubas, J., (2011). Shear design of high strength concrete beams - Canadian code perspective. Can. J. Civ. Eng. 23, 809–819. https://doi.org/10.1139/l96-890

Pratama, M.M.A., Vertian, T., Umniati, B.S., Yoh, W., (2019). Flexural behavior of the functionally graded concrete beams using two-layers and three-layers configuration. IOP Conf. Ser. Mater. Sci. Eng. 669, 012054. https://doi.org/10.1088/1757-899X/669/1/012054

Swamy, R., (1985). High-Strength Concrete -Material Properties and Structural Behavior. https://doi.org/10.14359/6527

Wafa, F., Ashor, S., (1992). Mechanical Properties of High-Strength Fiber Reinforced Concrete. https://doi.org/10.14359/2390

Yang, H.-M., Lee, H., Yang, K.-H., Ismail, M., Kwon, S.-J., 2018. Time and cold joint effect on chloride diffusion in concrete containing GGBFS under various loading conditions. https://doi.org/10.1016/J.CONBUILDMAT.2018.02.093

Yehia, S., (2020). Effect of Cold Joint on Stratified Slabs. Int. J. Eng. Res. V9. https://doi.org/10.17577/IJERTV9IS070278

Zega, B., Prayuda, H., Monika, F., Saleh, F., Wibowo, D.E., (2021). Effect of Cold Joint and Its Direction on The Compressive and Flexural Strength of Concrete. Int. J. GEOMATE 20, 86–92. https://doi.org/10.21660/2021.82

رایەڵی (١٢ و ١٣) جێبەجێکراوە لەژێر کاریگەری ڕێژەی دووری هێزەکەی دەکەوێتەسەری (a/d) ، رایەڵی (١٤-١٧) جێبەجێکراوە لەژێر کاریگەری چینی هێزی کۆنکرێتەکە بەبێ بەکارهێنانی شیشبەندی سوران (قەفیز)، وە رایەڵی (١٨ و ١٩) جێبەجێکراوە لەژێر کاریگەری دووری نێوان شیشبەندی سوران (قەفیز).

لەم توێژینەوەیە بۆمان دەرکەوت کە درزەکانی (cracks) رایەڵەکان کە پێکهاتووە لە دووچین کۆنکرێتی جیاواز ئەنجامەکەی نزیکە لە ئەنجامی رایەڵی یەک چینی. بەزیادکردنی چینی هێزی کۆنکرێت شکستی کۆتایی (ultimate failure) رایەڵی دووچینی زیاد دەبێ بە ڕێژەی (8.35%، 15.6%، 18.85%) بەراورد لەگەڵ رایەڵی کە لە یەک چین پێک هاتووە، هەوەها بەزیادکردنی چینی ئەستوری کۆنکرێتی بەهێز ئەوا نرخی هەریەک لە هێزی برین (Vc) و کۆتایی هێزی برین (Vu) زیاد دەبێ. هەوەها لەم توێژینەوەیە بۆمان دەرکەوت تاوەکو 30 دەقە دەتوابرێت چینی دووەم دابنرێت لە کۆنکرێتی شیشدار، لەدوای ئەم کاتەوە هێزی برین (Vc) و کۆتایی هێزی برین (Vu) کەم دەبێتەوە. بەزیاد کردنی دووری نێوان هێزەکان (a/d) لە (1 بۆ 1.5 و2) شکستی کۆتایی (ultimate failure load) کەم دەکات بە ڕێژەی (33% و 50%) . توانای هێزی برین (shear strength capacity) کەم دەبێتەوە بەزیادکردنی دووری نێوان شیشبەندی سوران (قەفیز). بەشێکی تری ئەم توێژتنەوەیە دۆزینەوەی هاوکێشەی نوێ بوو بۆ رایەڵی دووچینی شیشدار کە پێشنیازمان کرد بۆ گۆڕانکاری لە کۆدی (ACI-19) کە ئەنجامەکانی زۆرباش بوون.

پوختە

کۆنکرێت زۆر گرنگە لە کەرەستەی بیناسازیدا، بۆ بینای بەرز و پرد کۆنکرێتی هێزی بەرز بە بەکاردەهێنرێت، بۆ کەمکردنەوەی تێچووی کۆنکرێتی هێزی بەرز و قەبارەی رایەڵیەکان دەتوانرێت دوو چینی هێزی کۆنکرێتی جیاواز بەکاربهێنرێت. ئەم توێژینەوەیە لێکۆڵینەوە لە رەفتاری چەمانەوە و بڕینی رایەڵی شیشدار دەکات، کە لە دوو چینی هێزی کۆنکرێتی جیاواز پێکهاتووە، بەبەکارهێنانی شیشبەندی سوران (قەفیز) لەگەڵ بەکارنەهێنانی شیشبەندی سوران (قەفیز) بۆ رایەڵەکان، بە لەبەرچاوگرتنی کاریگەری چینی هێزی کۆنکریت، کاتی تێکردنی نێوان چینەکان، ئەستوری چینەکە، رێژەی دووری ئەو هێزەی دەکەوێتە سەری، وە دووری نێوان شیشبەندی سوران (قەفیز) . لێکۆڵینەوە کرداریەکە پێک هاتبوو لە دروست کردن و پشکنینی (19) ڕایەڵی لاکێشەیی کە دابەش کرابون بەسەرشەش کۆمەلە بە ئەندازەی 125 ملم پانی و250 ملم بەرزی و 1200 ملم درێژی، هەموو رایەڵەکان شیشبەندیان هەیە بە ئاراستەی درێژی رایەڵەکان ($4\Phi12$) ملم لەگەڵ بکارهێنانی ($\Phi8$) ملم شیشبەندی سوران (قەفیز) بۆ رایەڵەکان.

لە رایەڵی (١-٣) جێبەجێکراوە لەژێر کاریگەری چینی هێزی کۆنکرێتی (effect of layer compressive strength)، رایەڵی (٤-٧) جێبەجێکراوە لە ژێر کاریگەری کاتی تێکردنی نێوان دوو چینەکە(effect of casting overlap time) ، رایەڵی (٨-١١) جێبەجێکراوە لەژێر کاریگەری ئەستوری چینەکان (effect of layer thickness) ،

زانکۆی پۆلیتەکنیکی هەولێر
ERBIL POLYTECHNIC UNIVERSITY

ڕەفتاری چەمانەوە و بڕین لە دووچینی دارشتەی ڕایەڵی شیشبەندی کۆنکریتی

نامەیەکە

پێشکەشی ئەنجومەنی کۆلێژی تەکنیکی ئەندازیاری کراوە لەزانکۆی پۆلیتەکنیکی هەولێر

وەکو بەشێك لە پێداویستیەکانی بەدەست هێنانی بڕوانامەی ماستەر لە (ئەندازیاری شارستانی)

لەلایەن

هلمت برهان نجم

بەکالۆریۆس لە ئەندازیاری شارستانی

بەسەرپەرشتی

پ. د. میرین حسن فەهمی ڕەشید

کوردستان - هەولێر

November-2022